AD NUMBER

AD903418

NEW LIMITATION CHANGE

TO

Approved for public release, distribution unlimited

FROM

Distribution authorized to U.S. Gov't. agencies only; Test and Evaluation; 02 JUN 1972. Other requests shall be referred to Dean of Engineering, Air Force Institute of Technology, ATTN: AFIT-EN, Wright-Patterson AFB, OH 45433.

AUTHORITY

SFATL ltr dtd 15 May 1974

# AIR FORCE INSTITUTE OF TECHNOLOGY

AIR UNIVERSITY
UNITED STATES AIR FORCE

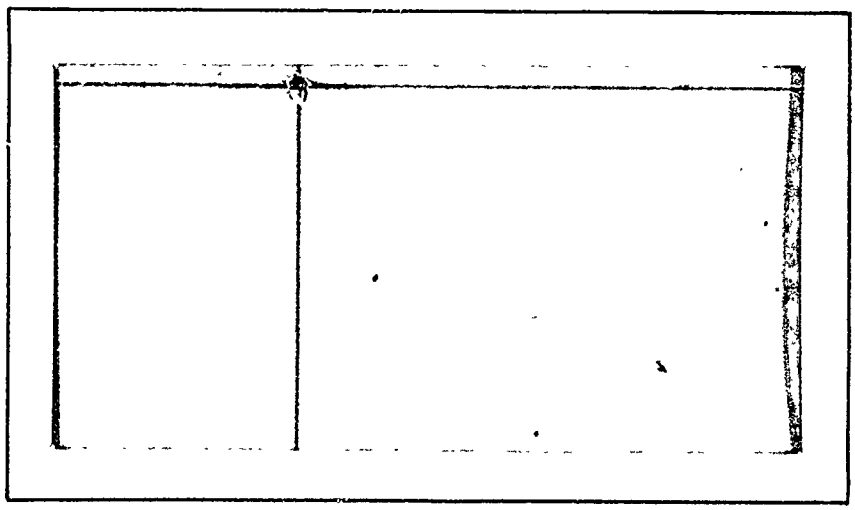

## SCHOOL OF ENGINEERING

WRIGHT-PATTERSON AIR FORCE BASE, OHIO

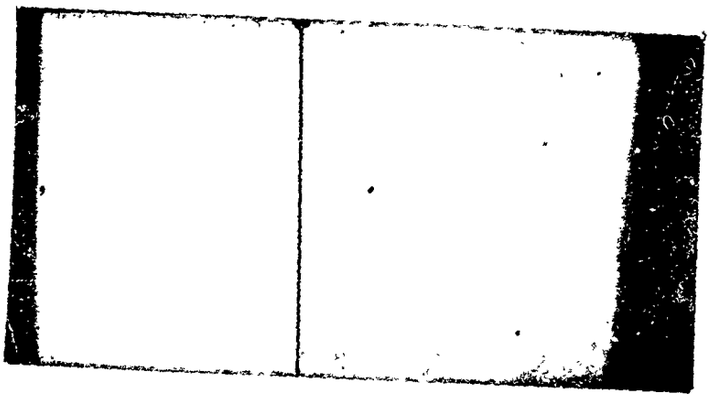

# THE EFFECT OF TARGET MANEUVERING ON KILL PROBABILITY IN AIR-TO-AIR GUNNERY

THESIS

GAW/MC/72-9

RICHARD E. GUILD
MAJOR USAF

# THE EFFECT OF TARGET MANEUVERING ON KILL PROBABILITY IN AIR-TO-AIR GUNNERY

THESIS

Presented to the Faculty of the School of Engineering

of the Air Force Institute of Technology

Air University

in Partial Fulfillment of the

Requirements for the Degree of

Master of Science

by

Richard E. Guild

Major USAF

Graduate Air Weapons

June 1972

## Preface

This report is the result of my attempts to analyze the effect of target maneuvering on kill probability in air-to-air gunnery. A primary motivation was a personal quest for a greater understanding of what might constitute an optimum ballistic dispersion for rapid firing cannons when used in air-to-air gunnery.

I wish to thank and express much appreciation to Mr. Hal Smith, of the Optimization Branch at the Air Force Armament Laboratory, for allowing me to use his mathematical model and for a great amount of patience in answering my questions over the telephone.

I would like to thank the following people for their efforts which allowed me to work this study in cooperation with the Air Force Armament Laboratory: Mr. Thomas P. Christie, Chief Analysis Division, Air Force Armament Laboratory, Dr. D. W. Breuer, Head of the Mechanics Department, Air Force Institute of Technology, and Major Robert O. Meitz, my advisor, Mechanics Department, Air Force Institute of Technology.

I also wish to acknowledge the patience and understanding of my wife, Alice while this study was being completed.

Major Richard E. Guild

# Contents

## Contents

## List of Figures

## List of Figures

## List of Tables

## List of Tables

## List of Symbols

| | |
|---|---|
| ABS | Absolute Value |
| AI | Radial Acceleration of Attacker |
| ALPHA | Exponential Ballistic Drag Factor |
| AMLC | Maximum Lead Capability |
| AO | Angle-off |
| APKD | Average Probability of Kill for Draws |
| AVP | Vulnerable Area of Part |
| BCDEF | Ballistic Coefficient |
| BD | Ballistic Dispersion |
| Cd | Drag Coefficient |
| COT | Center of Part in Width Direction |
| COY | Center of Part in Length Direction |
| CUHIT | Total Number of Hits |
| DELTA | Predicted Lead Angle |
| DELTF | Time Increment |
| DOS | Offset Distribution |
| exp | Base e Exponent |
| FLOS | Fire Line Offset |
| FR | Firing Rate |
| FRL | Fuselage Reference Line |
| FTD | Fire Timing Delay |
| Gamma | Flight Path Angle |
| GLF | Target g-loading |
| GLFDOT | g-loading Rate |

## List of Symbols

| | |
|---|---|
| GLFI | Attacker g-loading |
| GLFMAX | Maximum Permissible g-loading |
| IDP | Projectile Identifier |
| IGAMMA | Initial Flight Path Angle |
| IGLF | Initial g-loading |
| IPD | Pattern Density Identifier |
| IPHI | Initial Bank Angle |
| IPOL | Fire Pattern Symmetry Identifier |
| HWP | Half Width Pattern |
| KOS | Mils Offset |
| LAM | Predicted Impact Angle |
| OS | Displacement in width Direction |
| OSL | Displacement in length Direction |
| PHI | Bank Angle |
| PHIDOT | Roll Rate |
| $P_K$ | Probability of Kill |
| $P_{K_{AV}}$ | Kill Probability for Average Man uvering Target |
| PKOL | Kill Probability |
| PNR | Probable Number of Rounds |
| PRESGAM | Change in Flight Path Angle |
| PY(IDP) | Probability of Fire Point Location |
| r | Turn Radius |
| R | Line of Sight Range |
| RA | Radial Acc leration of Target |
| RB | Ballistic Range |

## List of Symbols

| | |
|---|---|
| S | Cross Sectional Area of Projectile |
| SIGB | Standard Deviation in Ballistic Dispersion Assuming a Circular Gaussian Distribution |
| SSL | Single-shot Kill Probability |
| TCR | Target Crossing Rate |
| TF | Time of Flight |
| TKSIG | Standard Deviation in Aim Wander |
| TLC | Tracking Lead Capability |
| TNLH | Total Number of Lethal Hits |
| TSIGMIN | Minimum Standard Deviation in Tracking Error |
| UBAR | Average Ballistic Velocity |
| UO | Total Initial Projectile Velocity |
| UP | Absolute Velocity of Projectile at Impact |
| USK | Velocity of Projectile Relative to Target at Time of Impact |
| VI | Velocity of Target Aircraft |
| VT | Velocity of Attacking Aircraft |
| W | Weight of Projectile |
| YDIS | Lateral Displacement of Maneuvering Target |
| YL | Distance of Fire Point along Fire Line |
| ZDIS | Vertical Displacement of Maneuvering Target |

## Abstract

A study was made to determine the effect of target maneuvering during projectile flight time on kill probability in air-to-air gunnery. The effect of target uncertainty was analyzed by comparing kill probabilities for a specified non-maneuvering target with kill probabilities for an average defensively maneuvering target. The kill probability of the average maneuvering target was defined as the average kill probability for the specified target when performing a negative-g jink, hard turn, and break. The kill probabilities were calculated using a mathematical model to approximate the gunnery attack. Firing conditions were parametrically varied from 500 feet to 3000 feet line of sight range and zero to 45 degrees angle-off. Two dissimilar rapid firing cannons are compared in the analysis. Kill probability was based on trackshoot aiming when the attacker's g-loading to establish lead for target motion was 5.6 g's or less, and snapshoot aiming when greater. It was concluded that target uncertainty has no effect on kill probability when the time of flight is less than .5 seconds, but that it significantly affects kill probability when the time of flight is greater than .8 seconds. It was also concluded, that for air-to-air gunnery, the ballistic dispersion of rapid firing cannons should be such that 80 percent of the rounds are within a circle of nine to ten mils diameter.

GAW/MC/72-9

# THE EFFECT OF TARGET MANEUVERING ON KILL PROBABILITY IN AIR-TO-AIR GUNNERY

## I. Introduction

In this study, the effect that a defensively maneuvering fighter aircraft has on the probability of kill in air-to-air gunnery is analyzed. The attempt is made to include in the analysis the pilot techniques used in making a gun attack and those used to avoid being hit.

A mathematical model, which calculates the probability of kill ($P_K$), is used in the analysis to describe the aerial gunnery engagement. The model is a combination of governing equations of motion, functional and geometric relationships and probability theory.

The model calculates the kill probability for a one second burst against a non-maneuvering target and for the same target making three violent defensive maneuvers. The probability of kill for the average-maneuvering target ($P_{K_{AV}}$) is defined to be the average of the kill probabilities for the three defensive maneuvers. The decrease in kill probability due to target maneuvering is the difference between the kill probability for the non-maneuvering target

and the average-maneuvering target. This difference is used to measure the effect of target maneuvering on kill probability in air-to-air gunnery.

The decrease in $P_K$ is found for two guns fired from various line of sight ranges and line of sight angles to the target at 5000 feet pressure altitude.

In addition to determining the decrease in kill probability due to target maneuvering, an investigation is made into the ballistic dispersion which produces the overall highest $P_K$ for the various angles-off and ranges. An effort is made to quantitatively describe the relative effectiveness of the three defensive maneuvers in decreasing $P_K$ as a function of the attacker's relative position. The relative position is also analyzed from the attacker's point of view. That is, for a given range what angle-off produces the highest kill probability against a maneuvering target?

The mathematical model used in this study was provided by the Optimization Branch, Analysis Division, Air Force Armament and Test Laboratory (AFATL), Eglin AFB, Florida. The model is named the Gun Design Model (GDMOD) and was developed by Mr. Hal Smith of the Optimization Branch. He originally developed the model to isolate gun design problems from fire control mechanization and related

encounter problems. It is written in Fortran language for use on the Control Data Corporation 6600 computer.

The GDMOD originally included only the prediction errors common to an aircraft attacking a co-airspeed, co-altitude, and non-maneuvering target. The model was modified by this author, through the addition of a target uncertainty subroutine, so that prediction errors for a maneuvering target are considered. Other modifications included a different interpretation to the offset of the fire line from the target and the weighting of various factors so that one overall $P_K$ is calculated for each firing burst rather than several average $P_K$'s.

In making the different interpretation to the offset of the fire line, this author has attempted to account for the way in which pilots use gunsights as an approximate rather than a precise reference for aiming guns in air-to-air combat.

A number of more minor modifications were also made to the model. Most are noted in the text of this study, but some are contained only in the program listing, which can be found in Appendix D. Although the Gun Design Model is the original work of Mr. Smith, it is thoroughly explained in this study since it has not been documented elsewhere.

The documentation here has been done both with his permission and advice; however, this author assumes the sole responsibility for any errors contained in this study.

Background

There are two basic approaches to predicting the outcome of a fighter versus fighter combat engagement. The earliest efforts used probability theory to predict kill probability. Conditional probabilities were calculated for a host of items such as: Given two fighters, what is the probability that one will achieve a maneuvering advantage over the other? Given that one does, what is the probability that he will achieve a position in which he can fire his guns at the other target; and if he fires his guns, what is the probability that he will hit the target, etc?

More recently, efforts have been made to simulate the air-to-air combat engagements on high speed digital computers. Optimization techniques using game theory and varational calculus techniques on the governing equations are being used to find optimum tactics and to study cost-effectiveness as well as design trade-offs for weapon systems.

Achieving realism has been particularly elusive in air-to-air combat studies and analysis. The difficulty is that

the number of variables involved are so numerous and so interdependent as to defy precise description.

This study uses a combination of the two basic approaches. That is, random variable relationships (one to one correspondance) and probability theory are combined with governing equations and functional relationships into a mathematical model that approximates the portion of an aerial combat engagement where the guns of one aircraft are being fired at another.

## Purpose

The purpose of this study is (1) to determine the decrease in kill probability due to target uncertainty during the flight time of the projectiles fired from rapid firing cannons in air-to-air combat, (2) to determine, for a particular gun, the ballistic dispersion that produces the highest value of kill probability against a maneuvering target, (3) to determine the relative effectiveness of presently accepted defensive air combat maneuvers in decreasing kill probability, and (4) to determine the offensive positions, relative to the target, which produce the highest kill probability.

Scope

This study is limited to computing the decrease in kill probability due to target motion during the flight time of the projectile. The initial conditions in the model place the attacker co-airspeed and co-altitude with the target. Kill probability is calculated both for the target continuing in straight and level flight and for the target as it performs three violent defensive maneuvers.

Kill probabilities for a particular target are calculated for two guns having the same firing characteristics, but differing in projectile muzzle velocity and aerodynamic drag coefficient. Results are obtained for ballistic dispersions of two, four, six, and eight mils; line of sight ranges of 500, 1000, 1500, 2000, 2500, and 3000 feet; and line of sight angles-off of 0, 15, 30, and 45 degrees.

## II. Air-to-Air Gunnery Considerations

The purpose of this chapter is to provide the reader with a general understanding of the factors and parameters of air-to-air gunnery that are represented in the mathmatical model. The chapter is written from a user's point of view with the purpose of providing the reader with clear reasons for the choice of parameters used in this analysis. To some, the contents of this chapter will be obvious considerations; to the others for whom the chapter is written, I trust it will be enlightening.

### General Situation

In general, the outcome of an aerial combat engagement between fighter aircraft is determined by (1) the number and types of aircraft involved, (2) the offensive and defensive tactics used by opposing sides, and (3) the maneuvers used by individual aircraft to provide mutual support to each other while attempting to gain an offensive advantage over an enemy aircraft. The term offensive advantage means a relative position from which it is possible, through more maneuvering, to launch a missile or to fire a burst from a cannon at the target.

In this study, it is assumed that such a position has been achieved. That is, the attacking aircraft has not only achieved an offensive advantage, but has maneuvered into a position where the pilot can fire a lethal burst from his gun at the target.

Defensive Maneuvering

If the pilot in the target aircraft is aware of the presence of the attacking aircraft, he will naturally make a violent maneuver with his aircraft to prevent being shot down. There are a number of defensive "last ditch" maneuvers which could be classified as "most violent;" however, the two common ones are the break and the negative-g jink.

Break. In making the most common type of break the pilot pulls the control stick full aft and, depending upon the aircraft, pushes it either to the right or to the left, or keeps it centered and uses full rudder deflection to roll the aircraft, or uses both. The resulting maneuver is a tight evasive turn. The pilot may also pull the throttle to idle and put out the speed brake in an attempt to force the attacker to overshoot the flight path. However, the primary purpose of the break maneuver is to avoid being hit by projectiles from the attacker's gun and to prevent the attacker from tracking with his gunsight.

The break maneuver is represented in the model by giving the target a roll rate (PHIDOT) of 90 degrees per second and a g-loading rate (GLFDOT) of six g's per second. The g-loading rate is maintained until the target has attained a g-loading (GLFI) of 7.0 g's, which is approximately the operating limit for most USAF fighter aircraft. The roll rate is continued throughout the maneuvering time of flight. Although higher roll rates can be achieved in fighter aircraft, 90 degrees per second is the approximate roll rate for a break.

Negative-g Jink. In making the negative-g jink the pilot rapidly pushes the control stick forward. Some amount of left or right roll may also be used as the stick is pushed forward. A couple of seconds later, the control stick is pulled aft and a roll in the opposite direction is made. The resulting maneuver is called jinking. Its purpose is to cause the attacking aircraft to get out of phase as the pilot tries to follow the maneuver and to prevent him from tracking the target.

Because of the short flight time involved, only the initial part of the jinking maneuver is represented in the mathematical model. This maneuver is represented by giving the target a negative-g loading rate (GLFDOT) of minus two g's per second. The g-loading rate is maintained until the

target has attained a g-loading (GLFI) of three negative g's, which is the operating limit for most USAF fighter aircraft. No roll rate is given to the target model for this maneuver, because a zero roll rate negative-g jink followed by a break is more effective than a rolling negative-g jink followed by a break in the opposite direction, since the pilot in the target aircraft is not "telegraphing" to the attacker, which way he is likely to roll next.

Hard Turn. One of the cardinal rules of flying in air-to-air combat is that one always turns into the attacker. The reason is to create a high angle-off so that the attacker is forced into shooting from a large deflection angle, which is very difficult to do. An equally important reason for turning into the attack is to keep the attacking aircraft in sight. By turning into the attack, the pilot in the target aircraft can keep the attacker in sight, and unless the attacker is careful, the defensive turn will cause the attacker to reach a "square corner" as the range between aircraft decreases. Since aircraft do not turn square corners, the attacker can overshoot the flight path of the target; then, by reversing his turn direction, the pilot of the target aircraft can maneuver behind his opponent.

The hard turn as considered in this analysis is used to represent the situation in which the pilot in the target aircraft has lost sight of the attacking aircraft. The target pilot knows he cannot afford to use gentle maneuvers, because the attacker might be behind him; yet he does not break since it causes a high loss of energy maneuverability.

The hard turn is represented in the model by giving the target a roll rate (PHIDOT) of 45 degrees per second and a g-loading rate (GLFDOT) of four g's per second. The roll rate is maintained throughout the maneuvering time of flight and the g-loading rate is maintained until a positive 7.0 g's is attained.

Non-Maneuvering Target

The non-maneuvering target flies at constant airspeed, constant heading, and constant altitude throughout the flight time of the projectile. The situation represented is one in which the pilot of the target aircraft doesn't see and is not aware that he is being attacked. It is represented in the model by giving the target zero roll rate (PHIDOT) and zero g-loading rate (GLFDOT).

Average-Maneuvering Target

The average-maneuvering target used in this study is defined only in terms of kill probability. The mathematical model calculates separate kill probabilities for the target making a jink, a hard turn, and a break. The average of the three resulting kill probabilities is defined as the kill probability for an average-maneuvering target.

Firing Parameters

To hit a moving target with a ballistic projectile, it is necessary to account for the motion of the target during the flight time of the projectile. This is called lead for target motion, and in air-to-air gunnery it presents the pilot in the attacking aircraft with a problem that is difficult to solve.

Since guns are rigidly mounted to fire forward on fighter aircraft, the pilot aims them by maneuvering his aircraft. To shoot down another aircraft, he must point the gun ahead of the target. The correct amount of lead required is determined by the flight path of the target

during the flight time of the projectile. The degree of difficulty in establishing the correct lead angle is determined by the relative rate at which the target is crossing the flight path of the attacker.

Angle-off. If the target is flying straight and level the task of leading for target motion is relatively easy to solve especially at close range (attacker less than 1500 feet from target) and low angle-off (attacker less than 20 degrees off target's tail). As angle-off increases, establishing the correct lead angle becomes more difficult, because the rate at which the target is crossing in front of the attacker increases.

Table I shows the effect of line of sight range and line of sight angle-off on firing parameters. Above 45 degrees angle-off the target crossing rate is, for ranges of approximately 1000 to 2000 feet, greater than the rate at which the attacking aircraft can turn. For this reason only angles-off of 45 degrees and less are considered in this study. Four angles-off ($0^{o}$, $15^{o}$, $30^{o}$, $45^{o}$) were chosen.

Table I

Firing Parameters for Attack against
Co-airspeed, Co-altitude, Non-maneuvering Target.

Results based on projectile muzzle
velocity of 3300 feet per second.

| Target Range (ft) | Attacker Angle-off (deg) | Target Cross. Rate (deg/sec) | Attacker Load Factor (g's) | Required Lead Angle (deg)[a] | Flight Time (sec) |
|---|---|---|---|---|---|
| 1000 | 0 | 0 | 1.0 | 0 | .357 |
| | 15 | 11.1 | 4.6 | 3.9 | .353 |
| | 30 | 22.5 | 9.1[b] | 7.5 | .343 |
| | 45 | 34.4 | 14.0[b] | 10.6 | .326 |
| 1500 | 0 | 0 | 1.0 | 0 | .585 |
| | 15 | 10.8 | 3.0 | 4.2 | .578 |
| | 30 | 22.0 | 5.9 | 8.0 | .558 |
| | 45 | 33.7 | 9.1[b] | 11.3 | .528 |
| 2000 | 0 | 0 | 1.0 | 0 | .856 |
| | 15 | 10.6 | 2.3 | 4.4 | .844 |
| | 30 | 21.5 | 4.2 | 8.5 | .810 |
| | 45 | 33.0 | 6.6 | 12.0 | .760 |
| 2500 | 0 | 0 | 1.0 | 0 | 1.182 |
| | 15 | 10.3 | 1.8 | 4.7 | 1.163 |
| | 30 | 20.9 | 3.3 | 9.1 | 1.108 |
| | 45 | 32.3 | 5.1 | 12.7 | 1.030 |
| 3000 | 0 | 0 | 1.0 | 0 | 1.582 |
| | 15 | 9.9 | 1.5 | 5.1 | 1.552 |
| | 30 | 20.3 | 2.7 | 9.7 | 1.466 |
| | 45 | 31.5 | 4.1 | 13.5 | 1.346 |

[a] 1 degree approximately equals 17.45 milliradians.

[b] Exceeds operating limitations on aircraft.

[c] Velocity of target and attacking aircraft is 1000 feet per second.

Range. The minimum range for using a gun to shoot down another aircraft is determined by survival considerations. At ranges of less than 1000 feet the possibility is very good that an attacking aircraft will ingest pieces of the target. The maximum range for using a gun is determined by the impact velocity of the projectile that is required to detonate it. A minimum impact velocity of 750 feet per second relative to the target is used in this analysis. At ranges greater than approximately 3000 feet, the projectiles of the guns used in this study have less than 750 feet per second velocity relative to the target at impact. Therefore, ranges of 500 to 3000 feet are considered in the analysis. Increments of 500 feet were chosen, because it is a convenient and perceptible increment for judging range in aerial combat. The ranges considered in the analysis are 500, 1000, 1500, 2000, 2500, and 3000 feet.

Attack Velocity. In envisioning aerial combat there is a tendency for one to think that the attacking aircraft will have a high overtake airspeed on the target. This is not necessarily so nor is it necessarily desirable. Turn radius is a function of velocity squared and the faster the speed of the attacking aircraft the greater will be the number of g's required to establish the correct lead angle. Hence, establishing the lead angle becomes more difficult as

the overtake airspeed increases as well as there being less time to do it in. High overtake airspeed also makes the attacker more vulnerable to overshooting the flight path of the target and ending up in front of a skilled defender. Thus, a higher kill probability for a single firing burst results if the attacking aircraft is co-airspeed with the target than if it has overtake airspeed.

This is not to say that a high speed attack is not appropriate. Depending upon the tactical situation and the relative energy maneuverability of the aircraft, high overtake airspeed attacks may be necessary. The advantage of an overtake airspeed attack is that the projectile time of flight decreases and the target has less time to react.

Because overtake is more a tactics parameter than it is a firing parameter, the analysis is based on a co-airspeed attack. Both the attacking aircraft and target aircraft have a velocity of 1000 feet per second. This airspeed is perhaps disputably high. However, since the lateral and vertical displacement of the target used in this study is affected only by acceleration normal to its flight path (g-load factor) and the projectile time of flight, the calculated kill probabilities are applicable to any co-airspeed attack velocity.

Altitude. Below 10,000 feet pressure altitude, the operational envelope of air-to-air guided missiles decreases markedly, whereas the effective firing envelope for guns is not as greatly affected. Because of this, there is a tendency for fighter pilots to think of the gun as a weapon to be used at low altitude and to want projectiles to be aerodynamically optimized for low altitude firing. For these reasons, a pressure altitude of 5000 feet is used in the analysis with the attacking aircraft and target aircraft co-altitude.

The term co-altitude should not imply to the reader that the attacking aircraft and target aircraft are necessarily flying straight and level, right side up. In this study, the position of the attacking aircraft and target aircraft are placed in that position; however, it is only for convenience in orienting the coordinate system.

In developing the target uncertainty subroutine for the mathematical model, the effect of the initial attitude of the target aircraft on its displacement during the time of flight of the projectile was found to be negligible for the three defensive maneuvers used in this analysis. Thus, the results are applicable whatever the initial attitude of the attacking and target aircraft and it makes little difference whether both are flying right side up, upside down, or going straight up.

Target Uncertainty

The prime difficulty in shooting an evasively maneuvering target is following its maneuver. As previously mentioned, in this study it is assumed that the attacker is following the defensive maneuver of the target. That is, until the instant the pilot in the attacking aircraft fires his gun, he has been able to follow whatever maneuver the target has made.

The task of establishing the correct lead angle for a target making a constant rate turn is more difficult than it is for a target flying straight and level because more lead is required. The reason more lead is required is that once a projectile leaves the gun, its flight path is relatively straight and the target's crossing rate relative to the projectile increases as the target continues a constant rate turn.

Assuming the attacker can follow the constant rate turn of the target, the correct lead angle can be approximately predicted by existing lead computing gunsight systems. However, if at the instant the gun is fired, the target makes a violent change in its flight path, such as changing its maneuver from a hard turn to a negative-g jink; then, the established lead angle for target motion is going to be incorrect and the projectile will likely miss the target. The displacement after the flight time of the projectile

between the target's actual position in space and the predicted position is called target uncertainty.

Determining the decrease in kill probability due to target uncertainty is the major objective of this study. The analysis is based on an attack against a target that is flying straight and level. At the instant the attacker fires his gun, the target makes a violent defensive maneuver. In the mathematical model, the target is given instantaneously a roll rate and a g-loading rate. Because of inertia, an airplane cannot instantaneously attain a roll rate or a g-rate, nor is it likely that a target will change its defensive maneuver at the precise instant the attacker's gun is fired. However, the error in the kill probability calculations due to the instantaneous rate approximations is offset by using a straight and level flight path as the initial condition for target maneuvering rather than a defensive turn.

Table II shows the lateral (YDIS), vertical (ZDIS), and radial displacements for a target making a break from straight and level flight. The time of flight is the same as in Table I. In Table II the load factor is for the target at the end of the time of flight, while in Table I the load factor is for the attacker at the beginning of the firing burst. The radial displacement of the target is

given in mils which is a term preferred in gunnery, because it is invariant with range.

Ballistic Dispersion

Because projectiles fired from guns follow a ballistic trajectory, the amount of target uncertainty, or miss error due to target maneuvering, during the flight time of the projectile is not predictable. Miss due to target uncertainty should not be confused with miss due to incorrect lead angle prediction or with miss due to the pilot being unable to establish the predicted lead angle. Incorrect lead angle prediction is classified as a sight system error and is inherent in the mechanization of the gunsight equations, which themselves are an approximate solution to the real ballistic situation. Miss due to pilot error in establishing the lead angle predicted by the gunsight is classified as aiming error. The trace or locus of the gun sight during the firing burst is called aim wander.

Ballistic dispersion is the "shot-gun" effect of projectile impacts common to rapid firing weapons. In this analysis, ballistic dispersion (SIGB) is defined as the diameter of the circle which contains 80 percent of the projectiles fired from a stationary, rigidly mounted gun.

Table II

Displacement of Break Maneuvering Target at end of Projectile Time of Flight.

Results based on target roll rate (PHIDOT) of 90 degrees per second and g-loading rate (GLFDOT) of 6 g's per second until 7.0 g's attained.

| Target Range (ft) | Attacker Angle-off (deg) | Flight Time (sec) | Final Target Load Factor (g's) | YDIS (ft) | ZDIS (ft) | Radial Distance (mils)[a,b] |
|---|---|---|---|---|---|---|
| 1000 | 0 | .357 | 3.1 | 0 | 1 | .7 |
| | 15 | .353 | 3.1 | 0 | 1 | .7 |
| | 30 | .343 | 3.0 | 0 | 1 | .8 |
| | 45 | .326 | 2.9 | 0 | 1 | .8 |
| 1500 | 0 | .585 | 4.5 | 3 | 6 | 3.2 |
| | 15 | .578 | 4.4 | 3 | 6 | 3.3 |
| | 30 | .558 | 4.3 | 2 | 5 | 2.7 |
| | 45 | .528 | 4.1 | 2 | 4 | 2.3 |
| 2000 | 0 | .856 | 6.1 | 13 | 16 | 6.9 |
| | 15 | .844 | 6.1 | 12 | 16 | 6.8 |
| | 30 | .810 | 5.8 | 10 | 14 | 6.3 |
| | 45 | .760 | 5.5 | 8 | 12 | 5.6 |
| 2500 | 0 | 1.18 | 7.0[c] | 43 | 31 | 14.4 |
| | 15 | 1.16 | 7.0[c] | 40 | 31 | 13.9 |
| | 30 | 1.11 | 7.0[c] | 34 | 28 | 12.6 |
| | 45 | 1.03 | 7.0[c] | 26 | 24 | 10.7 |
| 3000 | 0 | 1.58 | 7.0[c] | 111 | 40 | 25.7 |
| | 15 | 1.55 | 7.0[c] | 104 | 40 | 24.6 |
| | 30 | 1.47 | 7.0[c] | 88 | 40 | 22.3 |
| | 45 | 1.35 | 7.0[c] | 67 | 37 | 18.8 |

[a] Based on ballistic range of projectile.

[b] 1 mil equals approximately 1 foot at 1000 feet.

[c] Maximum operating limit attained before projectile arrives.

Achieving a satisfactory kill probability in air-to-air gunnery requires, among other factors, rapid firing cannons which fire projectiles at high muzzle velocity with some ballistic dispersion. As shown in Table II, the uncertainty of the target increases as the square of the projectile flight time. As the rate of fire, muzzle velocity, and size of the round increase, it is obvious that the lethality of the gun, as measured by kill probability, will increase. This does not necessarily hold for ballistic dispersion. Neither fighter pilots nor gun and fire control system engineers have ever been sure of the best ballistic dispersion. In this study, the influence of ballistic dispersion on kill probability is analyzed by comparing the kill probability at various ranges and angles-off for two, four, six, and eight mils ballistic dispersion.

It is recognized that "optimum" ballistic dispersion is directly related to the gunsight system and the results for various ballistic dispersions are applicable only to this model. However, the trend in kill probability as ballistic dispersion is varied at each of the ranges and angles-off holds for any sight system.

Gun Characteristics

Two different rapid firing cannons are used in the analysis. They are designated gun one and gun two, with gun two characterizing a cannon which fires a larger projectile at greater muzzle velocity than gun one. The characteristics of the two guns are shown in Table III.

Table III

Characteristics of Guns used in Analysis

| Characteristics | Gun 1 | Gun 2 |
|---|---|---|
| Firing rate (FR), rounds/sec | 100 | 100 |
| Muzzle velocity (VELM), ft/sec | 3300 | 4000 |
| Ballistic coefficient (BCOEF), $\frac{W^*}{SC_d}$ | 177.4 | 406.2 |

*W - Weight of projectile

S - Cross sectional area of projectile

$C_d$ - Aerodynamic drag coefficient

Pilots and Gunsights

Without the aid of a gunsight, a pilot finds it almost hopeless to judge where his gun is pointed, especially in the range direction (as opposed to azimuth). This is notwithstanding those pilots who through experience learn that a rivet or screw is located at some mil setting which can be used for aiming. However, the size of the forward windscreen is such that most pilots find aiming a gun impossible without a gunsight. Yet, when a pilot is provided a gunsight, he does not always try to superimpose the sight's pipper precisely on the center of the target when firing a gun. Rather, he will use the sight as a reference from which he uses his own judgement to make aiming corrections.

Sight dynamics, in the case of lead computing sight systems, and lack of dynamics, in the case of manually depressed sights, cause the sightline to be at an angle with the boreline of the gun. The motion of lead computing sights is intentionally damped to keep the sight reticle from moving too fast for the pilot to use it. Depending upon the load factor and bank angle of the aircraft, the sightline will intersect the trajectory of the projectiles at various ranges. During maneuvering flight, the damping causes the pipper or sightline to lag the boreline of the gun whether the g-loading on the aircraft is increasing or

decreasing. If the g-loading is constant, the sight settles to the "correct" lead prediction in approximately one second. This is also true for the so-called "Hot Line" gunsight. A relatively new development, it displays the approximate flight path of the projectiles and gives the pilot a dynamic sight picture in both the lead computing mode (with radar lock-on) and manual mode (without radar lock-on).

In gunnery training, pilots are taught to track a target for approximately one second and to use a short firing burst (less than one second). In combat flying, one seldom finds a situation where it is possible to use such a technique. It is more often that a pilot flies a lag pursuit course on the target and fires the gun while pulling the pipper through the target. This results in a firing burst of approximately three seconds. The reason the technique is appropriate is that during maneuvering flight the gunline is ahead of the sightline. As the target in this study is initially in steady state flight, the tracking technique is more appropriate to the mathematical model and so a firing burst of one second is used in the analysis.

Trackshooting and Snapshooting

In Table I it is shown that the g-load required to establish the correct lead angle may be greater than the

permissible operating limits of the attacking aircraft. In this situation the pilot is unable to establish the required lead angle by increasing the g-loading on his aircraft. When using a lead computing gunsight, the most desirable method for solving this problem is to maneuver to decrease the angle-off, so the necessary lead angle can be established within permissible operating limits. Another method for solving the problem is to use planned maneuvering to lead the target, with no intention of tracking it, and to time the firing burst so that the target flies into the bullet stream. The method of making this high deflection angle attack is called snapshooting.

A high rate of fire and a knowledge of the trajectory of the projectiles is required to successfully use the snapshoot method. Tracer bullets were once used to provide the pilot with trajectory information. More recently, the experience of tactical test pilots with the "Hot Line" gunsight has created a renewed interest in high deflection angle gunnery. For this reason, both trackshooting and snapshooting methods are included in the analysis.

If more than 5.6 g's are required to establish the lead angle, the assumption is made that the pilot will no longer be able to track a target when using a lead computing gunsight. The number of g's that a pilot can sustain and

at the same time track a target with a gunsight has been a continuing dispute. It is not too uncommon to find experienced pilots who are able to still see daylight at seven g's; however, most find it difficult to retain clear vision at six g's. If the g-load required to track the target is greater than 5.6 g's, the kill probability calculations are based on snapshoot firing. In the analysis, it is assumed that an attacker will sustain 5.6 g's and use planned maneuvering to snapshoot. This g-loading is perhaps too high to really simulate the snapshoot method, where low g-loadings are an advantage of the method. However, the difference in kill probability between a maneuvering and non-maneuvering target should be relatively constant regardless of the attacker's g-loading.

Kill Probability

Whether kill probability, the number of lethal hits, or the total number of hits per firing burst is the best measure of the effect of target maneuvering in air-to-air gunnery is disputable. In real life, one hit will sometimes bring down an aircraft and sometimes 20 hits may not be enough to keep it from returning to a friendly base. The kill probability calculated by the mathematical model used

in this analysis is based on the vulnerable area of the target to a single detonating projectile. The cumulative damage effect of more than one hit is not considered and therefore the calculated values of kill probability are less than what might result from a real gun system under the firing parameters used in the model. Nevertheless, kill probability, in spite of its inadequacy to precisely show the effect of multiple hits, was chosen as the best measure of the effect of target maneuvering in air-to-air gunnery.

## III. The Mathematical Model

The mathematical model is a combination of governing equations of motion, functional and geometric relationships, and probability theory. It is a computer program written in Fortran for the Control Data Corporation 6600. Mr. Hal Smith developed the model to isolate gun design problems from fire control and related encounter problems. This author modified the model so that target uncertainty can be included in its kill probability calculations. Perhaps, my more significant contributions to the model are a specified encounter description and a fire control interpretation which allows for the calculation of a single overall kill probability, rather than numerous ones, for each firing burst.

This chapter is written to provide the reader with an understanding of the way in which the air-to-air gunnery considerations of Chapter II are specified in the mathematical model. The inner workings of the model are contained in the Appendices to this study for those who are more interested in the functioning of the model.

### Coordinate System

The coordinate system originates at the center of the target aircraft as shown in Figure 1. The positive X direct-

ion passes through the nose of the aircraft along the FRL (fuselage reference line). The positive Y direction is along the left wing and the positive Z direction is up. The coordinate system moves at constant velocity along the flight path the target would follow in constant airspeed, constant altitude, non-maneuvering flight.

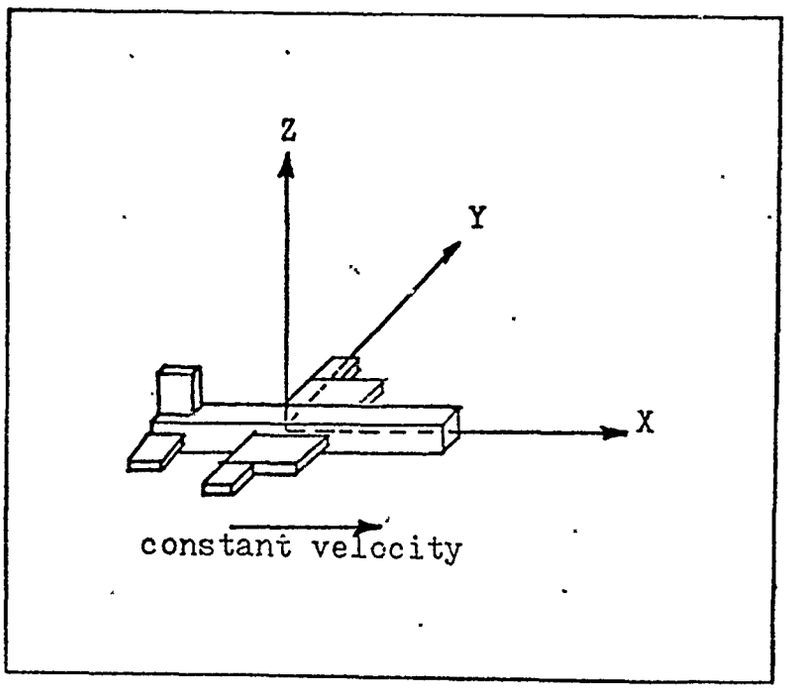


Figure 1 Coordinate Reference System

In maneuvering flight, the displacement of the target from the origin is considered negligible in the X direction, but not in the Y or Z directions.

Target

The target used in the model approximates a fighter aircraft. It is defined by eight rectangular parallelepipeds which represent the fuselage, right and left inboard wing sections, right and left outboard wing sections, right and left horizontal stabilators and a vertical stabilizer. Figure 2 shows a drawing of the target and Table IV contains the numerical designator and the dimensions for each of the target parts. The parts are numbered one through eight. The model calculates the fire pattern coverage of each part separately and sums the results, so that total target coverage is the sum of the coverage for the eight parts.

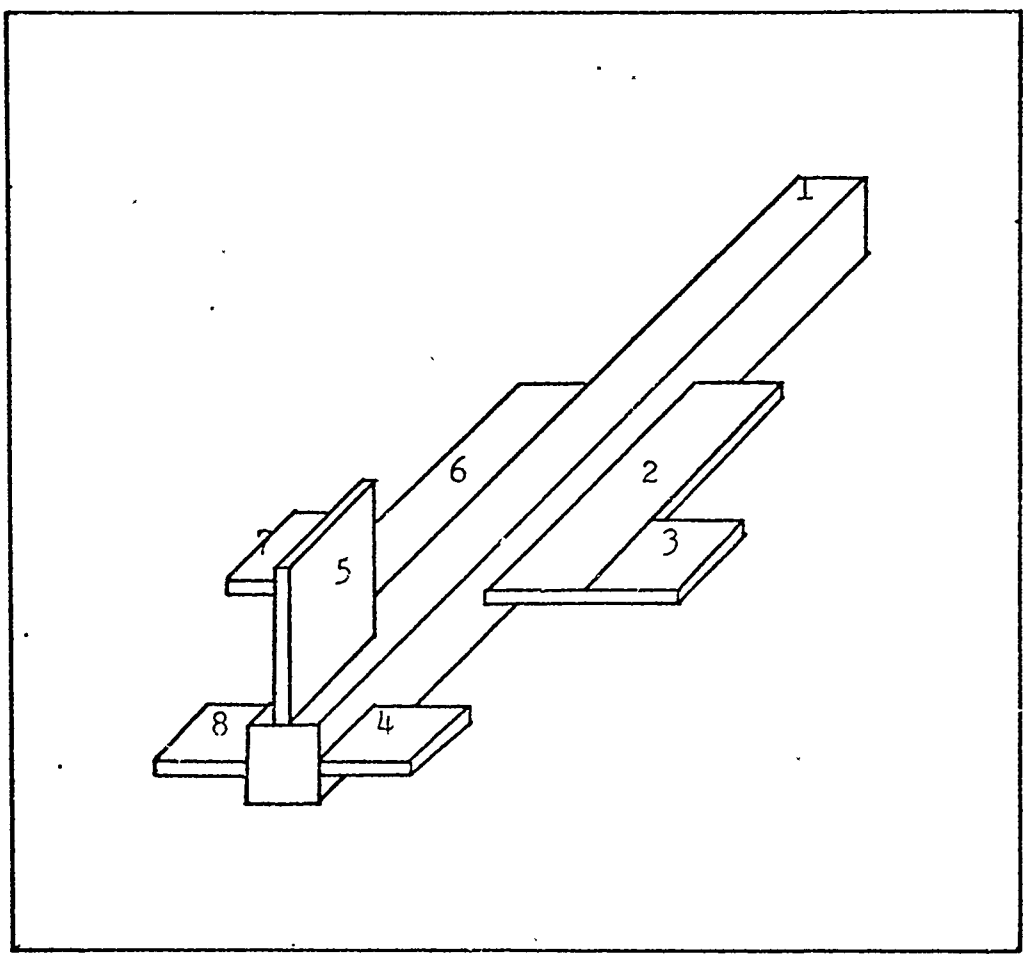


Figure 2 Target Aircraft

Table IV

Numerical Designator and Dimensions of Target Parts

| Part Number | Part Description | Dimensions (ft) |
|---|---|---|
| 1 | Fuselage | 40 X 4 X 4 |
| 2 | Right inboard wing section | 15 X 5 X $\frac{1}{2}$ |
| 3 | Right outboard wing section | 5 X 5 X $\frac{1}{2}$ |
| 4 | Right horizontal stabilizer | 4 X 5 X $\frac{1}{2}$ |
| 5 | Vertical stabilizer | 6 X 8 X $\frac{1}{2}$ |
| 6 | Left inboard wing section | same as 2 |
| 7 | Left outboard wing section | same as 3 |
| 8 | Left horizontal stabilizer | same as 4 |

Vulnerable Area of Target

The vulnerable target is shown in Figure 3 and its vulnerable areas to gun one and gun two are presented in Table V. Only the fuselage is vulnerable to a single detonating round from gun one, and just the fuselage and vertical stabilizer to gun two. The vulnerable areas are specified as functions of aspect angle in azimuth and elevation.

The vulnerable area of the target is based on the criteria of an A-type kill, which is defined to be at least enough damage to cause the aircraft to be uncontrollable within five minutes. The reason the other target parts are given zero vulnerable area is that only singly vulnerable components are considered.

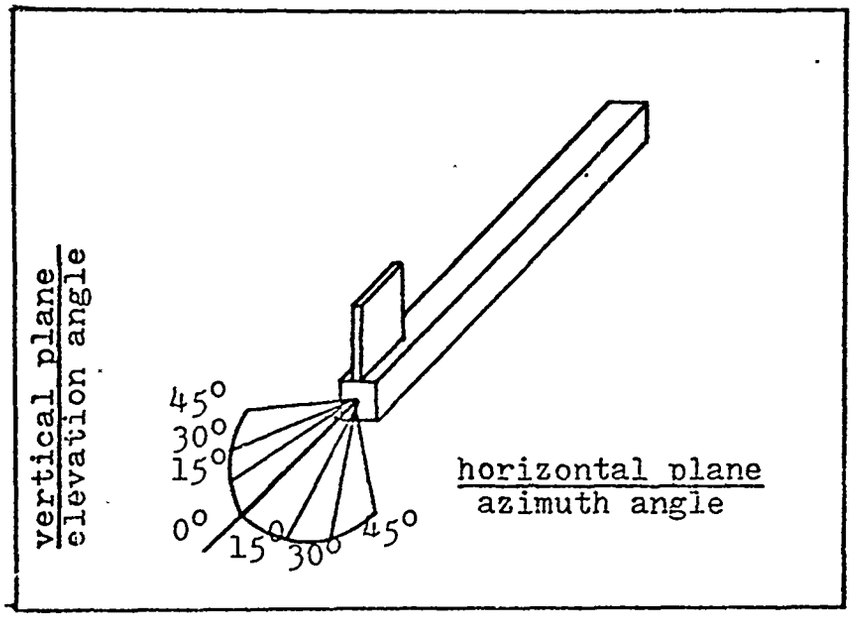


Figure 3 Vulnerable Target

Table V

Vulnerable Area of Target to
Single Detonating Projectile

| Aspect Angle | Gun 1 | Gun 2 | |
|---|---|---|---|
| Elevation (deg) | Fuselage ($ft^2$) | Fuselage ($ft^2$) | Vert. Tail ($ft^2$) |
| 0 | 1.5 | 6.3 | - |
| 15 | 7.3 | 36.3 | - |
| 30 | 21.3 | 62.6 | .1 |
| 45 | 23.6 | 70.7 | .4 |
| Azimuth (deg) | | | |
| 0 | 1.5 | 6.3 | - |
| 15 | 3.8 | 24.6 | - |
| 30 | 9.0 | 45.3 | .1 |
| 45 | 11.5 | 56.5 | .1 |

Ballistic Triangle

The general attack situation is shown in Figure 4. The target aircraft and attacking aircraft are assumed to be co-airspeed (1000 feet per second). The position of the attacking aircraft at the time of fire is defined by its line of sight range (R) and angle-off (AO) relative to the target. The total initial projectile velocity (UO) is equal to the muzzle velocity of the gun (VELM) plus the velocity of the attacking aircraft (VI).

The ballistic range to impact (RB) is calculated by an iterative process which uses R, AO, UO, the velocity of the target (VT), and the exponential ballistic drag factor (ALPHA). The average velocity of the projectile (UBAR) over the ballistic range is calculated by using RB, UO, and ALPHA. Details of the iteration and the equation for the average ballistic velocity are shown in the computer program listing for the ballistic triangle subroutine (SUBROUTINE BTRI), which can be found in Appendix E.

The predicted projectile time of flight (TF) is taken as the ballistic range divided by the average velocity of the projectile

$$TF = \frac{RB}{UBAR} \qquad (1)$$

and the predicted lead angle (DELTA) required to hit the target is taken as

$$\text{DELTA} = \arcsin \frac{\text{VT}\cdot\text{TF}\cdot\sin(\text{AO})}{\text{UBAR}\cdot\text{TF}} \qquad (2)$$

where VT·sin (AO) is the component of target velocity perpendicular to the trajectory of the projectile.

The angle at which the projectile impacts the target (LAM) is found from the angular relationship.

$$180\text{-AO} = 180\text{-DELTA-LAM} \qquad (3)$$

The absolute velocity of the projectile at the instant of impact with the target is approximately

$$\text{UP} = \text{UO}\cdot\exp(-\text{ALPHA}\cdot\text{RB}) \qquad (4)$$

and the velocity of the projectile relative to the target is

$$\text{USK} = \text{UP}-\text{VT}\cos(\text{LAM}) \qquad (5)$$

where VT cos(LAM) is the velocity component of the target along the trajectory of the projectile. If USK (the relative impact velocity) is less than 750 feet per second, it is assumed that the round will not detonate upon impact.

The g-loading (GLFI) required for the attacking aircraft to establish the lead angle for target motion (DELTA) is derived by considering what turn radius the constant velocity target must have to give it a turning rate equal to the target's crossing rate.

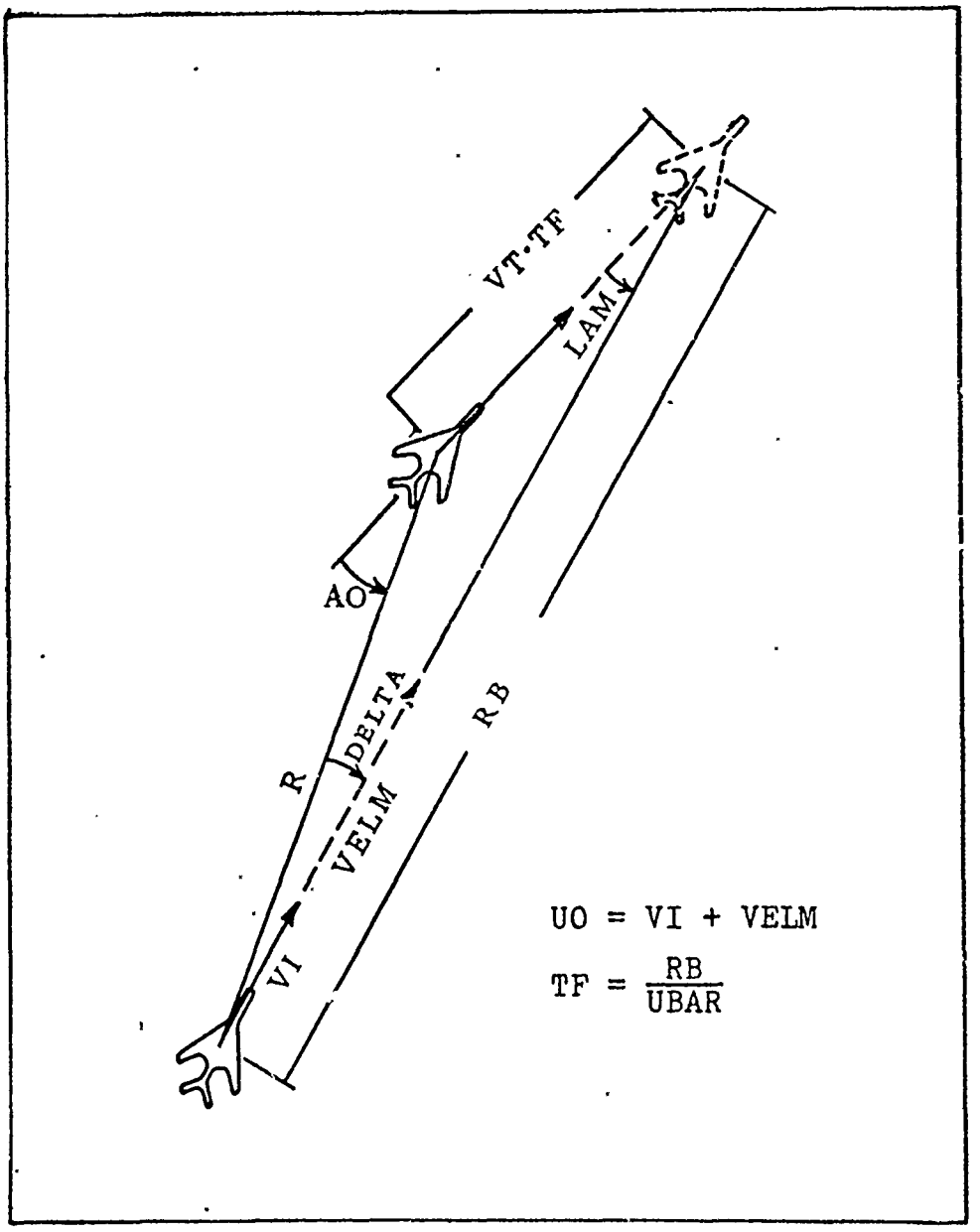


Figure 4 Two-dimensional ballistic triangle showing General Attack Situation

The crossing rate of the target (TCR) at the ballistic range (RB) is

$$TCR = \frac{VT \sin(LAM)}{RB} . \tag{6}$$

The turn radius (r) which gives the attacking aircraft the same angular velocity is

$$r = \frac{VI}{TCR} . \tag{7}$$

The radial acceleration (AI) the attacking aircraft must have to generate the turn radius r is

$$AI = r(TCR)^2 . \tag{8}$$

Substituting for r and TCR from equations (6) and (7) into equation (8), and dividing by 32.2 gives the radial acceleration on the attacking aircraft in terms of g-load factor.

$$AI = \frac{VI \cdot VT \cdot \sin(LAM)}{(32.2)RB} \tag{9}$$

Considering that gravity is acting perpendicular to this radial acceleration, the total g-loading (GLFI) required for the attacking aircraft to establish the predicted lead angle for target motion is

$$GLFI = \left\{ \left[ \frac{VI \cdot VT \cdot \sin(LAM)}{(32.2)RB} \right]^2 + 1^2 \right\}^{\frac{1}{2}} . \tag{10}$$

If GLFI (g-load factor on attacking aircraft) is greater than 5.6 g's, it is assumed that the attacker will snapshoot. If GLFI is less than or equal to 5.6 g's, it is assumed that the attacker will trackshoot.

Target Uncertainty

Target uncertainty is the difference between the predicted position of a target and its actual position due to maneuvering during the flight time of a projectile. Since the orientation of the coordinate system used in this analysis is determined by the initial velocity and orientation of the target aircraft, the location of the non-maneuvering target will always be at the origin of the coordinate system. A target which maneuvers will be displaced from the origin.

The longitudinal displacement (X direction) of a maneuvering aircraft is considered to be negligible in the analysis. The target is assumed to have a constant forward velocity and the shorter distance travelled in the X direction due to curvature in the flight is very small because of the short time of flight. The lateral displacement (YDIS) and the vertical displacement (ZDIS) are found by resolving the instantaneous radial acceleration of the target into its lateral and vertical components. The

derivation of the equations used in determining the displacement of a maneuvering target can be found in Appendix B.

The instantaneous radial acceleration (RA) is given by

$$RA = 32.2 \left[GLF - \cos(PHI)\cos(GAMMA)\right] \qquad (11)$$

where, GLF is the g-loading read by the pilot, PHI is the aircraft bank angle, and GAMMA its pitch attitude. By specifying the initial g-load factor (IGLF), bank angle (IPHI), and flight path angle (IGAMMA), and also the roll rate (PHIDOT) and g-loading rate (GLFDOT), the radial acceleration at any later time can be found.

The radial acceleration for a non-maneuvering aircraft is zero. The radial acceleration for an aircraft performing any of the three defensive maneuvers used in this study is continually changing in both magnitude and direction.

The displacement of a maneuvering target and the change in its orientation during the flight time of a projectile are found by dividing the time of flight (TF) into 100 time increments (DELTF). By considering the radial acceleration to be constant over each increment, but also allowing it to take on a new value at the end of each increment, the actual displacement of the target and change in its orientation can be closely approximated by summing over all the time intervals.

Using the time of flight, which is given by equation (1), and the initial target flight conditions shown in Table VI, the target uncertainty subroutine calculates YDIS, ZDIS, and PRESGAM, the change in the target's pitch attitude during the flight time of the projectile.

Table VI

The Initial Conditions of the Target Maneuvers

| Maneuver | IGLF (g's) | IPHI (deg) | IGAMMA (deg) | PHIDOT (deg/sec) | GLFDOT (g's/sec) |
|---|---|---|---|---|---|
| Non-Maneuvering | 1.0 | 0 | 0 | 0 | 0 |
| Negative-g Jink | 1.0 | 0 | 0 | 0 | -2 |
| Hard Turn | 1.0 | 0 | 0 | 45 | +4 |
| Break | 1.0 | 0 | 0 | 90 | +6 |

The initial value of the g-loading (GLFDOT) is maintained until the g-load (GLF) is a positive 7.0 g's or negative 3.0 g's, which approximate the maximum permissible operating limits on fighter aircraft.

The flight path for the target maneuvers used in this analysis and the displacement of the target for a flight time of 1.25 seconds is shown in Figure 5.

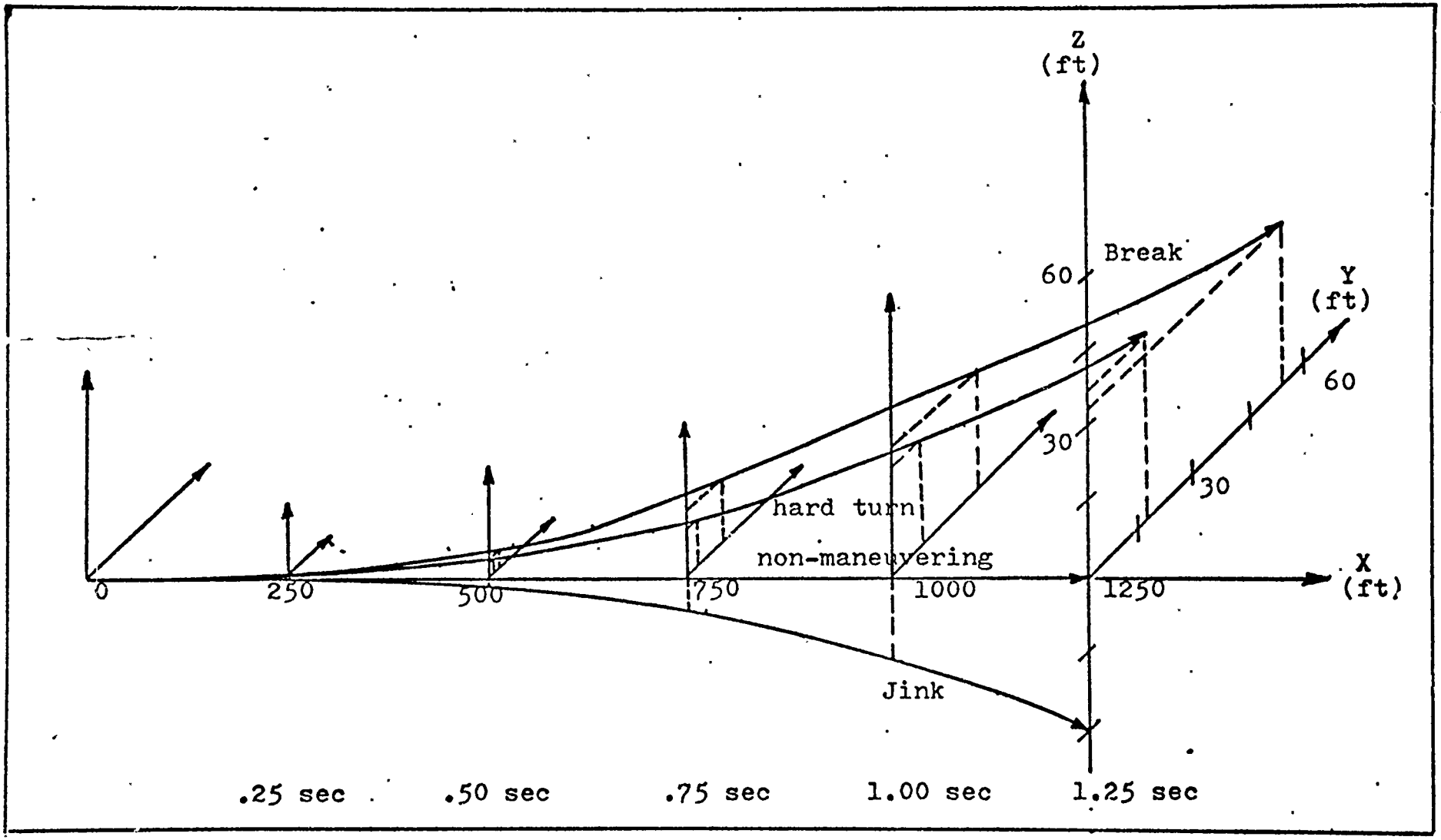


Figure 5 Flight Path of Defensive Maneuvers

Target Parts

The total hits on the target are calculated by considering the hits on each of the eight parts separately. The coordinates of the center of each part are specified in both width and length from the center of the target aircraft. The part area presented to the projectiles is determined by LAM (the predicted impact angle) for a non-maneuvering target, and by LAM plus PRESGAM (the change in flight path angle) for a maneuvering target. Only the half width and half length of the presented cross sectional part area are used in the calculations, because of the symmetric fire pattern used in the analysis.

The program listing of the target part subroutine (SUBROUTINE TGTPTS) can be found in Appendix E.

Fire Pattern

A method to precisely describe the fire pattern produced in air-to-air gunnery has yet to be developed. In air-to-ground gunnery, the location of the impact points from the aiming point can be scrutinized. While in air-to-air gunnery, only the hits on a small recoverable target can be studied. This inability to experimentally verify the air-to-air fire pattern makes the practice of assuming there is similarity between a fire pattern relative to a moving spatial target and a fire pattern relative to a fixed ground target somewhat questionable.

The significant difference between air-to-air gunnery and air-to-ground gunnery is target motion. The g-loading on an aircraft attacking a ground target is less than one-half g, even if the target is moving. In air-to-air gunnery, the g-loading is often four to six g's when the gun is fired. The result is large aiming errors and an uncertain distribution of projectiles in the fire pattern.

In air-to-ground gunnery, the aircraft's wings are level when the gun is fired. In air-to-air gunnery, although the roll attitude of the attacking aircraft and target are approximately matched at the time of fire, the target is generally rolling during the firing burst and flight time of the projectiles, and so it is impossible, in general, to predict the roll attitude of the target at the time of impact for each of the projectiles. That is, during a one second burst and a one second projectile time of flight, the roll attitude of a target aircraft can easily change 90 degrees. Thus, the cross sectional area of the target presented to the first projectile in a firing burst can vary significantly from the cross sectional area presented to the last projectile in the burst.

Rather than simulating a fire pattern that might be produced on a particular firing pass, a fire pattern which represents the average of many one second bursts is generated in the model.

Air-to-ground fire patterns are normally described by aim error and ballistic dispersion. Ballistic dispersion is used to describe the size of the impact pattern and aim error is used to locate the center of the impact points from the target. In air-to-air gunnery, the aim error is more dynamic than in air-to-ground gunnery and is a locus of the center of the aiming points. In this study, the aim error is divided into two categories, the tracking error due to the pilot and the system error of the sight.

Tracking Error. The tracking error is due to the pilot's inability to superimpose the sight pipper on the target. In the model, this error is described by generating a standard deviation in aim wander (TKSIG). In the unmodified model, the following relationship was used.

$$TKSIG = (.00375)R \qquad (12)$$

Where, R is the line of sight range in feet and TKSIG is the standard deviation in mils. It was felt that TKSIG should not be a function of range alone, but also a function of the angle-off. As the g-load factor required to establish lead for target motion is a function of line of sight range and angle-off, the following relationship from the GUN-Val studies is used (Ref 2).

$$TKSIG = \frac{TSIGMIN}{1 - \left(\frac{GLFI}{GLFMAX}\right)^2} \tag{13}$$

TSIGMIN is the minimum standard deviation in tracking error. A TSIGMIN of five mils is used for trackshooting.

GLFI is the g-loading required for the attacking aircraft to establish lead for target motion.

GLFMAX is the maximum permissible operating g-load on the attacking aircraft. GLFMAX is 7.0 g's in this study.

The tracking error is greater for snapshooting than for trackshooting. At 5.6 g's, equation (13) gives a TKSIG of 13.9 mils. For snapshoot fire, a minimum value of 15.0 mils is assumed.

The value of TKSIG for snapshooting is generated in the model by taking the difference between the target's crossing rate and the lead capability of the attacking aircraft at 5.6 g's,

$$TLC = (AMLC - TCR)TF \tag{14}$$

where, the target's crossing rate (TCR) is given by

$$TCR = \frac{VT \cdot \sin(LAM)}{RB} \tag{15}$$

and the attacker's max lead capability (AMLC) by

$$AMLC = \frac{(5.6)(32.2)}{VI} \tag{16}$$

Assuming a uniform distribution for tracking error in snapshooting, the standard deviation in mils for one second of fire is

$$TKSIG = \frac{.5773}{2} ABS(TLC) \qquad (17)$$

where ABS(TLC) is the absolute value of the tracking lead capability of the attacking aircraft and the coefficient is the probability for one standard deviation of a uniform distribution. The value of TKSIG used for snapshooting is given by equation (17) or 15 mils, whichever is greater.

Length of Fire Line. The length of the fire line is three standard deviations times the range RB. The location of each fire point from the center of aim is determined by TKSIG according to the following relationship.

$$YL = \frac{3}{50} (IDP-.5) TKSIG \cdot RB \cdot IPOL \qquad (18)$$

IPOL produces fire pattern symmetry taking on the values of plus or minus one.

IDP is the round number which takes on integer numbers from 1 to 50. The midpoint between rounds is used in the calculations.

TKSIG is the standard deviation for aiming.

RB is the ballistic range.

The coefficient is due to the fire line being three standard deviations long and consisting of 50 fire points.

The probable number of rounds (PNR) at each fire point is given by

$$PNR = PY(IDP) \cdot FR \cdot DOB \qquad (19)$$

PY(IDP) is the frequency distribution for each round as shown in Figure 6.

FR is the firing rate of the gun and DOB is the duration of burst, which are 100 rounds per second and one second, respectively.

Fire Point Density. A normal distribution of fire points along the fire line is approximated by grouping the frequency distribution of fire points into sets of 10 rounds. The frequency distribution of fire points for one-half of the symmetric fire line is shown in Figure 6.

Size of Fire Pattern. By definition, ballistic dispersion is the diameter of a circle which encompasses 80 percent of the projectile impacts. Laboratory test firings on rigidly mounted, rapid firing cannons show a circular distribution of impact points. A similar distribution of slightly greater diameter results when the same cannon is mounted on an aircraft and fired with the aircraft on jacks (Ref 8 ). It is assumed that circular ballistic dispersion

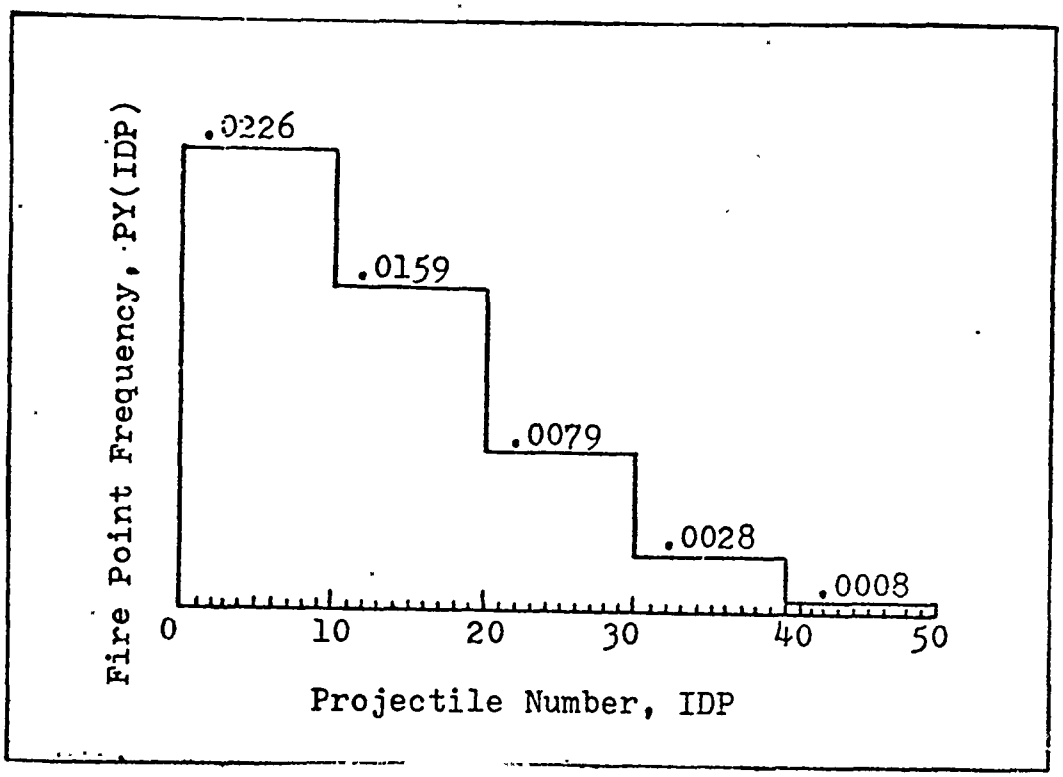


Figure 6 Frequency Distribution of Fire Points along Fire Line

can be approximated by a circular normal distribution. The standard deviation of a normal distribution contains approximately 67 percent of the projectile impact points. In this analysis, then the relationship between a standard deviation in ballistic dispersion (SIGB) and the diameter of the 80 percent circle (BD) defined to be ballistic dispersion is

$$BD = 1.825SIGB \tag{20}$$

Germond calculated that 98.89 percent of the impacts are within three standard deviations for the integrated

Table VII

Projectile Flight Time and Attacker g-loading for Various Flight Conditions

| Firing Conditions | | Gun 1 | | Gun 2 | |
|---|---|---|---|---|---|
| Angle-off (deg) | Range (ft) | TF (sec) | GLF (g's) | TF (sec) | GLF (g's) |
| 0° | 500 | .164 | 1.0 | .129 | 1.0 |
| | 1000 | .357 | 1.0 | .266 | 1.0 |
| | 1500 | .585 | 1.0 | .413 | 1.0 |
| | 2000 | .856 | 1.0 | .569 | 1.0 |
| | 2500 | 1.182 | 1.0 | .736 | 1.0 |
| | 3000 | 1.582 | 1.0 | .913 | 1.0 |
| 15° | 500 | .163 | 9.3[a,b] | .128 | 10.3[a,b] |
| | 1000 | .353 | 4.6 | .264 | 5.2 |
| | 1500 | .577 | 3.0 | .410 | 3.5 |
| | 2000 | .834 | 2.3 | .564 | 2.7 |
| | 2500 | 1.163 | 1.8 | .729 | 2.2 |
| | 3000 | 1.552 | 1.5 | .904 | 1.9 |
| 30° | 500 | .158 | 18.8[a,b] | .125 | 20.8[a,b] |
| | 1000 | .342 | 9.1[a,b] | .259 | 10.3[a,b] |
| | 1500 | .558 | 5.9[b] | .400 | 6.8[b] |
| | 2000 | .810 | 4.3 | .550 | 5.1 |
| | 2500 | 1.108 | 3.3 | .710 | 4.1 |
| | 3000 | 1.466 | 2.7 | .880 | 3.4 |
| 45° | 500 | .152 | 28.9[a,b] | .121 | 31.3[a,b] |
| | 1000 | .326 | 14.0[a,b] | .250 | 15.5[a,b] |
| | 1500 | .527 | 9.1[a,b] | .385 | 10.3[a,b] |
| | 2000 | .760 | 6.6[b] | .529 | 7.7[a,b] |
| | 2500 | 1.030 | 5.1 | .681 | 6.1[b] |
| | 3000 | 1.346 | 4.1 | .842 | 5.1 |

[a]Exceeds aircraft operating limitations

[b]Snapshoot

gaussian distribution (Ref 3). A ballistic dispersion of three SIGB is used in the mathematical model. As shown in Figure 7, the ballistic fire pattern is represented by making a square approximation to a circular distribution and using two uniform distributions to generate 80 percent of the impacts within one standard deviation (SIGB). Further explanation of the square and uniform approximations can be found in Appendix A.

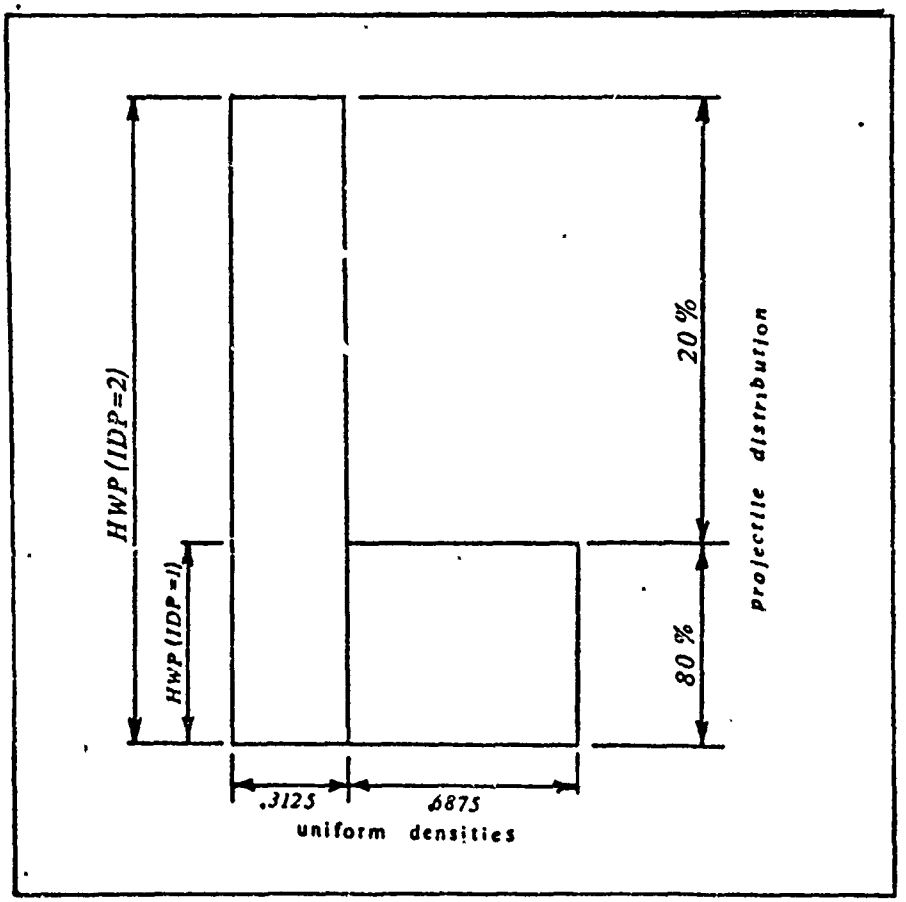


Figure 7 Ballistic Dispersion

The half width of the fire pattern (HWP) is greater for snapshooting than it is for trackshooting. The relationship between SIGB and HWP is given by equations (30) and (31) from Appendix A.

The amount of target coverage and the probability that a given projectile hits the target is calculated in the mathematical model by weighting each projectile for ballistic dispersion. That is, 80 percent of each round is considered to be within one SIGB and 20 percent is considered to be in the area between one and three SIGB.

By treating each round separately, an approximation to an elliptical normal distribution, with the major axis along the fire line, is achieved as each of the 100 fire points is considered.

Center of Fire Pattern. The center of the fire pattern is located with respect to the origin of the moving coordinate reference system. An offset distribution is generated in the width direction and a firing time delay distribution in the length direction. Width and length are defined with respect to the fire line direction and the fire line direction of draw is defined with respect to the target's fuselage reference line (FRL).

The distribution in offset (KOS) and fire timing delay (FTD) models pilot technique. There are three pilot

techniques for establishing lead angle for target motion. The one preferred by most is lag pursuit. The pilot lags the target with the gunsight as he makes the attack. He attempts to stabilize the gunsight just short of the target to allow the sight to settle. As the sight is settling, the pilot squeezes the trigger and increases his g-loading to pull the fire pattern through the target.

A second technique is the lead pursuit. The pilot attempts to stabilize the sight in front of the target. Then ever so slightly (while sustaining three to six g's) he eases off the g-loading and squeezes the trigger, so that the fire pattern goes through the target. The third technique is to stabilize the sight on the target and fire when it is superimposed and settled. These three tracking techniques should not be confused with snapshooting where the pilot always establishes a large lead angle and shoots the gun so that the target flies into the fire pattern.

As can be imagined, the location of the center of the fire pattern is impossible to locate. It is found that pilots have greater difficulty in locating the pattern in the forward-aft direction with respect to the target than in the vertical. This is due to the forward motion of the target. The forward-aft error of the fire pattern is called lateral error and the above-below error with respect to the target is vertical error. In the mathematical model these

errors are defined with respect to the fire line, where length is along the fire line and width is perpendicular to it. The fire line draw direction is defined with respect to the target's fuselage reference line (FRL) and gives an equal likelihood of being along the fuselage or perpendicular to it. Thus, offset and fire time delay can be either perpendicular or parallel to the target's FRL.

In the mathematical model, error in the length direction is generated by assuming that the pilot has an equal likelihood of being early, on time, or late in squeezing the trigger. Early and late timing are given a distance equivalent to an error in timing of approximately .2 seconds for trackshooting and approximately .3 seconds for snapshooting according to the following equation for firing time delay (FTD),

$$FTD = TKSIG \cdot RB(IFT-2) \qquad (21)$$

where IFT takes on values of one, two, and three for early, perfect, and late.

Error in the width direction is generated by selecting offsets in the width direction of -18, -12, -6, 0, 6, 12, 18 mils, which are converted to feet by the following equation for fire line offset (FLOS),

$$FLOS = (.001)KOS \cdot RB \tag{22}$$

where KOS takes on the above values.

The location of the center of the fire pattern with respect to the origin of the coordinate system is at FTD and FLOS, which take on 21 combinations of values for each one second firing burst. For calculating kill probability it is assumed that FTD has a uniform distribution and that FLOS has a normal distribution about zero.

Target Coverage

In the model, the origin of the coordinate system moves at constant velocity along the flight path the target would follow in constant airspeed, constant altitude non-maneuvering flight. Target coverage is determined by taking the difference between the displacement of each projectile and the target part. The number of hits is estimated by the amount the fire pattern overlaps the presented area of the target part and the projectile density.

The distance between the center of the part and a projectile is given for the width direction by

$$OS = ABS\left[FLOS - COT(I,L) - YDIS\right] \tag{23}$$

and in the length direction by

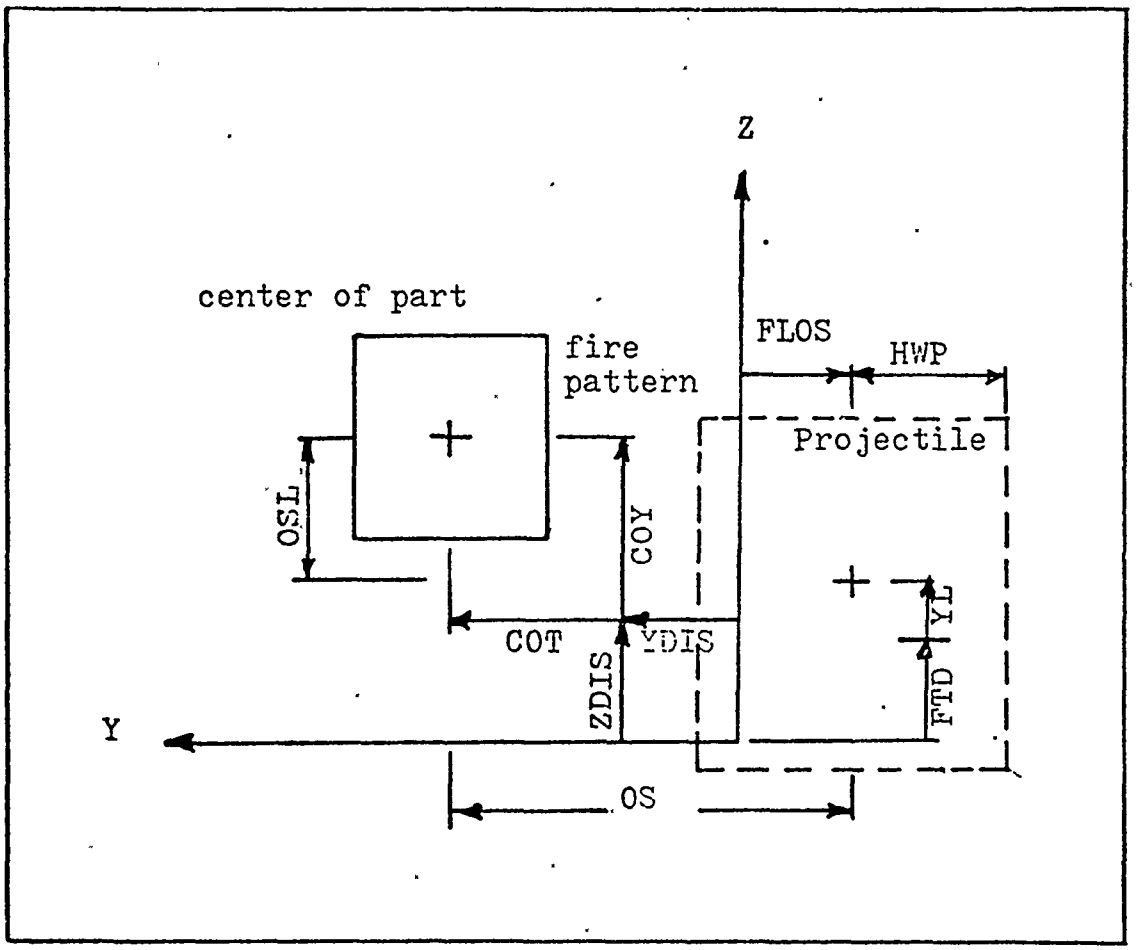


Figure 8 Coverage of Target Part

$$OSL = ABS\ [YL + FTD - COY(I,L) - ZDIS] \ . \qquad (24)$$

FLOS, the fire line offset, is given by equation (22).

FTD, the firing time delay, is given by equation (21).

YL, the location of the projectile along the fire line, is given by equation (18).

YDIS and ZDIS, the displacement of the target during the flight time of the projectile, are given by equations (38) and (39).

COT(K,L) and COY(K,L) specify the location of the center of the part from the center of the target, where I is the part number and L is the orientation of the fire line with respect to the target's fuselage reference line (FRL).

The coverage of each target part is determined from the amount of overlap between its presented area and the size of the fire pattern (HWP). A more detailed explanation of target coverage can be found in Appendix A.

Kill Probability

The kill probability is calculated from the total number of lethal hits on the target (TNLH) according to the following approximation for CUHIT| independent attacks, each with a single-shot kill probability of SSL (Ref 3 ).

$$PKOL = 1 - \exp(-TNLH) \qquad (25)$$

TNLH, the total number of lethal hits, is equal to the product of CUHIT (the total number of hits) times SSL (the single-shot kill probability). The probability of a single-shot kill is the vulnerable area of a part (AVP) divided by the presented area of the part (PAREA), provided the part is hit.

$$SSL = \frac{AVP}{PAREA} \tag{26}$$

CUHIT is the sum of the hits on all parts and is calculated by the target coverage subroutine. An explanation how CUHIT is calculated can be found in Appendix A under target coverage.

Four PKOLS are calculated for each firing burst and the average of the four (APKD) is taken as the value of kill probability for each of the 21 combinations of seven fire line offsets and three firing time delays. The four PKOLS result from the orientation of the fire line with respect to the target's FRL; that is, whether the fire line or direction of draw is parallel or perpendicular to the FRL. Both are considered equally likely. Since the vulnerable area is given as a function of the aspect angle in the horizontal and vertical planes, each direction of draw is broken into a horizontal and vertical component. A more detailed explanation of the four equally likely draws can be found in Appendix A.

To summarize the last two sections, the model calculated 84 kill probabilities for each firing burst (four draws, three fire timing delays, and seven offsets). For a given burst of one second duration, only a portion of the 84 combinations produce lethal hits depending upon the ballistic dispersion, angle-off, and line of sight range to the target at the time of fire.

A weighted average kill probability is calculated for each combination of gun, ballistic dispersion, angle-off, and range. The four draws are weighted equal as are the three fire timing delays (early, perfect, late). The offsets of the fire line are weighted by the following approximation to a normal distribution. An offset of minus six to plus six mils is considered to occur 70 percent of the time. This corresponds to one standard deviation in aiming bias at the middle of the firing burst. For a non-maneuvering, air- to-air target, Captain Dick Hackford calculated the standard deviation in aiming bias to be 5 mils (Ref 4 ). The other weighting factors for offset are 20% for 6 to 12 mils, and 10% for 12 to 18 mils. It is considered a pilot will not fire if he estimates that the offset will be greater than 18 mils.

## IV. Results

The effect of target uncertainty on kill probability in air-to-air gunnery is shown by comparing the kill probability for a specified non-maneuvering target with the kill probability for an average maneuvering target. The average maneuvering target is defined only in terms of kill probability. It is the average of the kill probabilities for the specified target making a negative-g jink, hard turn, or break.

Kill probabilities were calculated for the two dissimilar, but representative, rapid firing cannons for various ballistic dispersions. The firing conditions were parametrically varied in both range and angle-off. Line of sight range was varied from 500 feet to 3000 feet in increments of 500 feet, and initial angle-off was varied from zero degrees to 45 degrees in increments of 15 degrees.

Both tracking fire and snapshoot firing are included in the calculated kill probabilities. Tracking fire is assumed if the attacking aircraft can establish lead for target motion while sustaining 5.6 g's or less. If more than 5.6 g's are required to track the target, snapshoot firing is assumed. The approximate regions for trackshooting and snapshooting are shown in Figure 8. The projectile

flight time and the attacker's g-loading for various attack parameters are shown in Table VII.

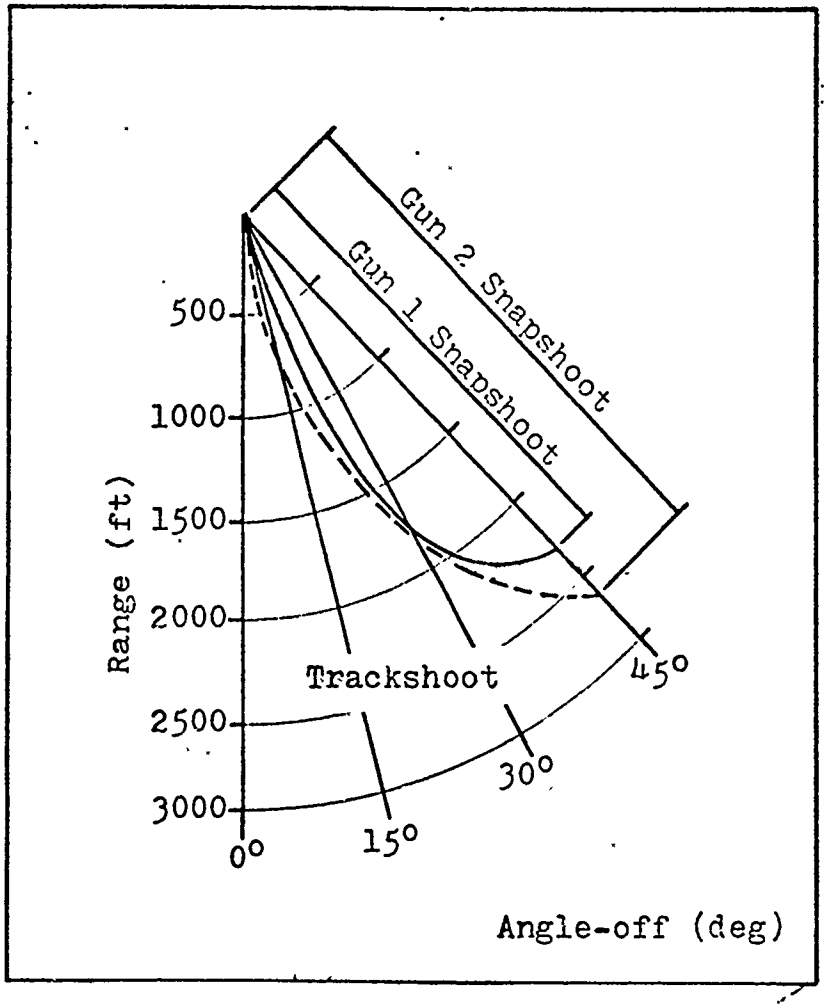


Figure 9 Approximate Regions for Trackshoot and Snapshoot Aiming.

The results of the analysis are presented by grouping the data into four sets of graphs. The first set shows the decrease in kill probability due to target maneuvering during the flight time of the projectile. The second set shows the

effect of ballistic dispersion on kill probability. The relative effectiveness of the three defensive maneuvers in decreasing kill probability is shown in the third set, and the best attack parameters in the fourth.

The kill probabilities from which the graphs were constructed can be found in Appendix C. No attempt was made to verify the degree of accuracy or realism of the calculated values. The probabilities were calculated to three significant digits. It is not claimed they are that accurate or to, perhaps, even one significant digit.

The intent was to establish a baseline of kill probabilities for a specified non-maneuvering target and then find the deviations from that baseline caused by target maneuvering. Perhaps the greatest source of inaccuracy in the model is the use of vulnerable area, which does not account for cumulative damage of multiple hits and which considers only damage to singly vulnerable components. The model calculates both the total hits and total number of lethal hits; however, they were not used to measure the effect of target maneuvering, because it is felt they can be more misleading than kill probability. The second most important item to keep in mind when using the results is that they are calculated for a one second firing burst.

A plot of kill probability versus the total number of lethal hits is shown in Figure 10. The probability of kill for a particular draw and a particular set of firing conditions was often higher than .9. However, as the weighted averaging is applied, the kill probability decreases substantially.

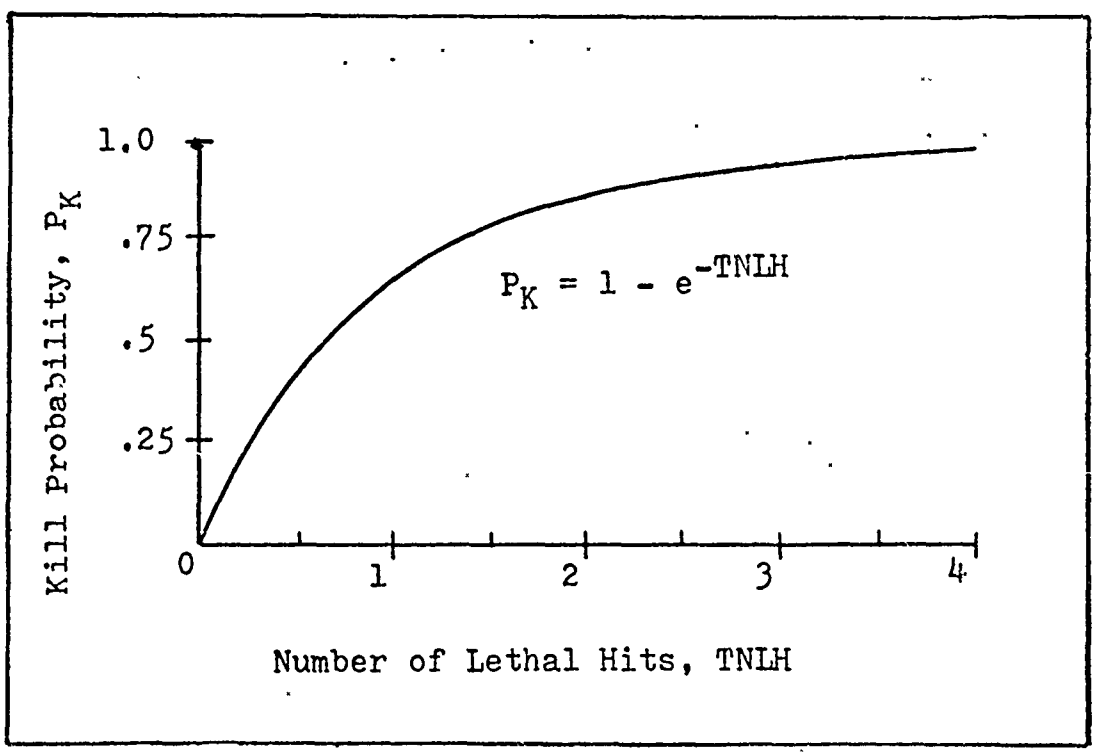


Figure 10 Kill Probability versus Total Number of Lethal Hits.

From an engineering design point of view, the results show the relative lethality of two dissimilar rapid firing cannons for various ballistic dispersions. From a pilot's point of view, Figures 16 and 17 quantize the relative effectiveness of defensive maneuvers. Figures 18 and 19 show the line of sight range that a pilot should try to achieve when shooting at an aircraft from various angles-off.

Decrease in Kill Probability

Table VIII shows the percentage decrease in kill probability due to target maneuvering during projectile flight time. The values for the percentage decrease have a five percent round off.

It is noted that target maneuvering causes a much higher decrease in kill probability for gun one than for gun two. The primary reasons are the higher muzzle velocity of gun two and higher ballistic coefficient, which results in the projectile having a short flight time.

The effectiveness of gun one decreases markedly beyond ranges of 2000 feet, which corresponds to a flight time of approximately .8 seconds as shown by Table VII. Gun two's

effectiveness against a maneuvering target starts a marked decrease at a range of 3000 feet, which corresponds to a flight time of approximately .875 seconds.

In Table VIII no preferred ballistic dispersion is noticeable for gun one. Gun two shows an increase in kill probability due to target uncertainty at ranges of 2000 feet and 2500 feet for a SIGB of 6 mils.

Figures 10, 11, 12, and 13 show kill probability for the non-maneuvering and average maneuvering target. Each figure shows the kill probability for a particular SIGB (standard deviation in ballistic dispersion) and the BD equivalent (diameter of circle containing 80 percent of rounds).

The graphs were constructed by averaging the kill probabilities of the four angles-off considered in the study ($0^{o}$, $15^{o}$, $30^{o}$, $45^{o}$). Each angle-off was weighted equally in calculating the average. The kill probabilities as a function of angle-off can be found in Appendix C.

The results in Appendix C show how dependent the value of kill probability is on angle-off. One is tempted to not consider 30 degrees and 45 degrees in combining kill probability, since pilots try to avoid having to fire with high angle-off. However, there is evidence to suggest that in combat these angles-off occur

Figure 11 shows the kill probability for an 80 percent ballistic dispersion (BD) of approximately 3.6 mils diameter. The greater lethality of gun two is clearly displayed. Whereas percentage decrease in kill probability, Table VIII, shows the effect of differences in muzzle velocity and ballistic drag coefficient between the two guns, Figure 11 shows the effect of the target having a greater vulnerability to gun two than to gun one. This vast difference in lethality between the guns is the primary reason that the total number of hits was not used to measure the effect of target uncertainty in air-to-air gunnery. At ranges of 1000 feet and less both guns produce an equal number of hits on the target.

By comparing Figure 11 with Figure 12, the importance of ballistic dispersion on the effectiveness of air-to-air cannons is seen. At 1200 feet, Gun one with 7.3 mils ballistic dispersion shows a 50 percent higher kill probability against a non-maneuvering target and 40 percent higher kill probability against an average maneuvering target than it does for 3.6 mils dispersion. Gun two shows a greater percentage decrease for target uncertainty at BD = 7.3 mils than for BD = 3.6 mils; however, the kill probability remains

Figure 11 shows the kill probability for an 80 percent ballistic dispersion (BD) of approximately 3.6 mils diameter. The greater lethality of gun two is clearly displayed. Whereas percentage decrease in kill probability, Table VIII, shows the effect of differences in muzzle velocity and ballistic drag coefficient between the two guns, Figure 11 shows the effect of the target having a greater vulnerability to gun two than to gun one. This vast difference in lethality between the guns is the primary reason that the total number of hits was not used to measure the effect of target uncertainty in air-to-air gunnery. At ranges of 1000 feet and less both guns produce an equal number of hits on the target.

By comparing Figure 11 with Figure 12, the importance of ballistic dispersion on the effectiveness of air-to-air cannons is seen. At 1200 feet, Gun one with 7.3 mils ballistic dispersion shows a 50 percent higher kill probability against a non-maneuvering target and 40 percent higher kill probability against an average maneuvering target than it does for 3.6 mils dispersion. Gun two shows a greater percentage decrease for target uncertainty at BD = 7.3 mils than for BD = 3.6 mils; however, the kill probability remains

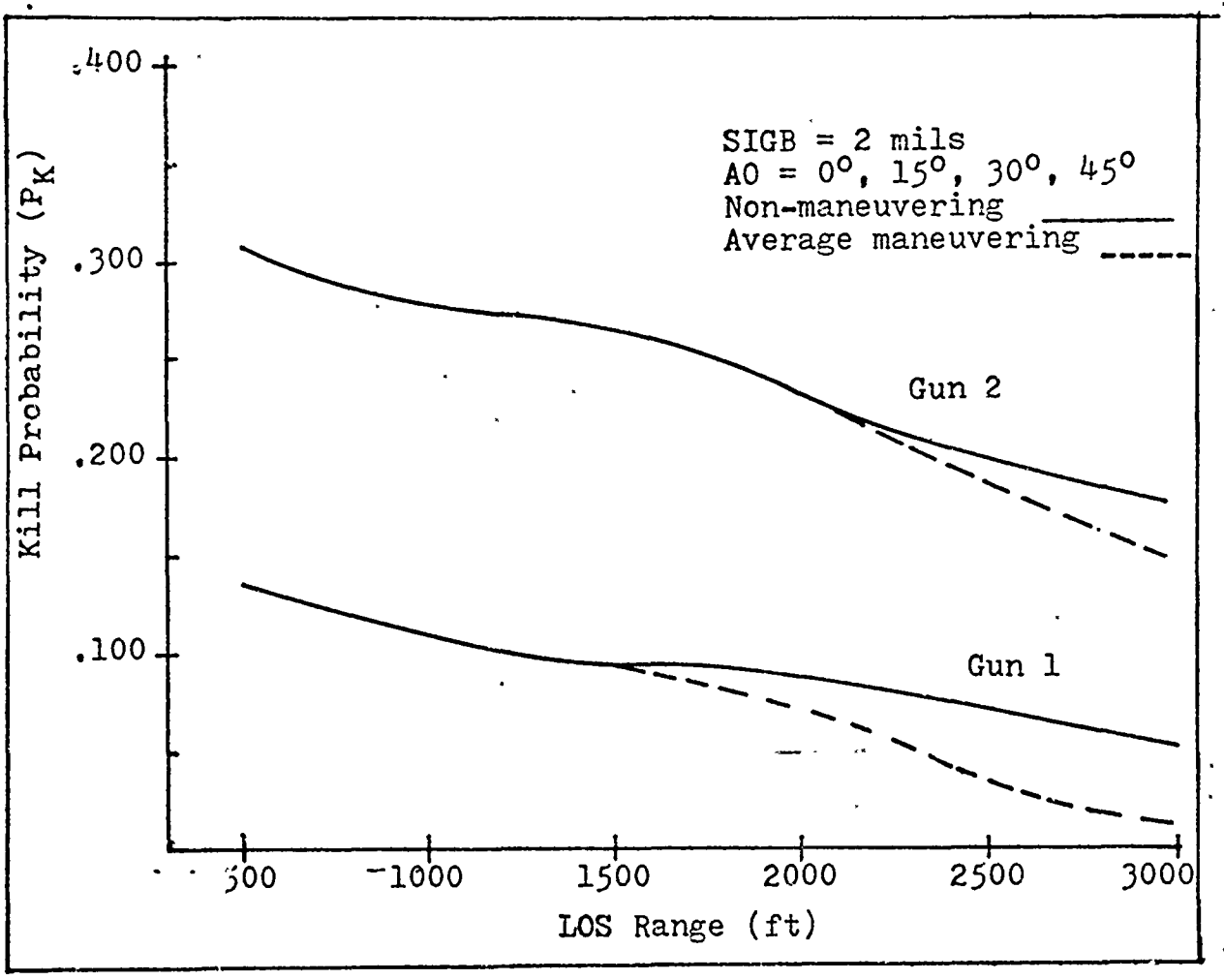


Figure 11 Kill Probability for Non-Maneuvering and Average Maneuvering Target. BD = 3.6 mils.

higher at all ranges for the larger dispersion.

A further effect of ballistic dispersion can be seen by comparing Figure 13 with Figure 12. The smaller dispersion of Figure 12 (BD = 7.3 mils) shows a higher kill probability against a non-maneuvering target. However, the kill probability for an average maneuvering target is approximately the same for both dispersions. At certain ranges the larger dispersion, Figure 13 (BD = 10.9 mils), shows a greater kill probability for an average maneuvering target than for a non-maneuvering target. This anomaly results from the increase in presented area as the target maneuvers, but has yet to escape the central or high density portion of the fire pattern.

Comparing Figure 14 (BD = 14.5 mils) with Figure 13 (BD = 10.9 mils), it can be seen that any additional increase in ballistic dispersion will cause the kill probability to decrease. Except for very short ranges, the results for BD = 10.9 mils are higher than for BE = 14.5 mils for both guns and both the average maneuvering and non-maneuvering target.

If Figure 14 (BD = 14.5 mils) is compared with Figure 11 (BD = 3.6 mils) the effectiveness of large dispersions at short ranges can be seen. It should also be noted that at long gun ranges a smaller dispersion produces a higher kill

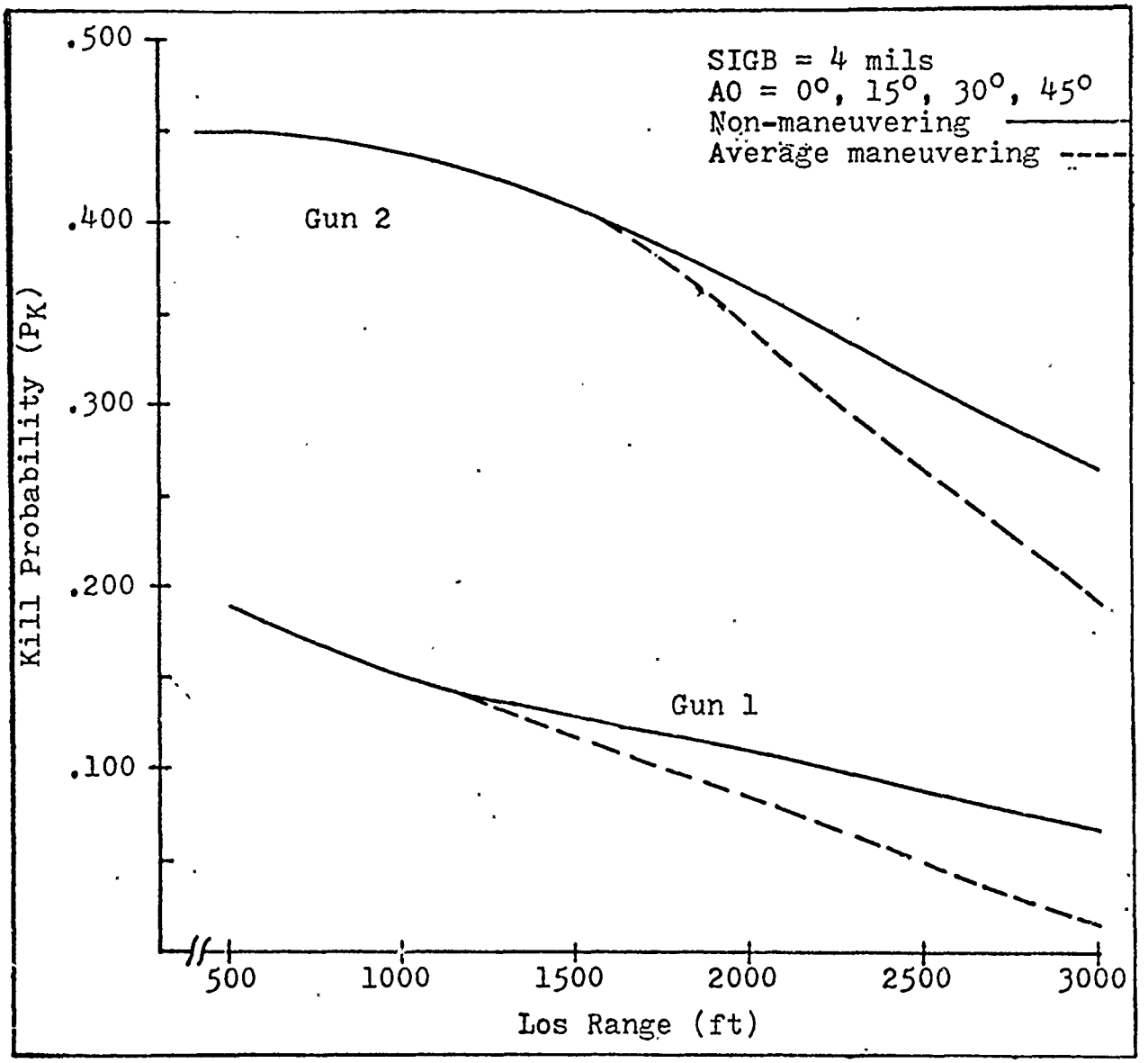


Figure 12 Kill Probability for Non-Maneuvering and Average Maneuvering Target. BD = 7.3 mils.

probability against a non-maneuvering target than a large dispersion does. This is more obvious if one compares the results for SIGB = 2 mils and SIGB = 8 mils for gun one against a non-maneuvering target, which can be found in Appendix C. Both dispersions show a low kill probability at long ranges; however, the kill probability they do have is due to different factors. The small dispersion creates an aiming problem and the large dispersion creates a projectile density problem against a non-maneuvering target. This can be verified by comparing the results for the break maneuvering target. The larger dispersion has a greater kill probability for a maneuvering target, which is the reverse of the results for the non-maneuvering target. These points suggest that (1) the ballistic dispersion should be optimized for the range at which the gun is most likely to be used, and (2) the optimum ballistic dispersion is dependent upon the sight system and pilot proficiency at aiming the gun with it.

A further look at Figure 14 shows that at long gun ranges (greater than 2000 feet where projectile flight time is on the order of one second) a maneuvering target decreases the kill probability even for large ballistic dispersions.

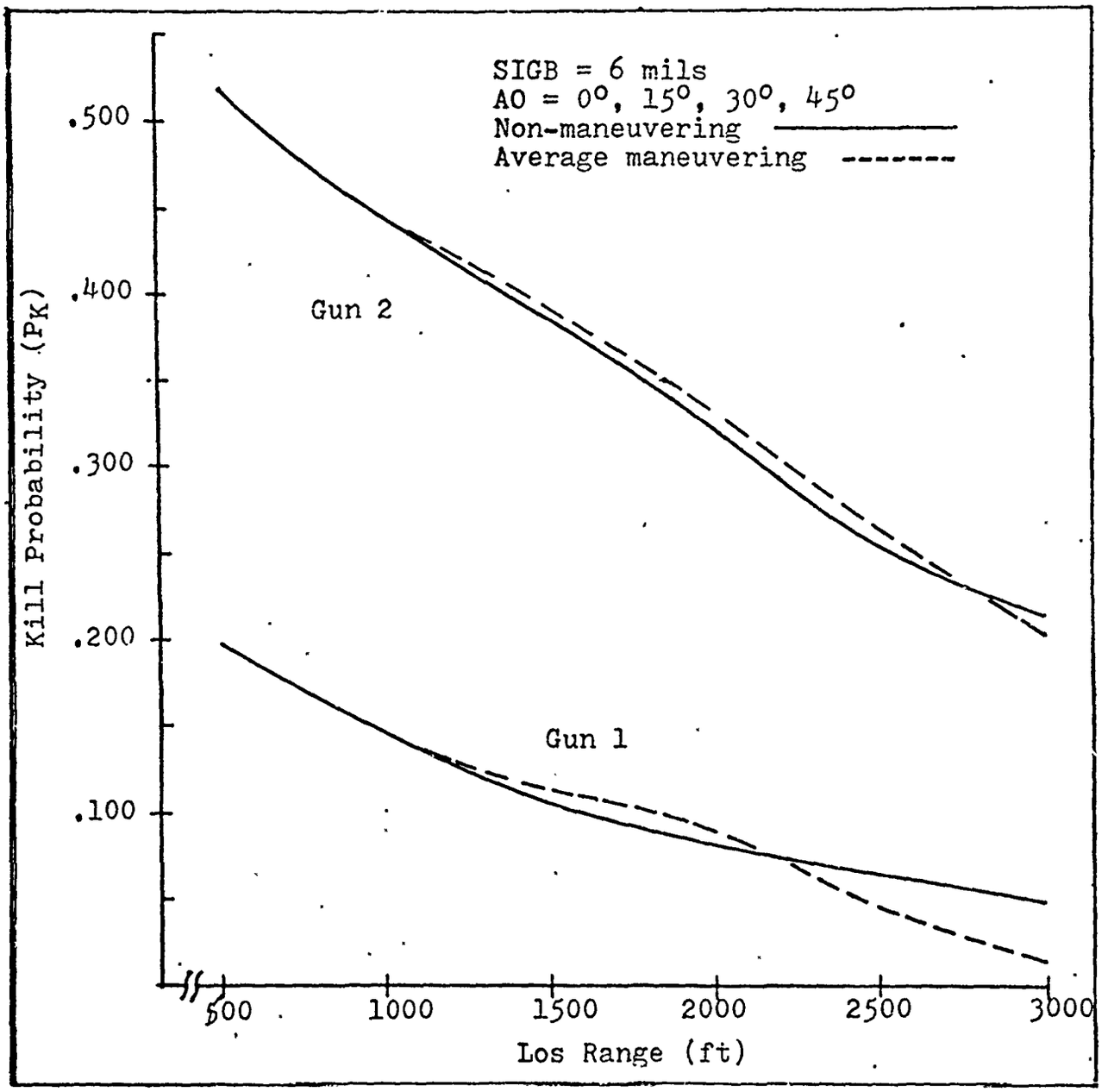


Figure 13 Kill Probability for Non-Maneuvering and Average Maneuvering Target. BD = 10.9 mils.

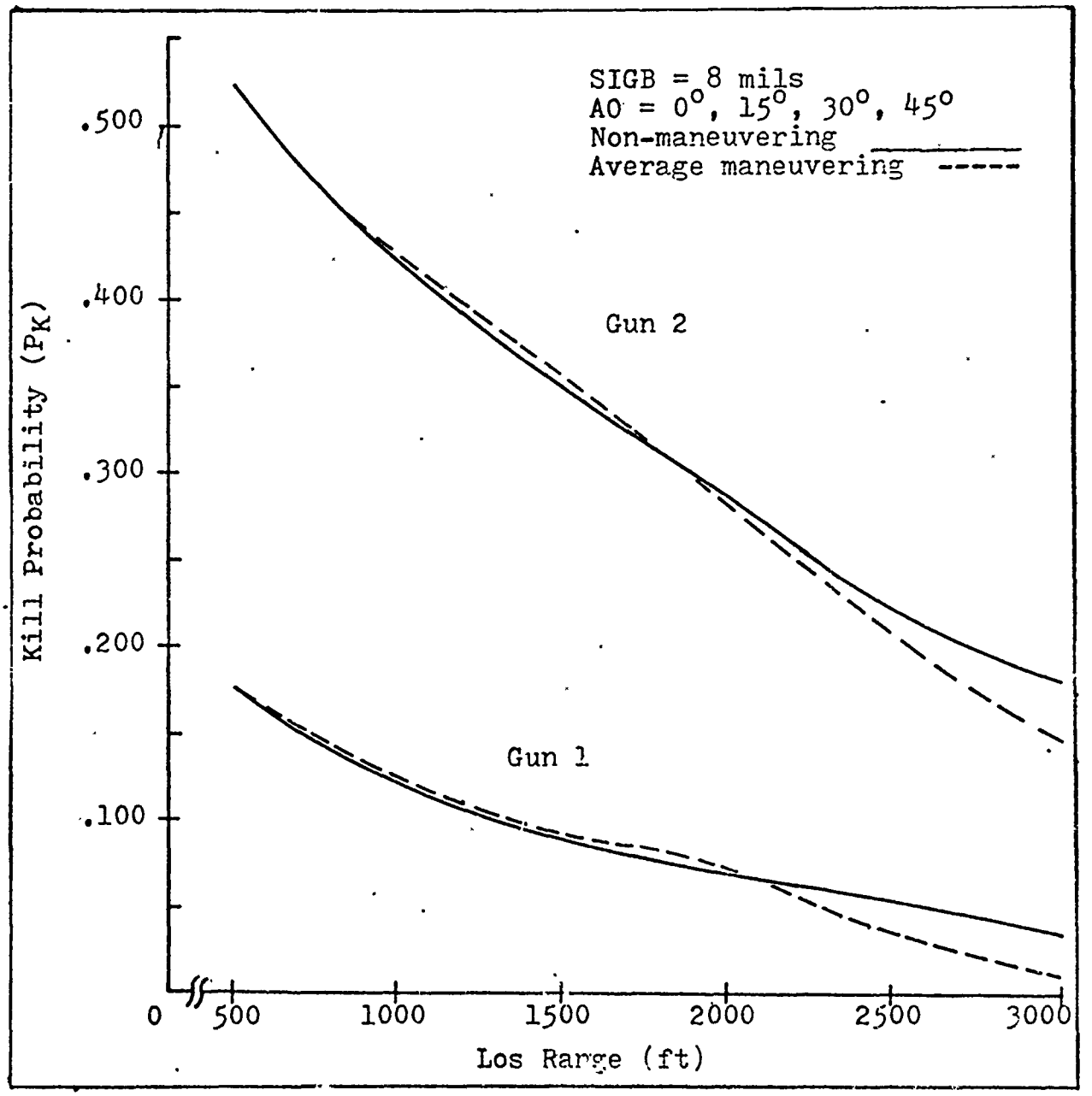


Figure 14 Kill Probability for Non-maneuvering and Average Maneuvering Target. BD = 14.5 mils.

"Optimum" Ballistic Dispersion

Figure 15 shows the overall average kill probability for gun one and gun two against the average maneuvering and non-maneuvering target for various ballistic dispersions. The overall average is the average kill probability for all four angle-offs (0°, 15°,30°, 45°) and all six ranges (500 ft, 1000 ft, 1500 ft, 2000 ft, 2500 ft, 3000 ft).

Against a non-maneuvering target, shown by the solid line, the highest overall average kill probability for both gun one and gun two is achieved at a ballistic dispersion of approximately seven mils (SIGB = 4 mils).

Against an average maneuvering target, shown by the dashed line, the highest overall average kill probability is achieved at a ballistic dispersion of approximately nine mils (SIGB = 5 mils) for gun one, and at a ballistic dispersion of approximately 11 mils (SIGB = 6 mils) for gun two.

Perhaps the most significant phenomena indicated by the curves in Figure 15 is the rapidity with which the kill probability decreases as the ballistic dispersion is made smaller, especially for gun two. That the kill probability decreases at approximately the same rate for both the average maneuvering and non-maneuvering target shows the rapid fall in kill probability to be an aiming problem. That is, the projectile density is very high within the

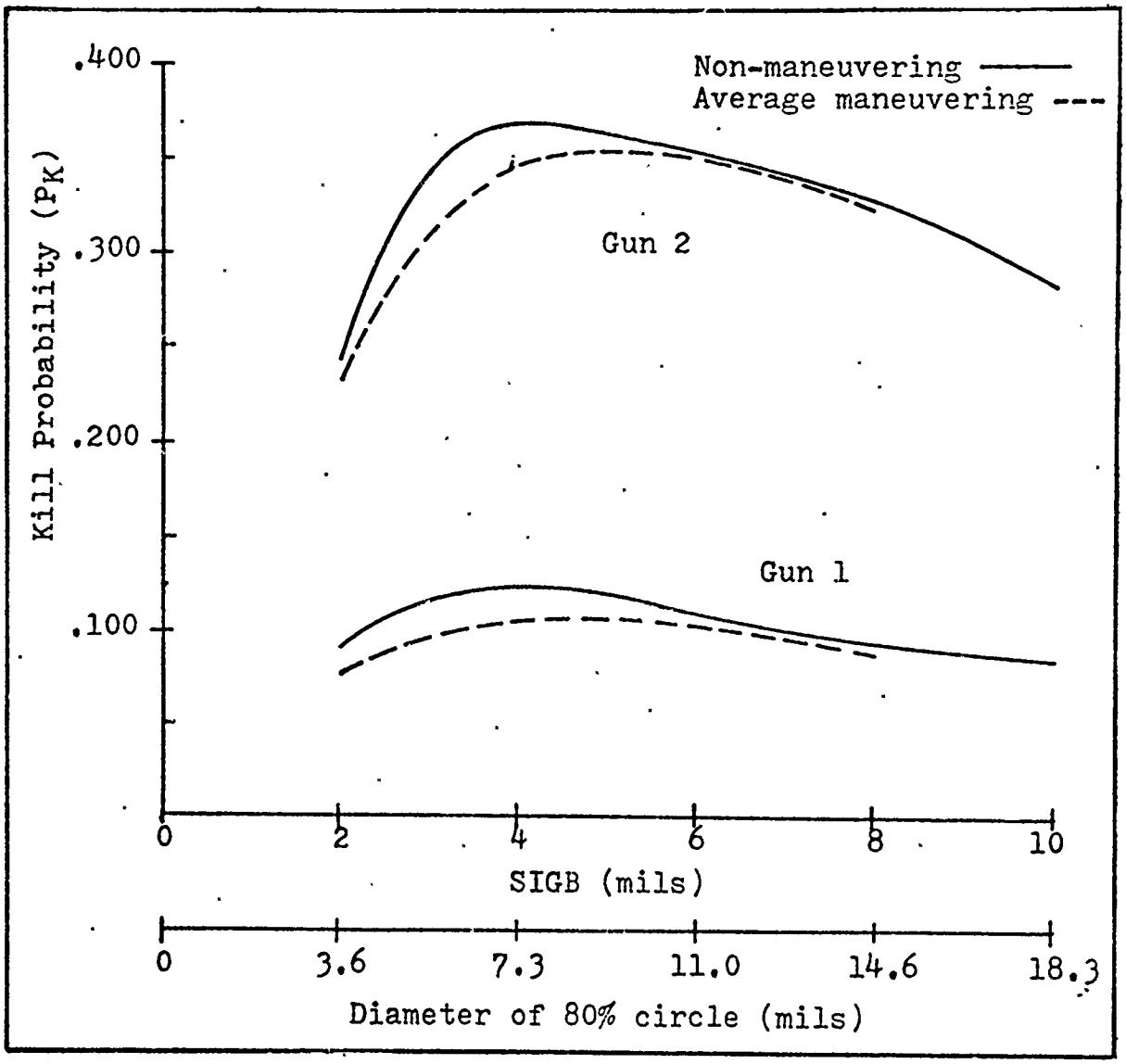


Figure 15 "Optimum" Ballistic Dispersion

fire pattern, but the pattern is not being superimposed on the target because of aiming error.

A better sight system, better aircraft dynamics, and greater pilot proficiency at aiming the gun (than has been mathematically modeled) will improve the kill probability for small ballistic dispersions. However, there is another factor which must be considered; during the flight times of approximately .8 seconds or longer, a maneuvering target can escape the fire pattern from a gun which has a small ballistic dispersion.

This effect of tight ballistic dispersion on kill probability at long gun range can be seen most vividly in Figure 11 for gun one, where the decrease in kill probability due to target uncertainty is significant for line of sight ranges of 2000 feet and greater. The target uncertainty problem can also be seen by comparing the kill probability between a non-maneuvering and break maneuvering target at SIGB = 2 mils for gun one in Appendix C.

A check was made of the ballistic dispersion for the 20-millimeter Vulcan cannon installed in the F-4E aircraft. The specifications for the M-61 Vulcan cannon when mounted on a test firing rig is that 80 percent of 100 rounds or more will be within an eight mil diameter circle. The

center of the 80 percent group is to be within 2.5 mils in elevation or depression and 4.75 mils azimuth of the true boresight point (Ref 8). When installed in the F-4E the maximum allowable dispersion increases to a 10 mil diameter circle (Ref 6).

The question of the actual dispersion of a Vulcan cannon was posed to several people in weapons requirements at TAC Headquarters (Ref 1). The ballistic dispersion of a 20-MM Vulcan cannon when installed in aircraft and fired on a harmonization range is approximately four mils (SIGB = 2 mils). According to the calculations of this analysis, the actual dispersion is too small. As shown in Figure 15, against an average maneuvering air-to-air target a ballistic dispersion of approximately nine mils (SIGB = 5 mils) is indicated as being optimum for gun one and approximately 11 mils (SIGB = 6 mils) for gun two.

Although this study is limited to air-to-air gunnery, the question of "optimum" ballistic dispersion for both air-to-air and air-to-ground gunnery is quickly brought up when ballistic dispersion is discussed. For low angle air-to-ground strafing, everyone questioned agreed

that a tight dispersion is desirable. However, low angle strafing at slant ranges of 1000 feet to 2000 feet can be disastrous in combat; high angle strafing at slant ranges of 3000 feet to 4000 feet is preferable. At these ranges, where the flight time of the projectile is one second or longer, the gravity drop of the projectile and the difficulty in aiming the gun at long slant ranges suggest that the high angle strafing problem is similar to firing from zero degrees angle-off at a non-maneuvering air-to-air target.

If this argument is accepted, then the "optimum" ballistic dispersion for high angle air-to-ground strafing is approximately seven mils (SIGB = 4 mils) for both gun one and gun two. This can be verified by considering the kill probability for various ballistic dispersions against a non-maneuvering target at zero degrees angle-off in Appendix C. That is, the values of kill probability for a non-maneuvering target at zero degrees angle-off are higher in Table X than in Tables IX, XI, or XII.

Effectiveness of Defensive Maneuvers

The relative effectiveness of the jink, hard turn, and break, in decreasing kill probability during projectile flight time, is shown in Figures 16 and 17. Figure 16 shows the effectiveness of the maneuvers as a function of angle-off and Figure 17 shows the effectiveness of the maneuvers as a function of range.

The increase in kill probability for the jink at low angle-off, as shown in Figure 16, occurs because this maneuver shows a higher kill probability than a non-maneuvering target does at certain ranges. This is more clearly shown in Figure 17.

Both figures show the break to be the most effective maneuver in decreasing kill probability during the flight time of the projectile. The jink is probably a much more effective maneuver than is indicated in these Figures. It is especially effective in destroying an attacking pilot's aiming solution both from the standpoint of the sight's lead angle computation and from the standpoint of a pilot's ability to aim while under negative g-loads.

That the jink maneuver produces a higher kill probability for certain ranges (between 1000 feet and 2500 feet for gun one) at angles-off of less than $10^{o}$ is due to greater presented vulnerable area as the target rotates in the vertical plane before maneuvering out of the central part of

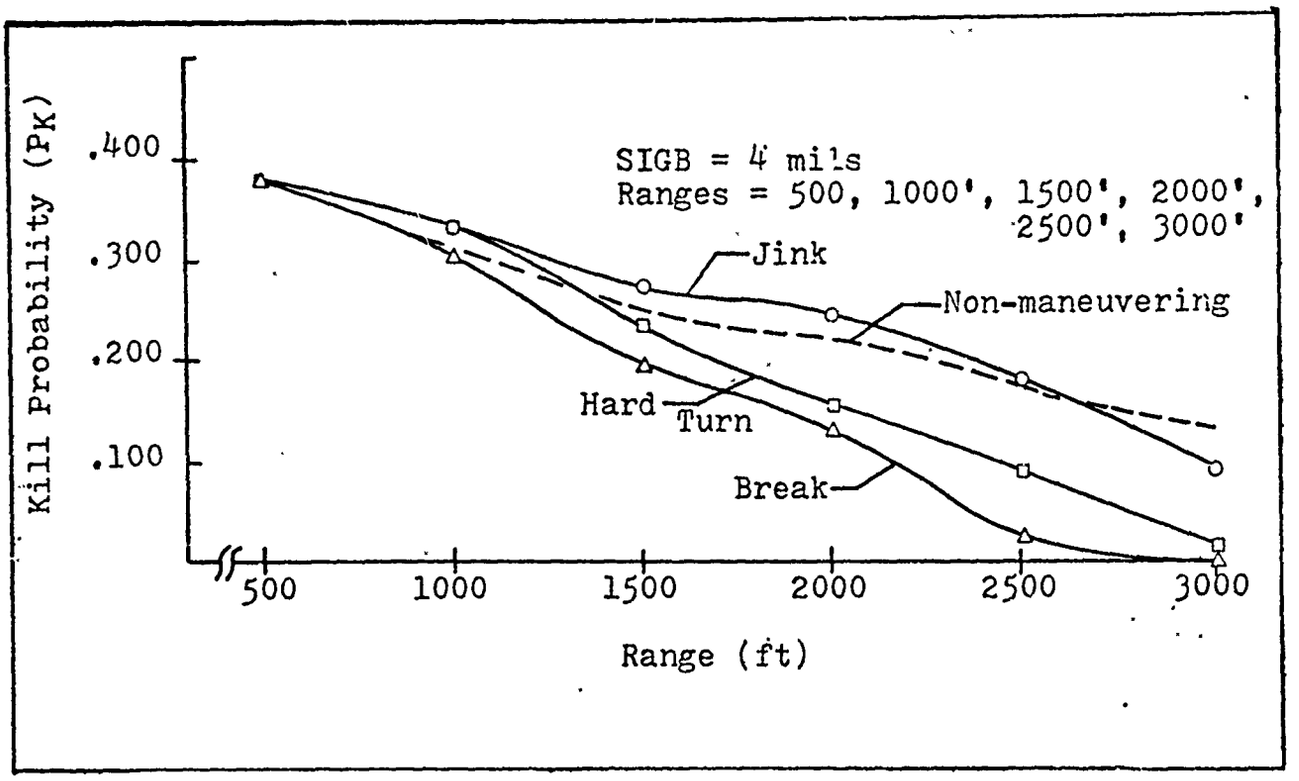


Figure 16 Relative Effectiveness of Defensive Maneuvers against Gun One

the fire pattern.

Best Attack Parameters

The "optimum" parameters for shooting at an aerial target are shown in Figures 18 and 19. Figure 18 shows the angle-off and line of sight range combination which produces the highest kill probability against a non-maneuvering target. Figure 19 shows the same for the average maneuvering target. Both Figures are for gun one with a

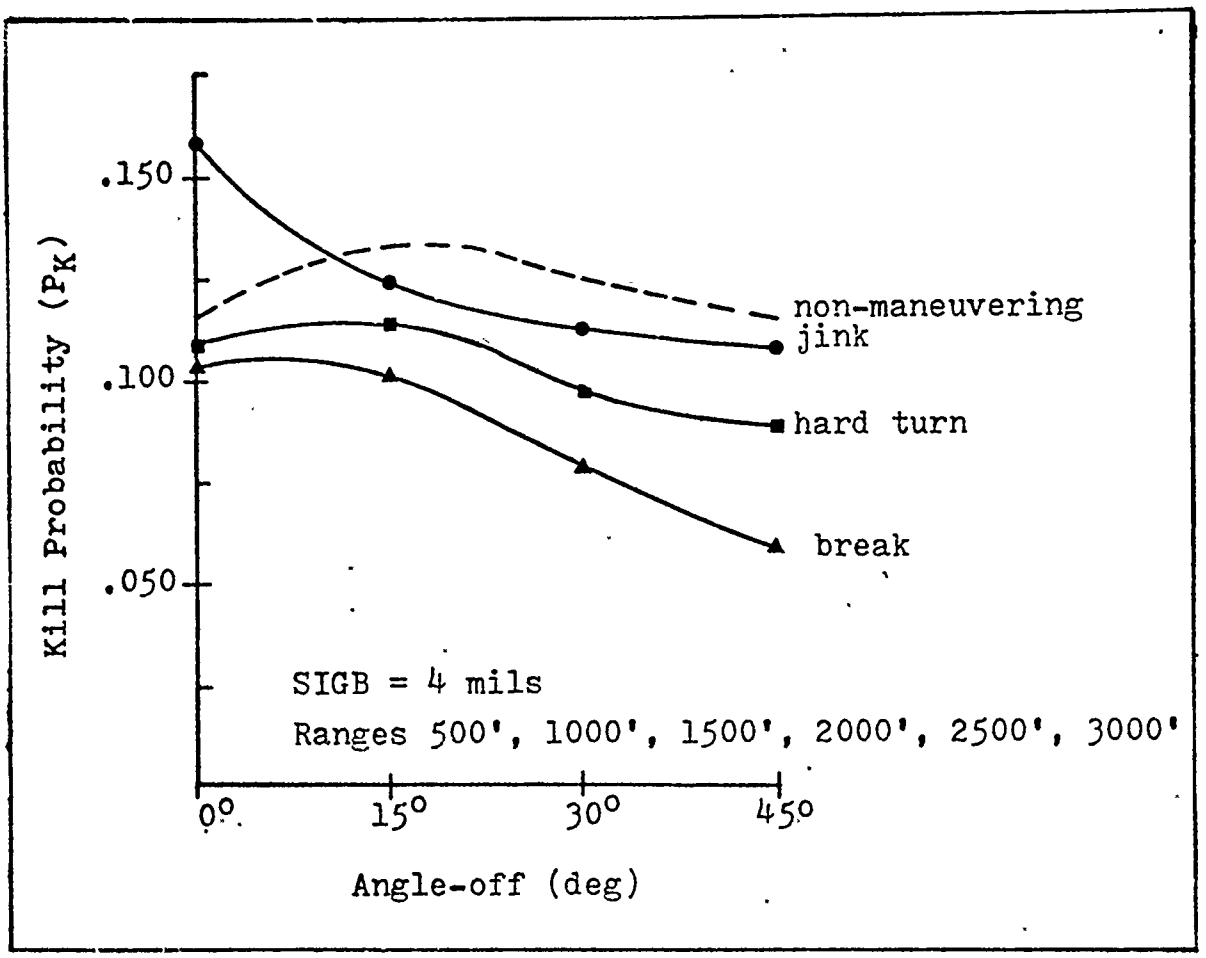


Figure 17 Relative Effectiveness of Defensive Maneuvers against Gun One

ballistic dispersion of approximately seven mils (SIGB = 4 mils).

A close check of both curves shows that the effect of target maneuvering is to decrease the range at which the "optimum" angle-off for firing occurs. Again, it is only noticeable for ranges greater than 2000 feet (time of flight approximately .8 sec. and greater).

The dashed line shows the region for snapshooting and the solid line shows the region for trackshooting. The

double-dash line shows the "optimum" firing parameters.

It should be noticed that the "optimum" line was not drawn through the peaks of the curves for the various angles-off. The reason is that a peak represents 5.6 g's or the crossover between trackshoot aiming and snapshoot aiming. That is, each peak is a so-called "square corner" of air-to-air gunnery.

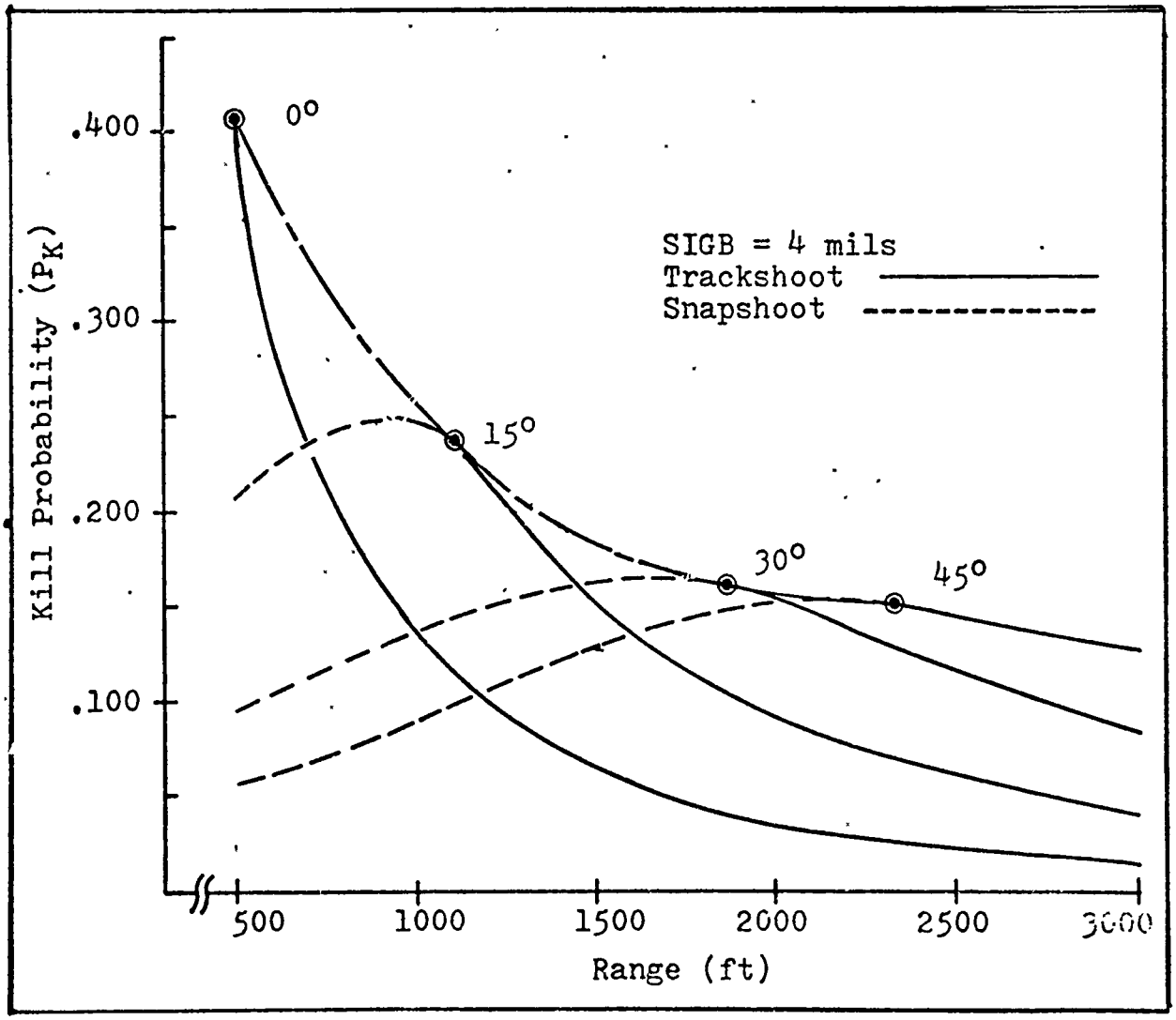


Figure 18 "Optimum" Angle-off versus Line of Sight Range for Gun One against Non-maneuvering Target.

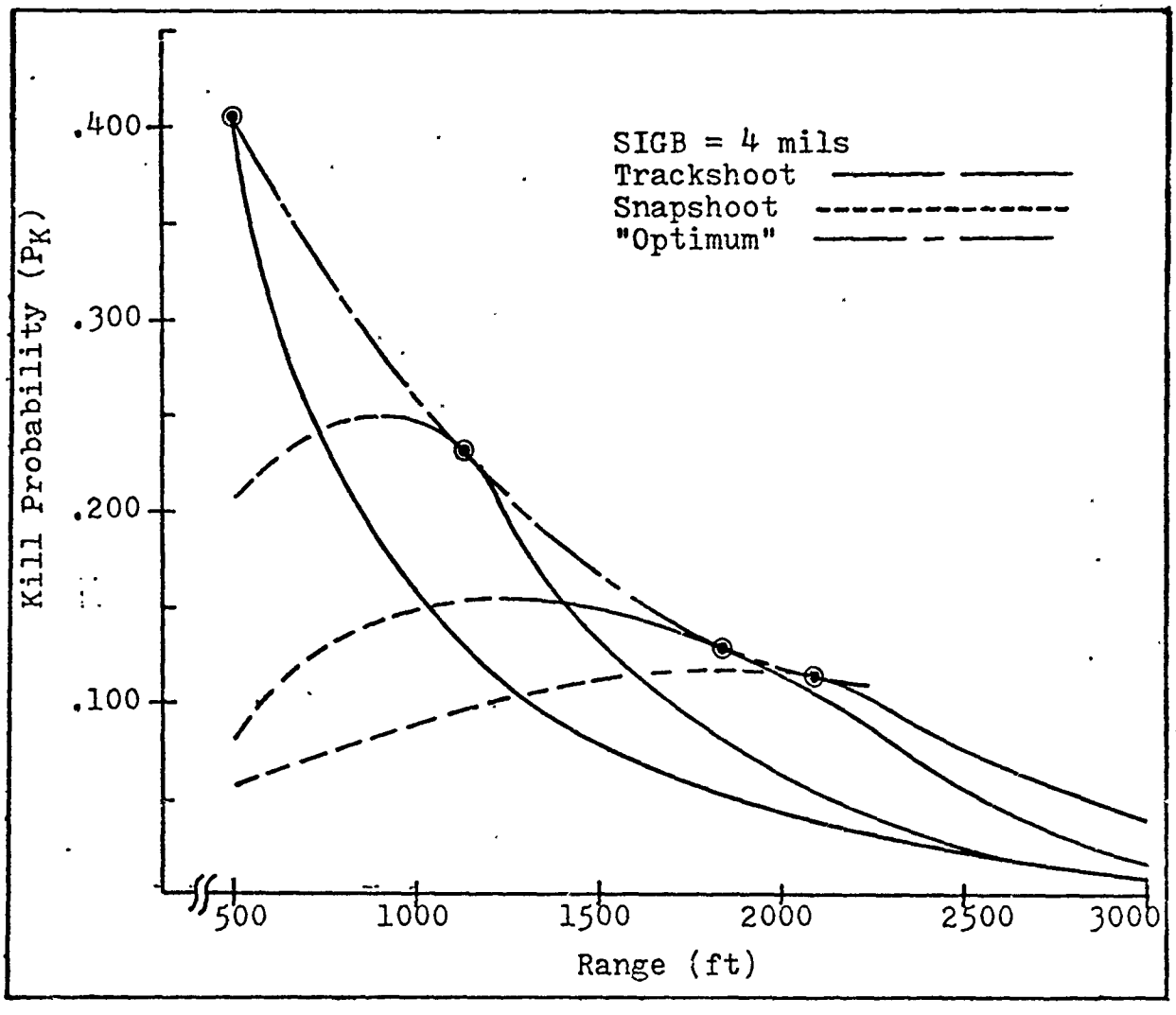


Figure 19 "Optimum" Angle-off versus Line of Sight Range for Gun Two against Average Maneuvering Target.

## V. Conclusions

1. Uncertainty in a target's position and attitude due to defensive maneuvering during projectile flight time in air-to-air gunnery significantly decreases kill probability when the time of flight is greater than .8 seconds. Target uncertainty has no effect on kill probability when the time of flight is less than .5 seconds.
2. To the degree that actual air-to-air gunnery was modeled, the results of this study show the "optimum" ballistic dispersion for rapid firing cannons in air-to-air gunnery to be such that 80% of rounds fired should fall within a circle of approximately nine to ten mils diameter when the installed gun is harmonized. No analysis was conducted to determine the effect of bias in gun alignment.

## Bibliography


1. Craig, Major James T., Headquarters Tactical Air Command (TAC - DRT), Langly AFB, Virgina. Telephone Conversation 22 May 1972.

2. Final Gun-Val Report: An Evaluation of Fighter Aircraft Guns by Engineering Tests and Mathematical Analysis. AF Reprot 55J01. Wright-Patterson AFB, Ohio: Air Force Armament Center, 1 October 1955.

3. Germond, H. H., The Circular Coverage Function, The RAND Corporation, RM-330, 26 January 1950.

4. Hackford, R. H., Analysis of Piloted Weapons Delivery: F-4E Aerial Gunnery. Unpublished Masters Thesis, GGC/EE/72-3. Wright Patterson AFB, Ohio: Air Force Institute of Technology, May, 1972.

5. Meyer, Paul L., Introductory Probability and Statistical Applications (Second Edition). Reading, Mass: Addison Wesley Publishing Company, 1970

6. Request for Proposal (RFP) for F-4E aircraft dated March 1966.

7. Schaffer, M. B., Basic Measures for Comparing the Effectiveness of Conventional Weapons, The RAND Corporation, RM-4647-PR, January 1966.

8. Smith, H., Optimization Branch, Analysis Division, Air Force Armament and Test Laboratory, Eglin AFB, Florida. Numerous telephone conversations and several face to face conversations between July 1971 and May 1972.

9. Springfield Armory Purchase Description, SAPD - 265A Ammendment 1, for GAU-4 M61A1.

# Appendix A

This section contains the development of selected topics for the mathematical model.

## Square Approximation to Circular Dispersion

The approximation is made by representing probability as the area under a surface, where the height of the surface is specified by the density distribution (Ref 5). For the same density distribution, d, the differential area of a square equivalent to the differential area of a circle is found by equating probability.

$$b^2 \cdot d = \frac{\pi}{4} D^2 \tag{27}$$

where b is a side of the incremental square and D is the diameter of the circle. The diameter of interest is for a circle which contains 80 percent of the projectiles, which is by definition ballistic dispersion (BD).

For a Gaussian circular distribution, 80 percent of the distribution is within 1.825 standard deviations of the mean. Letting SIGB represent one standard deviation in projectile density, the ballistic dispersion is

$$BD = 1.825 \text{ SIGB}. \tag{28}$$

Substituting for D in equation 27, with BD from equation 28, the side of the square which contains 80 percent of the distribution is approximated.

$$b = 1.6 \text{ SIGB} \tag{29}$$

The half width of a square fire pattern (HWP) needed to encompass 80 percent of the rounds as a function of range is

$$\text{HWP} = \frac{1.6 \text{ SIGB} \cdot \text{RB}}{1000} \tag{30}$$

and the half width of a square pattern needed to encompass the remaining 20 percent of the rounds is approximately

$$\text{HWP} = \frac{(1.6)^2 \text{SIGB} \cdot \text{RB}}{1000} \tag{31}$$

Referring to Figure 7, it can be seen that through the small surface the probability density is

$$.6875 + 1/3(.3125) = .79 \doteq .8 \tag{32}$$

and through the large surface.

$$2/3(.3125) = .21 \doteq .2 \tag{33}$$

Part Coverage

Figure 20 shows partial part coverage by the fire pattern. The probable number of hits on the part (CUHIT) is calculated according to the following equation.

$$CUHIT = SAR \cdot COV \cdot PNR \cdot DPD(IPD) \tag{34}$$

SAR is the ratio of area between the part and the pattern.

$$POW = \frac{PHW}{HWP} \text{ or } 1.0 \text{ whichever less}$$

$$POL = \frac{PHL}{HWP} \text{ or } 1.0 \text{ whichever less}$$

$$SAR = POW \cdot POL \tag{35}$$

COV is the ratio of the part which is covered by the pattern

$$OSC = \tfrac{1}{2} \frac{OSCR}{PHW}$$

$$OSLC = \tfrac{1}{2} \frac{OSLCR}{PHL}$$

$$COV = OSC \cdot OSLC \tag{36}$$

The probable number of rounds is given by equation 19 for trackshooting and by the following equation for snapshooting, where a uniform density of fire along the fire line is assumed

$$PNR = .01\ FR \cdot DOB \tag{37}$$

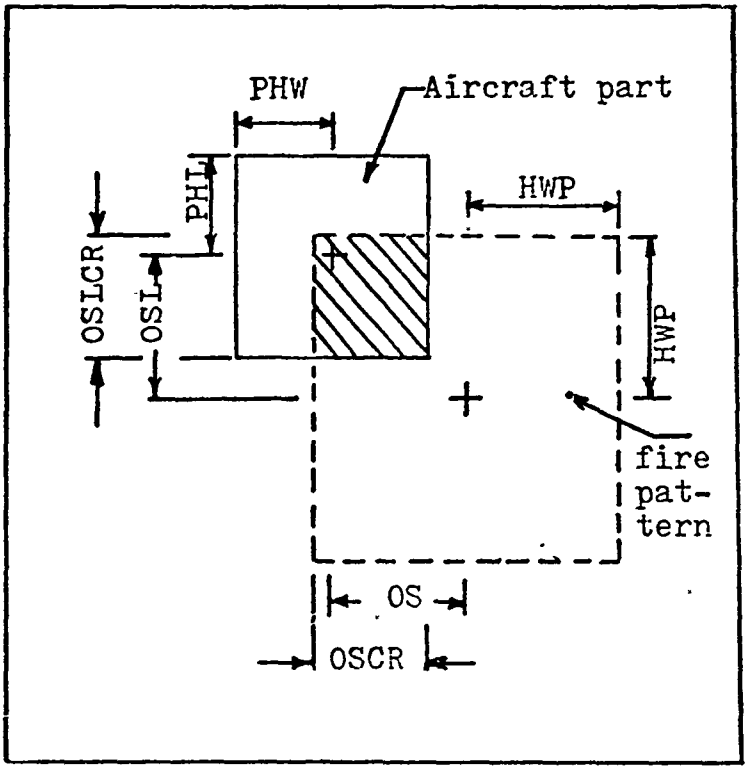


Figure 20 Partial Coverage of Part by Fire Pattern

Draws

Four draws are used to average the locus of the projectiles in the vicinity of the target. The upper drawing in Figure 21 shows how the projectile flight path is broken into two component flight paths. One component is in the horizontal plane (side-rearview aspect) and the other in the vertical plane (top-rearview aspect). This is necessary, because methods of calculating vulnerable area for other than a few aspects have not yet been developed.

The lower drawing in Figure 21 shows that from each aspect two draw directions are used. One draw is parallel to the FRL and the other is perpendicular. Each draw is given a numerical designator as shown in the drawing. The reason the fire line is oriented in two directions for each aspect is to produce an average kill probability. Each draw is weighted equally since the roll attitude of the target at the instant of projectile impact is very unpredictable. The predicted projectile impact angle (LAM) is taken to be equal in both the vertical plane and horizontal plane.

Figure 22 shows how the part number and draw number determine the area of a target part presented to an impacting projectile.

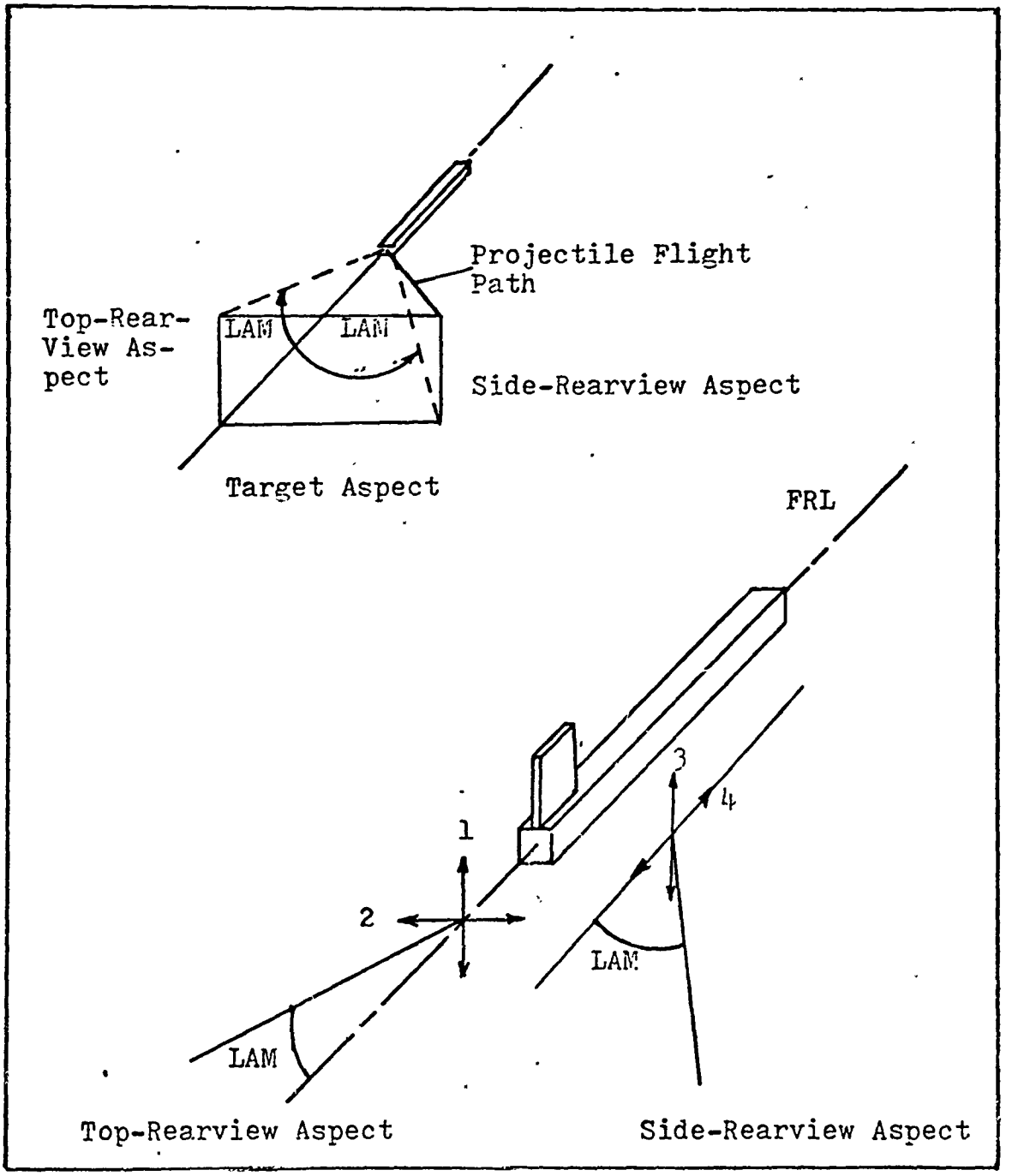


Figure 21 Draws of Fire Line

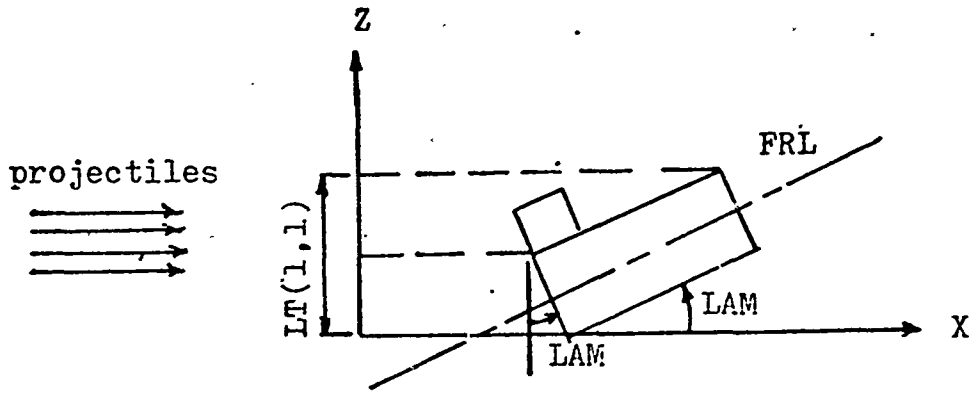


LT(1,1) = 4cos(LAM) + 40sin(LAM)

draw number
part number

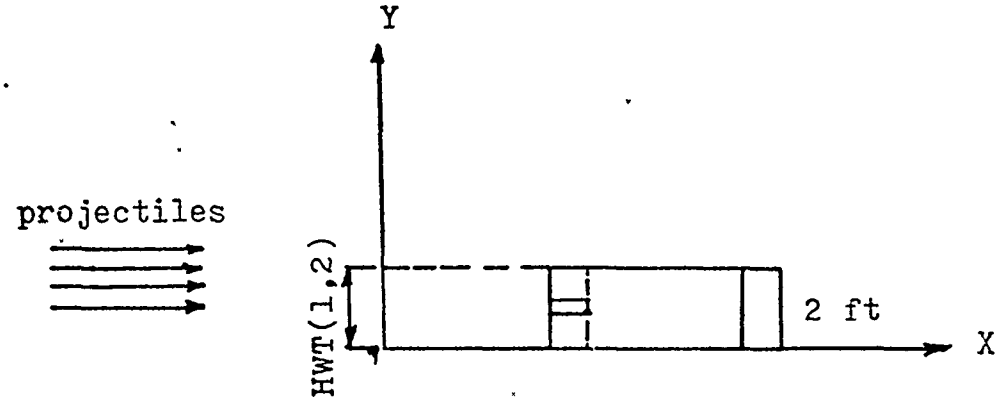


HWT(1,2) = 2

Figure 22 Half width Target (HWT) and Length of Target (LT)

# Appendix B

This section contains the development of the equations used to calculate the displacement and change in attitude of the target during the flight time of the projectile.

## Target Uncertainty Model

Figure 23 shows the acceleration forces acting on a maneuvering aircraft flying at constant velocity. The kinematic radial acceleration (RA) is equal to the g-loading read by the pilot on the accelerometer minus the gravity component along the instantaneous radius of turn.

$$RA = 32.2 \left(GLF - \cos(gamma)\cos(phi)\right) \qquad (11)$$

where, GLF is the g-load factor read by the pilot, phi is bank angle and gamma is flight path angle.

The displacement of the target is approximated by dividing the flight time into 100 time increments. The instantaneous radial acceleration is assumed to be constant in both magnitude and direction for the duration of each increment. The lateral and vertical displacements of the maneuvering target is approximated by summing the incremental displacements over each of the time increments. The model calculates the displacement by updating the magnitude and

direction of the acceleration and velocity components at the end of each time increment.

Since the roll rate of the maneuvering aircraft is much greater than the pitch rate, and because the coordinate system is such that the initial flight path angle is always zero, the direction of the radial acceleration can be approximated by using only the bank angle. Figure 24 shows the instantaneous components of radial acceleration in the Y and Z directions.

The displacement of the target during each time increment (DELTF) is the sum of the displacements caused by the acceleration components during the present time increment and the displacement due to the velocity components from acceleration during the previous time increment. The lateral displacement (YDIS) is the sum of the incremental displacements (DELYDIS) and the vertical displacement (ZDIS) is the sum of the incremental displacements (DELZDIS).

$$DELYDIS = RA \cdot \sin(PHI) \cdot \left(\frac{DELTF}{2}\right)^2 + DELV \cdot DELTF \qquad (38)$$

$$DELZDIS = RA \cdot \cos(PHI) \cdot \left(\frac{DELTF}{2}\right)^2 + DELW \cdot DELTF \qquad (39)$$

where,
$$DELV = RA \cdot \sin(PHI \cdot DELTF \qquad (40)$$

and
$$DELW = RA \cdot \cos(PHI) \cdot DELTF \qquad (41)$$

are the velocity components due to acceleration during the previous time increment.

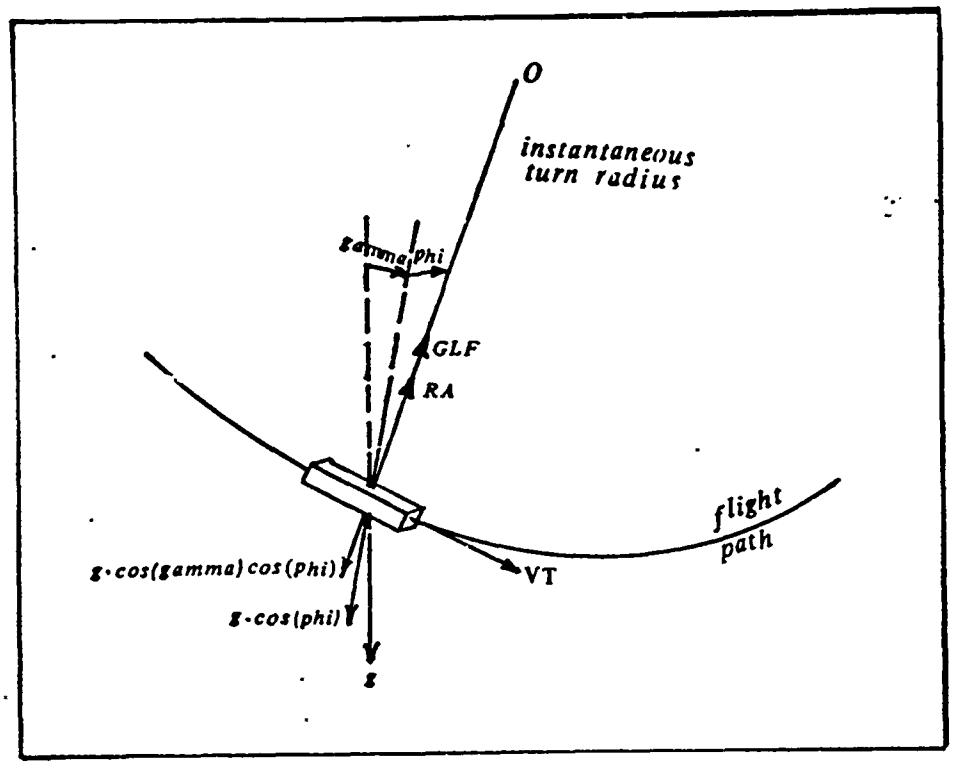


Figure 23 Kinematic Acceleration

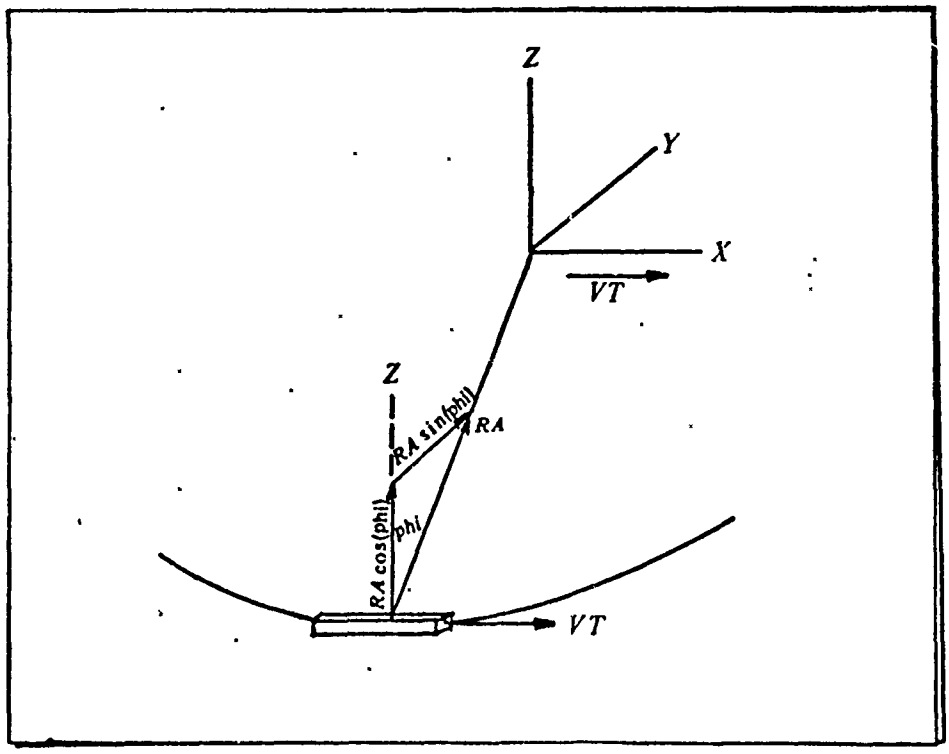


Figure 24 Components of Instantaneous Radial Acceleration

# Appendix C

Presented in this appendix are the kill probabilities calculated by the mathematical model.

## Table IX

Kill Probabilities for Gun 1, SIGB = 2 mils

### Non-Maneuvering

| | PHIDOT = 0<br>GLFDOT = 0 | | | |
|---|---|---|---|---|
| Range | 0° | 15° | 30° | 45° |
| 500 | .321 | .120 | .049 | .031 |
| 1000 | .120 | .190 | .088 | .046 |
| 1500 | .056 | .126 | .114 | .068 |
| 2000 | .030 | .078 | .126 | .102 |
| 2500 | .019 | .051 | .092 | .106 |
| 3000 | - | .034 | .067 | .099 |

### Jink

| PHIDOT = 0<br>GLFDOT = -2 g/sec | | | |
|---|---|---|---|
| 0° | 15° | 30° | 45° |
| .321 | .120 | .049 | .031 |
| .152 | .187 | .087 | .046 |
| .099 | .122 | .112 | .069 |
| .079 | .070 | .119 | .103 |
| .062 | .037 | .073 | .104 |
| .013 | .013 | .034 | .076 |

### Hard Turn

| PHIDOT = 45°/sec<br>GLFDOT = 4 g/sec | | | |
|---|---|---|---|
| 0° | 15° | 30° | 45° |
| .325 | .120 | .049 | .031 |
| .126 | .188 | .087 | .045 |
| .061 | .122 | .109 | .063 |
| .036 | .068 | .106 | .090 |
| .004 | .012 | .039 | .064 |
| - | - | - | .003 |

### Break

| PHIDOT = 90°/sec<br>GLFDOT = 6 g/sec | | | |
|---|---|---|---|
| 0° | 15° | 30° | 45° |
| .325 | .119 | .049 | .030 |
| .125 | .182 | .085 | .044 |
| .064 | .112 | .102 | .059 |
| .008 | .024 | .051 | .059 |
| - | - | - | .003 |
| - | - | - | - |

### Average Maneuvering

| | Average<br>Maneuvering | | | |
|---|---|---|---|---|
| Range | 0° | 15° | 30° | 45° |
| 500 | .323 | .120 | .049 | .031 |
| 1000 | .134 | .186 | .086 | .045 |
| 1500 | .074 | .117 | .107 | .064 |
| 2000 | .041 | .054 | .092 | .084 |
| 2500 | .022 | .016 | .037 | .057 |
| 3000 | .004 | .004 | .011 | .026 |

## Table X

## Kill Probabilities for Gun 1, SIGB = 4 mils

### Non-Maneuvering

| PHIDOT = 0<br>GLFDOT = 0 | | | | |
|---|---|---|---|---|
| Range | 0° | 15° | 30° | 45° |
| 500 | .405 | .204 | .094 | .058 |
| 1000 | .136 | .247 | .151 | .089 |
| 1500 | .064 | .152 | .161 | .123 |
| 2000 | .037 | .093 | .158 | .153 |
| 2500 | .024 | .060 | .115 | .142 |
| 3000 | .016 | .041 | .082 | .126 |

### Jink

| PHIDOT = 0<br>GLFDOT = -2 g/sec | | | |
|---|---|---|---|
| 0° | 15° | 30° | 45° |
| .406 | .204 | .094 | .058 |
| .181 | .244 | .150 | .089 |
| .125 | .146 | .156 | .123 |
| .111 | .084 | .145 | .151 |
| .092 | .045 | .092 | .136 |
| .021 | .018 | .043 | .099 |

### Hard Turn

| PHIDOT = 45°/sec<br>GLFDOT = 4 g/sec | | | |
|---|---|---|---|
| 0° | 15° | 30° | 45° |
| .409 | .204 | .094 | .058 |
| .142 | .248 | .152 | .088 |
| .065 | .143 | .157 | .114 |
| .025 | .061 | .118 | .114 |
| .012 | .026 | .059 | .080 |
| - | .001 | .005 | .019 |

### Break

| PHIDOT = 90°/sec<br>GLFDOT = 6 g/sec | | | |
|---|---|---|---|
| 0° | 15° | 30° | 45° |
| .411 | .204 | .094 | .058 |
| .140 | .243 | .148 | .086 |
| .048 | .112 | .133 | .097 |
| .024 | .047 | .093 | .093 |
| - | .001 | .009 | .020 |
| - | - | - | - |

| Average Maneuvering | | | | |
|---|---|---|---|---|
| Range | 0° | 15° | 30° | 45° |
| 500 | .408 | .204 | .094 | .058 |
| 1000 | .154 | .245 | .150 | .087 |
| 1500 | .079 | .133 | .148 | .111 |
| 2000 | .043 | .064 | .118 | .119 |
| 2500 | .024 | .024 | .053 | .078 |
| 3000 | .007 | .006 | .016 | .039 |

## Table XI

## Kill Probabilities for Gun 1, SIGB = 6 mils

### Non-Maneuvering

| | PHIDOT = 0<br>GLFDOT = 0 | | | |
|---|---|---|---|---|
| Range | 0° | 15° | 30° | 45° |
| 500 | .358 | .234 | .125 | .080 |
| 1000 | .104 | .218 | .149 | .103 |
| 1500 | .046 | .121 | .141 | .112 |
| 2000 | .025 | .069 | .130 | .132 |
| 2500 | .015 | .042 | .088 | .119 |
| 3000 | .010 | .027 | .059 | .098 |

### Jink

| PHIDOT = 0<br>GLFDOT = -2 g/sec | | | |
|---|---|---|---|
| 0° | 15° | 30° | 45° |
| .3 9 | .234 | .125 | .080 |
| .140 | .216 | .147 | .103 |
| .091 | .116 | .137 | .111 |
| .076 | .062 | .120 | .130 |
| .062 | .033 | .070 | .114 |
| .015 | .014 | .033 | .079 |

### Hard Turn

| PHIDOT = 45°/sec<br>GLFDOT = 4 g/sec | | | |
|---|---|---|---|
| 0° | 15° | 30° | 45° |
| .362 | .235 | .125 | .080 |
| .112 | .221 | .152 | .103 |
| .055 | .126 | .147 | .111 |
| .034 | .072 | .133 | .126 |
| .010 | .023 | .068 | .099 |
| .001 | .003 | .018 | .032 |

### Break

| PHIDOT = 90°/sec<br>GLFDOT = 6 g/sec | | | |
|---|---|---|---|
| 0° | 15° | 30° | 45° |
| .365 | .235 | .126 | .079 |
| .116 | .222 | .153 | .102 |
| .059 | .124 | .146 | .110 |
| .018 | .041 | .101 | .110 |
| .002 | .006 | .026 | .044 |
| - | - | - | .001 |

### Average Maneuvering

| | Average<br>Maneuvering | | | |
|---|---|---|---|---|
| Range | 0° | 15° | 30° | 45° |
| 500 | .362 | .234 | .125 | .080 |
| 1000 | .112 | .218 | .150 | .103 |
| 1500 | .068 | .122 | .143 | .110 |
| 2000 | .034 | .058 | .118 | .120 |
| 2500 | .024 | .021 | .054 | .085 |
| 3000 | .005 | .005 | .017 | .037 |

## Table XII

Kill Probabilities for Gun 1, SIGB = 8 mils

### Non-Maneuvering

| | PHIDOT = 0<br>GLFDOT = 0 | | | |
|---|---|---|---|---|
| Range | 0° | 15° | 30° | 45° |
| 500 | .281 | .210 | .132 | .094 |
| 1000 | .080 | .182 | .137 | .095 |
| 1500 | .036 | .095 | .123 | .103 |
| 2000 | .019 | .054 | .107 | .116 |
| 2500 | .012 | .033 | .070 | .101 |
| 3000 | .008 | .021 | .046 | .080 |

| Jink | | | | Hard Turn | | | | Break | | | |
|---|---|---|---|---|---|---|---|---|---|---|---|
| PHIDOT = 0<br>GLFDOT = -2 g/sec | | | | PHIDOT = 45°/sec<br>GLFDOT = 4 g/sec | | | | PHIDOT = 90°/sec<br>GLFDOT = 6 g/sec | | | |
| 0° | 15° | 30° | 45° | 0° | 15° | 30° | 45° | 0° | 15° | 30° | 45° |
| | | | | .285 | .211 | .132 | .094 | .287 | .212 | .133 | .094 |
| | | | | .085 | .186 | .189 | .098 | .087 | .186 | .140 | .098 |
| Not Calculated | | | | .041 | .098 | .188 | .102 | .041 | .094 | .126 | .098 |
| | | | | .023 | .051 | .107 | .108 | .025 | .051 | .102 | .098 |
| | | | | .015 | .029 | .065 | .084 | .008 | .016 | .033 | .047 |
| | | | | .004 | .008 | .019 | .043 | - | - | .003 | .005 |

| | Average Maneuvering | | | |
|---|---|---|---|---|
| Range | 0° | 15° | 30° | 45° |
| 500 | .286 | .211 | .132 | .094 |
| 1000 | .086 | .186 | .139 | .098 |
| 1500 | .041 | .096 | .127 | .100 |
| 2000 | .024 | .051 | .104 | .103 |
| 2500 | .022 | .022 | .049 | .065 |
| 3000 | .002 | .004 | .011 | .024 |

## Table XIII

### Kill Probabilities for Gun 2, SIGB = 2 mils

#### Non-Maneuvering

| | PHIDOT = 0<br>GLFDOT = 0 | | | |
|---|---|---|---|---|
| Range | 0° | 15° | 30° | 45° |
| 500 | .592 | .377 | .159 | .090 |
| 1000 | .292 | .461 | .235 | .129 |
| 1500 | .188 | .356 | .343 | .169 |
| 2000 | .122 | .259 | .306 | .233 |
| 2500 | .084 | .210 | .266 | .224 |
| 3000 | .067 | .173 | .222 | .238 |

#### Jink

| PHIDOT = 0<br>GLFDOT = -2 g/sec | | | |
|---|---|---|---|
| 0° | 15° | 30° | 45° |
| .593 | .377 | .159 | .090 |
| .299 | .460 | .235 | .129 |
| .203 | .350 | .342 | .169 |
| .147 | .257 | .305 | .233 |
| .121 | .210 | .269 | .231 |
| .109 | .171 | .237 | .227 |

#### Hard Turn

| PHIDOT = 45°/sec<br>GLFDOT = 4 g/sec | | | |
|---|---|---|---|
| 0° | 15° | 30° | 45° |
| .595 | .377 | .159 | .090 |
| .297 | .461 | .235 | .128 |
| .196 | .344 | .333 | .163 |
| .137 | .249 | .288 | .219 |
| .108 | .200 | .236 | .210 |
| .086 | .155 | .195 | .192 |

#### Break

| PHIDOT = 90°/sec<br>GLFDOT = 6 g/sec | | | |
|---|---|---|---|
| 0° | 15° | 30° | 45° |
| .596 | .377 | .159 | .090 |
| .295 | .455 | .233 | .127 |
| .187 | .303 | .310 | .156 |
| .145 | .233 | .262 | .208 |
| .117 | .178 | .208 | .176 |
| .026 | .070 | .103 | .127 |

| | Average Maneuvering | | | |
|---|---|---|---|---|
| Range | 0° | 15° | 30° | 45° |
| 500 | .594 | .377 | .159 | .090 |
| 1000 | .297 | .458 | .235 | .128 |
| 1500 | .195 | .332 | .328 | .163 |
| 2000 | .143 | .246 | .285 | .220 |
| 2500 | .115 | .196 | .237 | .205 |
| 3000 | .073 | .132 | .187 | .182 |

## Table XIV

## Kill Probabilities for Gun 2, SIGB = 4 mils

### Non-Maneuvering

| PHIDOT = 0<br>GLFDOT = 0 | | | | |
|---|---|---|---|---|
| Range | 0° | 15° | 30° | 45° |
| 500 | .729 | .592 | .296 | .174 |
| 1000 | .449 | .640 | .402 | .247 |
| 1500 | .264 | .546 | .517 | .300 |
| 2000 | .168 | .428 | .469 | .378 |
| 2500 | .116 | .329 | .422 | .350 |
| 3000 | .085 | .256 | .358 | .359 |

### Jink

| PHIDOT = 0<br>GLFDOT = -2 g/sec | | | |
|---|---|---|---|
| 0° | 15° | 30° | 45° |
| .731 | .591 | .296 | .174 |
| .468 | .638 | .402 | .247 |
| .299 | .541 | .514 | .300 |
| .215 | .418 | .463 | .377 |
| .164 | .310 | .408 | .346 |
| .121 | .218 | .323 | .339 |

### Hard Turn

| PHIDOT = 45°/sec<br>GLFDOT = 4 g/sec | | | |
|---|---|---|---|
| 0° | 15° | 30° | 45° |
| .730 | .592 | .296 | .174 |
| .462 | .640 | .402 | .246 |
| .283 | .546 | .515 | .294 |
| .182 | .413 | .454 | .363 |
| .108 | .272 | .363 | .305 |
| .065 | .167 | .247 | .254 |

### Break

| PHIDOT = 90°/sec<br>GLFDOT = 6 g/sec | | | |
|---|---|---|---|
| 0° | 15° | 30° | 45° |
| .731 | .592 | .296 | .174 |
| .465 | .638 | .399 | .244 |
| .278 | .532 | .503 | .285 |
| .145 | .345 | .396 | .322 |
| .094 | .213 | .292 | .247 |
| .072 | .144 | .193 | .208 |

### Average Maneuvering

| Range | 0° | 15° | 30° | 45° |
|---|---|---|---|---|
| 500 | .731 | .592 | .296 | .174 |
| 1000 | .465 | .639 | .401 | .246 |
| 1500 | .286 | .540 | .510 | .293 |
| 2000 | .180 | .392 | .437 | .354 |
| 2500 | .122 | .265 | .354 | .299 |
| 3000 | .086 | .176 | .254 | .267 |

## Table XV

## Kill Probabilities for Gun 2, SIGB = 6 mils

### Non-Maneuvering

| | PHIDOT = 0<br>GLFDOT = 0 | | | |
|---|---|---|---|---|
| Range | 0° | 15° | 30° | 45° |
| 500 | .779 | .678 | .386 | .235 |
| 1000 | .387 | .668 | .430 | .289 |
| 1500 | .203 | .520 | .507 | .303 |
| 2000 | .121 | .365 | .443 | .353 |
| 2500 | .078 | .262 | .373 | .315 |
| 3000 | .055 | .197 | .294 | .317 |

### Jink

| PHIDOT = 0<br>GLFDOT = -2 g/sec | | | |
|---|---|---|---|
| 0° | 15° | 30° | 45° |
| .782 | .678 | .386 | .235 |
| .407 | .666 | .429 | .289 |
| .233 | .514 | .504 | .302 |
| .156 | .356 | .437 | .352 |
| .117 | .248 | .363 | .313 |
| .095 | .175 | .282 | .310 |

### Hard Turn

| PHIDOT = 45°/sec<br>GLFDOT = 4 g/sec | | | |
|---|---|---|---|
| 0° | 15° | 30° | 45° |
| .783 | .679 | .386 | .234 |
| .404 | .671 | .432 | .288 |
| .230 | .530 | .511 | .302 |
| .152 | .380 | .446 | .353 |
| .112 | .280 | .375 | .309 |
| .089 | .210 | .296 | .299 |

### Break

| PHIDOT = 90°/sec<br>GLFDOT = 6 g/sec | | | |
|---|---|---|---|
| 0° | 15° | 30° | 45° |
| .784 | .679 | .386 | .234 |
| .413 | .672 | .433 | .288 |
| .243 | .531 | .510 | .302 |
| .168 | .388 | .439 | .348 |
| .129 | .278 | .360 | .295 |
| .053 | .126 | .218 | .260 |

### Average Maneuvering

| Range | 0° | 15° | 30° | 45° |
|---|---|---|---|---|
| 500 | .783 | .679 | .386 | .234 |
| 1000 | .408 | .583 | .431 | .288 |
| 1500 | .235 | .525 | .508 | .302 |
| 2000 | .158 | .374 | .441 | .351 |
| 2500 | .119 | .268 | .363 | .305 |
| 3000 | .079 | .170 | .265 | .291 |

## Table XVI

## Kill Probabilities for Gun 2, SIGB = 8 mils

### Non-Maneuvering

| | PHIDOT = 0<br>GLFDOT = 0 | | | |
|---|---|---|---|---|
| Range | 0° | 15° | 30° | 45° |
| 500 | .756 | .666 | .411 | .274 |
| 1000 | .324 | .654 | .413 | .297 |
| 1500 | .163 | .468 | .479 | .287 |
| 2000 | .096 | .314 | .405 | .332 |
| 2500 | .062 | .216 | .325 | .284 |
| 3000 | .043 | .155 | .249 | .279 |

### Jink

| PHIDOT = 0<br>GLFDOT = -2 g/sec | | | |
|---|---|---|---|
| 0° | 15° | 30° | 45° |
| Not Calculated | | | |

### Hard Turn

| PHIDOT = 45°/sec<br>GLFDOT = 4 g/sec | | | |
|---|---|---|---|
| 0° | 15° | 30° | 45° |
| .760 | .667 | .411 | .274 |
| .340 | .659 | .415 | ? |
| .184 | .476 | .483 | ? |
| .118 | .323 | .408 | ? |
| .083 | .223 | .324 | ? |
| .060 | .152 | .232 | ? |

### Break

| PHIDOT = 90°/sec<br>GLFDOT = 6 g/sec | | | |
|---|---|---|---|
| 0° | 15° | 30° | 45° |
| .762 | .668 | .411 | .274 |
| .347 | .660 | .415 | .297 |
| .192 | .476 | .481 | .283 |
| .122 | .315 | .398 | ? |
| .087 | .211 | .303 | ? |
| .071 | .153 | .224 | ? |

### Average Maneuvering

| Range | 0° | 15° | 30° | 45° |
|---|---|---|---|---|
| 500 | .761 | .667 | .411 | .274 |
| 1000 | .343 | .659 | .415 | .297 |
| 1500 | .188 | .476 | .482 | .283 |
| 2000 | .120 | .319 | .403 | ? |
| 2500 | .085 | .217 | .314 | ? |
| 3000 | .065 | .152 | .228 | ? |

## Appendix D

The figures in this section show the general flow of information within the mathematical model.

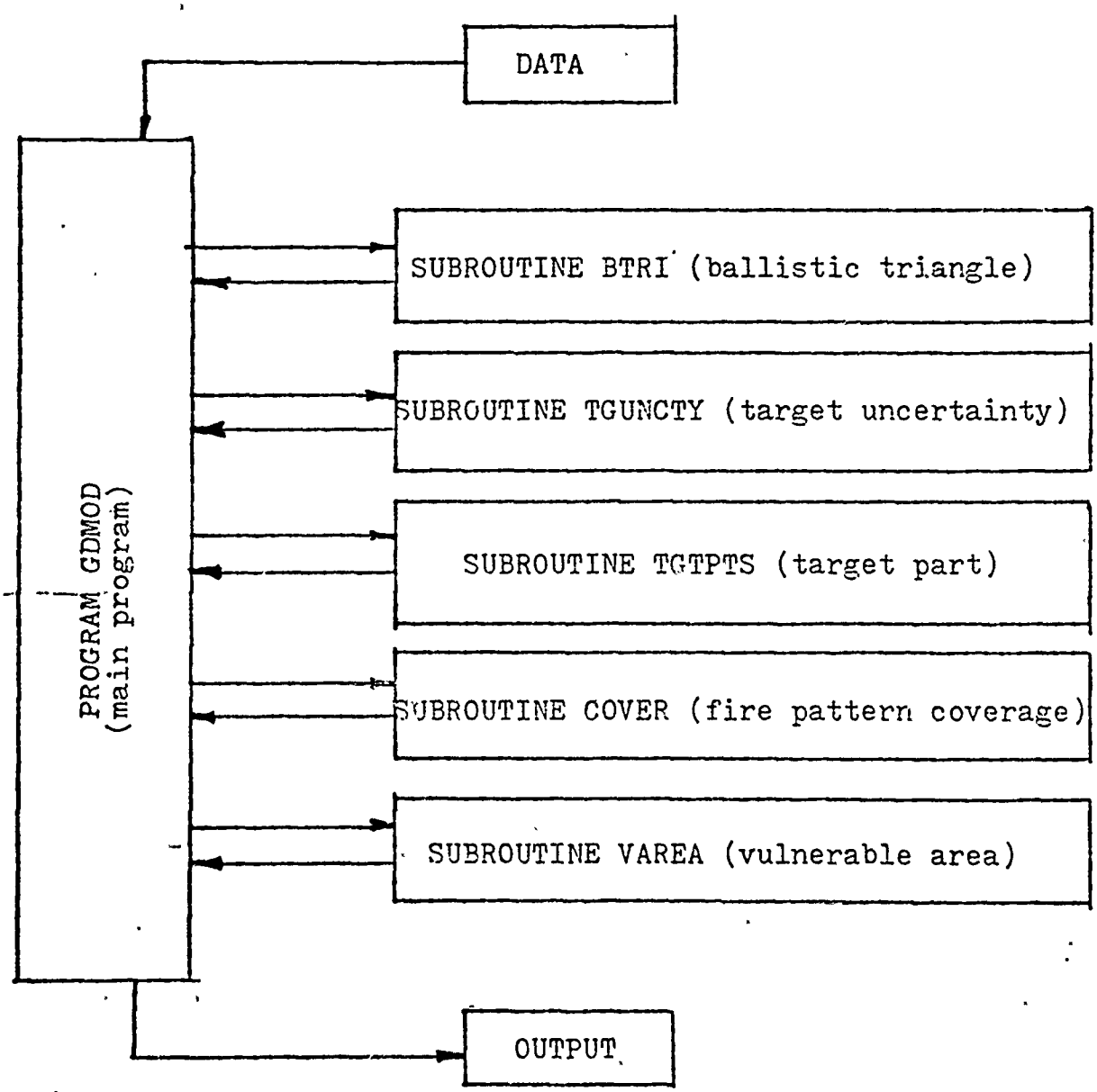


Figure 25 General Flow of Information Within Mathematical Model

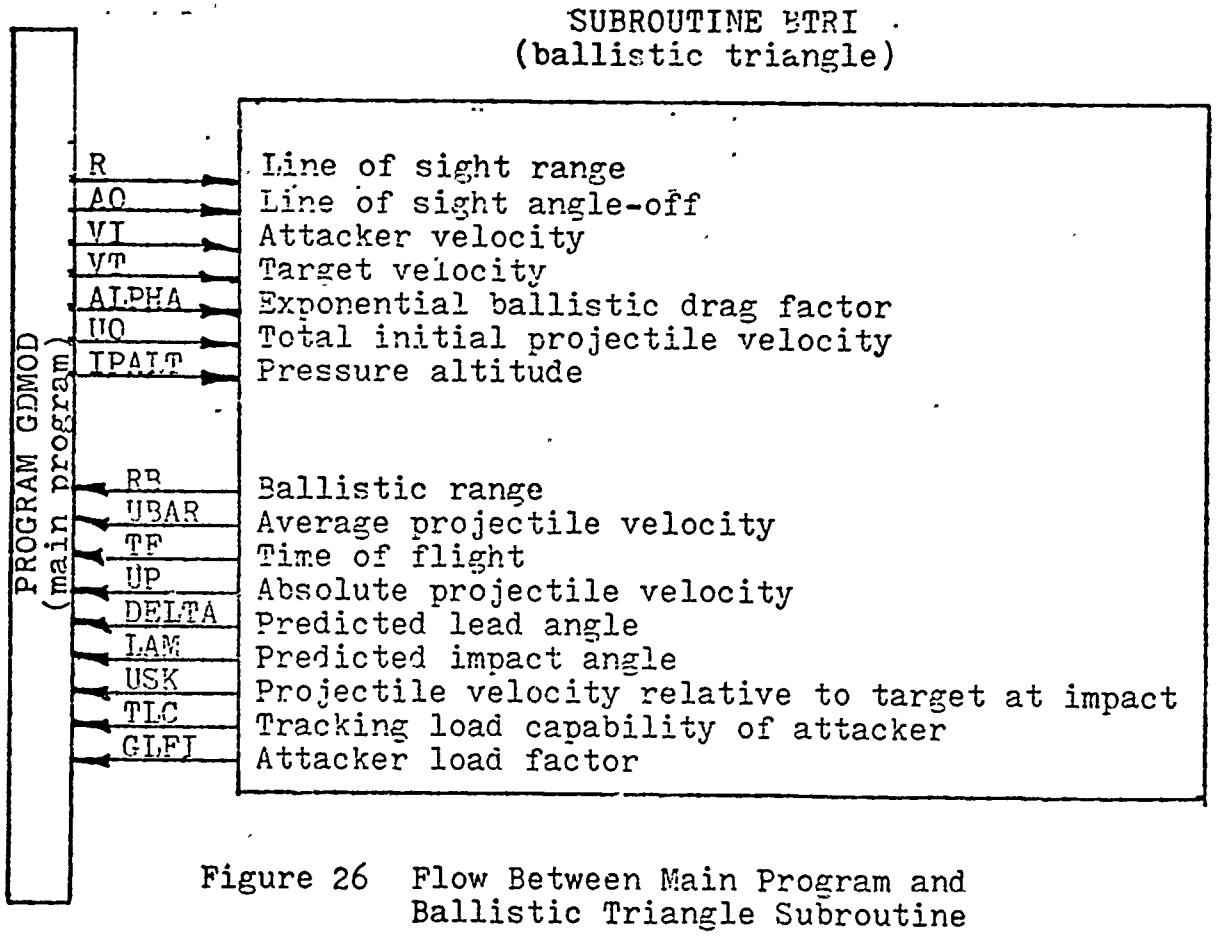


Figure 26 Flow Between Main Program and Ballistic Triangle Subroutine

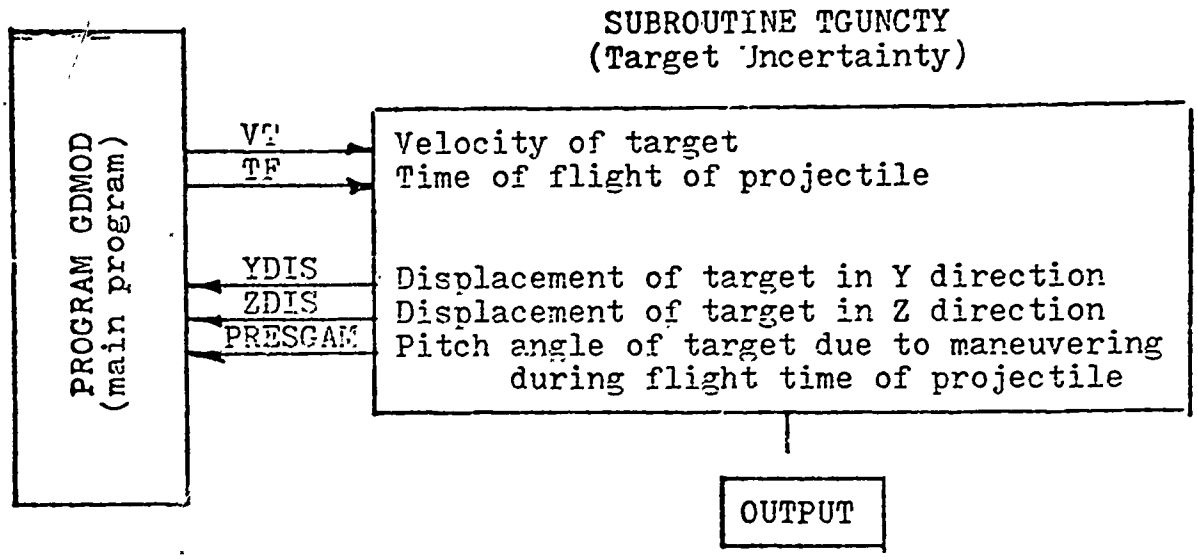


Figure 27 Flow Between Main Program and Target Uncertainty Subroutine

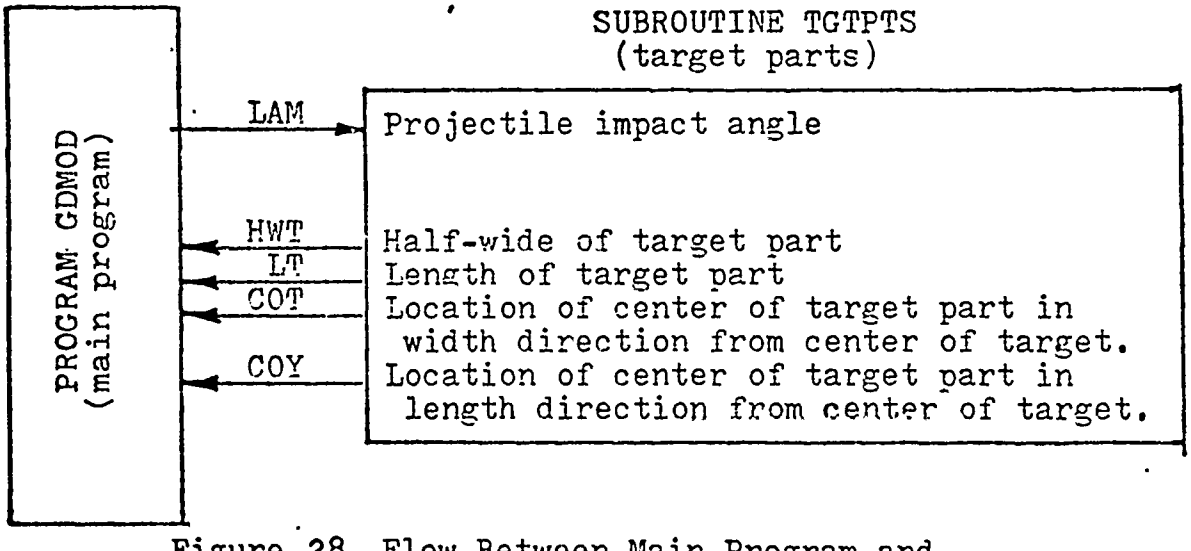


Figure 28 Flow Between Main Program and Target Parts Subroutine

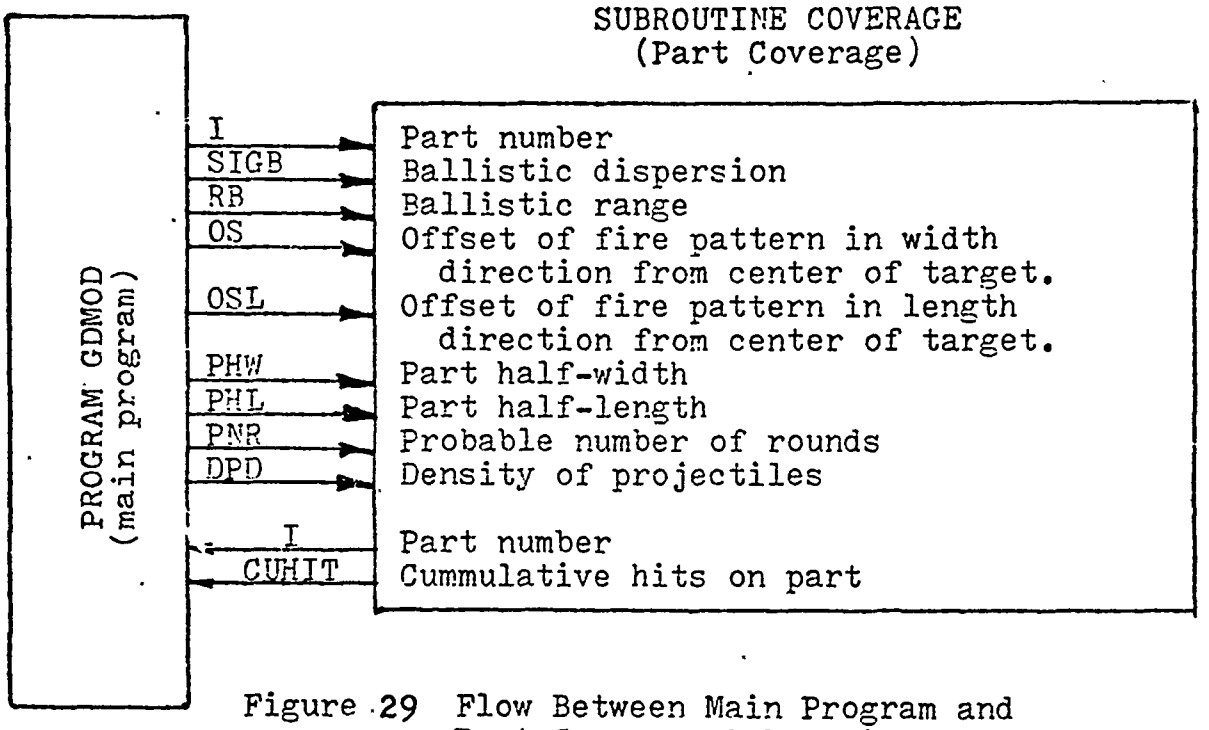


Figure 29 Flow Between Main Program and Part Coverage Subroutine

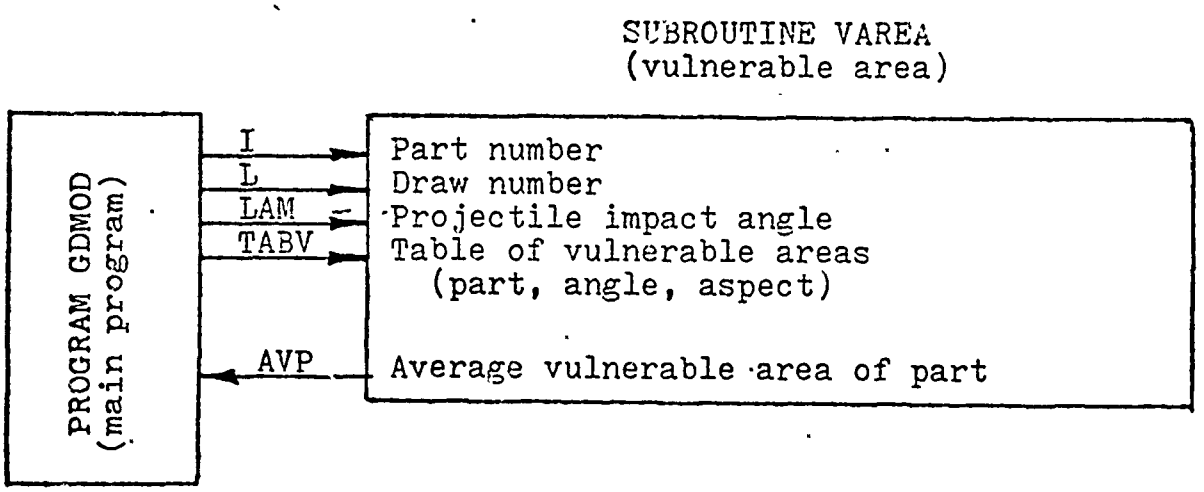


Figure 30 Information provided to main program by vulnerable area subroutine.

# Appendix E

This section contains the program listing for the mathematical model. The computer processing time is approximately 500 seconds per maneuver on a CDC 6600 and the printed output is approximately 500 pages. If the Print 5, Print 6, and Print 7 cards are removed, the output is approximately 100 pages per maneuver.

```
      PROGRAM GOMOD (INPUT,OUTPUT)
      DIMENSION DPD (2),HWT(8,4),COT(8,4),CCY(8,4),CUHIT(8),ANLH(8),
     1TABVA(8,4,2),TABVB(8,4,2),TABV(8,4,2)
      DIMENSION PY(50)
      REAL LAM,LT(8,4)
      DATA DPD/.6875,.3125/
      DATA PY/10*.0226,10*.0159,10*.0079,10*.0028,10*.0008/
      DATA TABVA/1.5,7*0.,7.3,7*0.,21.3,7*0.,23.6,7*0.,1.5,7*0.,3.8,7*0.
     1,9.0,7*0.,11.5,7*0./
      DATA TABVB/6.3,7*0.,36.3,7*0.,62.6,3*0.,.1,3*0.,70.7,3*0.,.4,3*0.,
     16.3,7*0.,24.6,7*0.,45.3,3*0.,.1,3*0.,56.5,3*0.,.1,3*0./

C     GUN TYPE
      DO 10 N=1,2
      IGUN=N
C     TARGET VULNERABILITY IS A FUNCTION OF GUN TYPE
      DO 92 I=1,8
      DO 92 J=1,4
      DO 92 K=1,2
      IF(IGUN.EQ.2) GO TO 91
      TABV(I,J,K)=TABVA(I,J,K)
      GO TO 92
   91 TABV(I,J,K)=TABVB(I,J,K)
   92 CONTINUE
      IF(IGUN.EQ.2) GO TO 11
C     GUN ONE CHARACTERISTICS
      VELM=3300.
      BCOEF=177.4
      GO TO 12
C     GUN TWO CHARACTERISTICS
   11 VELM=4000.
      BCOEF=406.2
C     FIRING CHARACTERISTICS
   12 FR=100
      DOB = 1.0
```

```
C  PRESSURE ALTITUDE (FEET)
      DO 20 IPALT=5,5
C  ATTACKER VELOCITY @ 5000 FT (FT/SEC)
      VI = 1000.
C  AIR DENSITY @ 5000 FT (LBM/FT3)
      RHOA=.0659
      IF(IPALT.EQ.5) GO TO 19
C  AIR DENSITY @ 35,000 FT (LBM/FT3)
      RHOA=.0237
C  ATTACKER VELOCITY @ 35,000 FT (FT/SEC)
      VI=900.
C  ATTACKER AND TARGET ARE COAIRSPEED
   19 VT=VI

C  EXPONENTIAL BALLISTIC DRAG FACTOR
      ALPHA=.5*RHOA/BCOEF
C  TOTAL INITIAL VELOCITY OF PROJECTILE (FT/SEC)
      UO = VELM + VI
C  BALLISTIC DISPERSION
      DO 100 IGD=4,5
      SIGB = 2.+(IGD-1)*2.
      ISIB=SIGB
      PRINT 1,IGUN,ISIB,IPALT
    1 FORMAT(1H1,4X,*GEM RESULTS FOR ONE SEC BURST OF GUN*,I2,*,*,I3,1X,
     1*MILS GUN DISPERSION AT*,I3,1X,*KFT PALT*///)
      PRINT 4
    4 FORMAT(2X,*IFT=1/EARLY,2/PERFECT,3/LATE TIMING,KOS=MIL OFFSET,L=
     11/2=TOP-EL/AZ, 3/4=SIDE-EL/AZ VIEW-FIRE DRAW DRN*)
C  LINE OF SIGHT ANGLE OFF
      DO 200 IAO=1,4
      AO = .26180 * (IAO-1.)
C  LINE OF SIGHT RANGE
      DO 200 IIR=1,6
      R=500.*IIR
      CALL BTRI(R,AO,VI,VT,RB,DELTA,LAM,TF,ALPHA,UO,UBAR,UP,USK,
     1GLFI,TLO,IPALT)
```

```
C  TRACKSHOOT FLAG
      IFLAG=0
C  TRACKSHOOT IF ATTACKER CAN TRACK WITH 5.6 G,S OR LESS
      IF(TLC.GT.0) GO TO 196
C  SNAPSHOOT AIM DISPERSION (RADIANS)
      ATLC=ABS(TLC)/3.464
      TKSIG=AMAX1(ATLC,.015)
C  SNAPSHOOT FLAG
      IFLAG=1
      PRINT 2
    2 FORMAT(25X,*ATTKR IS SNAPSHOOTING*/)
      GO TO 197
C  MIN STANDARD DEVIATION OF AIMING ERROR IS 5 MILS
  196 TSIGMIN=.005000
C  MAX LOAD FACTOR OF ATTACKING AIRCRAFT
      GLFMAX=7.33
C  STANDARD DEVIATION OF AIMING ERROR
      TKSIG=TSIGMIN/(1.0-(GLFI/GLFMAX)**2)
  197 PRINT 3,AO,R,RB,DELTA,LAM,LBAR,UP,USK,TLC,TKSIG,TF,GLFI
    3 FORMAT(1X,*ANGLE*,6X,*LOS*,6X,*FIRE*,5X,*LEAD*,7X,*CROSS*,6X,
     1*AVER*,5X,*PIP*,6X,*HIT*,6X,*LEAD*,7X,*TRACKING*,7X,*FLIGHT*
     2,7X,*ATTKR*,/01X,*OFF*,8X,
     3*RANGE*,4X,*RANGE*,4X,*ANGLE*,6X,*ANGLE*,6X,*RVEL*,5X,*VEL*,6X,
     4*VEL*,6X,*CAP.RES*,4),*SIGM.RES*,8X,*TIME*,9X,*LF*//,01X,F8.5,3X,
     5F6.0,3X,F6.0,3X,
     6F8.5,3X,F8.5,3X,F6.0,3X,F6.0,3X,F6.0,2X,F8.5,3X,F8.5,8X,F7.4,
     77X,F7.4/)
C  MIN ACCEPTIBLE PROJECTILE IMPACT VELOCITY
      IF(USK.GT.750.) GO TO 40
      PRINT 9
    9 FORMAT(40X,*BULLETS TOO SLOW*)
      GO TO 200
   40 CONTINUE
      CALL TGUNCTY(VT,TF,YDIS,ZDIS,PRESGAM)
C  INCREASE IN PROJECTILE IMPACT ANGLE DUE TO MANEUVERING TARGET
      TLAM=LAM+PRESGAM
```

```
      PRINT 8,TLAM
    8 FORMAT(/,35X,23HWITH TARGET UNCERTAINTY,4X,6HTLAM =,F6.5,/)
      PRINT 5
    5 FORMAT(1X,*AIRCRAFT PART*,3X,*FUSEL*,4X,*RIEWS*,4X,*ROBWS*,4X,*RHO
     1RS*,4X,*VSTAB*,4X,*LIEWS*,4X,*LOBWS*,4X,*LHORS*,4X,*TOTAL*,4X,*FLE
     2FF*,2X,*IFT/KCS/L*)
      LAM=TLAM
      CALL TGTPTS(LAM,HWT,LT,COT,CCY)
C  INITIAL VALUE OF AVE WEIGHTED PROB KILL FOR DRAWS, FIRE TIMING, OFFSETS
      AWPKOTO=0.
C  LATERAL ERROR IN AIMING
      DO 300 IOS=1,19,6
C  INITIAL VALUE OF AVE PROB KILL FOR DRAWS AND FIRE TIMING
      APKOT=0.
C  FIRING TIME DELAY (FT EQUIV OF STND DEV EARLY/PERFECT/LATE IN BURST TIMING)
      DO 301 IFT=1,3
      IFTT=IFT
      FTO=(IFT-2)*TKSIG*RB
C  SYMMETRY FLAG FOR LATERAL LAG OR LEAD
      KSYM=-1
C  ISYM PREVENTS PLUS ZERO AND MINUS ZERO FROM BEING SYMMETRIC
      ISYM=0
   81 ISYM=ISYM+1
      IF(IOS.LT.19) GO TO 82
      ISYM=ISYM+1
   82 CONTINUE
C  LATERAL OFFSET IN FEET OF PATTEN
      KOS=(19-IOS)*KSYM
      FLOS=.001*KOS*RB
C  INITIAL VALUE OF AVE PROB KILL FOR DRAWS
      APKO=0.
C  DRAWS OF FIRE PATTERN
C     DRAW 1 - TAIL VIEW, DRAW PARALLEL TO FRL
C     DRAW 2 - TAIL VIEW, DRAW PERPENDICULAR TO FRL
C     DRAW 3 - SIDE VIEW, DRAW PERPENDICULAR TO FRL
C     DRAW 4 - SIDE VIEW, DRAW PARALLEL TO FRL
      DO 400 L=1,4
```

```
C  INITIAL VALUES OF HITS AND LETHAL HITS FOR DRAW ON EACH PART
      DO 401 I=1,8
      CUHIT(I)=0.
  401 ANLH(I)=0.
C  INITIAL VALUES OF TOTAL HITS AND TOTAL LETHAL HITS FOR DRAW
      TNH=0.
      TNLH=0.
C  CONSIDERED VULNERABLE PART
      DO 500 I=1,5,4
C  PART HALF WIDTH
      PHW=HWT(I,L)
C  PART HALF LENGTH
C  PART CENTER IN WIDTH DIRECTION
      PHL=0.5*LT(I,L)
      CCP=CCT(I,L)+YDIS
C  OFFSET IN WIDTH DIRECTION OF FIRE PATTERN AND PART
      OS=ABS(FLCS-CCP)
C  INDIVIDUAL FIRE POINTS
      DO 600 IDP=1,50
C  FIRE PATTERN SYMMETRY FLAG
      IPOL=1
C  SYMMETRY OF FIRE PATTERN
      DO 600 IDPP=1,2
      IPOL=-1*IPOL
C  DISTANCE ALONG FIRELINE (DRAW) OF FIRE POINT
       YL=.06*(IDP-.5)*TKSIG*RB*IPOL
C  OFFSET OF INDIVIDUAL FIRE POINT FROM TARGET CENTER FOR SNAPSHOOT
      IF(IFLAG.EQ.1) YL=.5773*YL
C  COMBINED OFSET DUE TO TRKSIG AND FIREING TIME DELAY
      YOS=YL+FTD
C  OFFSET IN LENGTH DIRECTION OF FIRE POINT FROM PART CENTER
      OSL=ABS(YOS-COY(I,L)-ZDIS)
C  PROBABLE NUMBER OF ROUNDS AT PARTICULAR FIRE POINT  (TRACKSHOOT)
      PNR=PY(IDP)*FR*DOE
C  PROBABLE NUMBER OF ROUNDS AT PARTICULAR FIRE POINT  (SNAPSHOOT)
      IF(IFLAG.EQ.1) PNR=.01*FR*DOE
```

```
      CALL CCVER(SIGB,RE,CS,CSL,PHW,PHL,PNR,DPD,CUHIT,I)
  600 CONTINUE
C   IF CUMULATIVE HITS (AFTER 100 RDS) LESS THAN .001 SELECT NEXT PART
      IF(CUHIT(I).LT.0.001) GO TO 500
      CALL VAREA(I,L,LAM,TAEV,AVP)
C   PART AREA
      PAREA=4.*PHW*PHL
C   SINGLE SHOT VULNERABLE AREA RATIO OF PART
      SSV=AVP/PAREA
C   PREVENTS VULNERABLE AREA RATIO FROM BEING LARGER THAN ONE
      SSL=AMIN1(SSV,1.0)
C   AVE NUMBER OF LETHAL HITS ON TARGET FOR DRAW
      ANLH(I)=CUHIT(I)*SSL+ANLH(I)
C   TOTAL HITS AND TOTAL LETHAL HITS
      TNH=TNH+CUHIT(I)
      TNLH=TNLH+ANLH(I)
  500 CONTINUE
C   IF TOTAL NUMBER LETHAL HITS LESS THAN .001 GO TO NEXT DRAW
      IF(TNLH.LT.0.001)GO TO 400
C   PROBABILITY OF KILL FOR DRAW
      PKCL=1.-EXP(-TNLH)
C   AVE PROB KILL FOR FOUR DRAWS
      APKD=APKD+PKCL/4.
      PRINT 6, (CUHIT(I),I=1,8),TNH,PKOL,IFT,KOS,L
    6 FORMAT(3X,*TOTAL HITS*,   10F9.3,2X,I1,*/*,I3,*/*,I1)
      PRINT 7 ,(ANLH(I),I=1,8),TNLH,APKD
    7 FORMAT(3X,*EFF. HITS*,   10F9.3/)
  400 CONTINUE
C   AVE PROB KILL FOR DRAWS AND FIRE TIMING
      APKDT=APKDT+APKD
C   LATERAL OFFSET SYMMETRY
      KSYM=KSYM+2
      IF(ISYM.LT.2) GO TO 81
  301 CONTINUE
```

```
C  WEIGHTING FACTORS FOR LATERAL OFFSET (LAG OR LEAD)
C  BETWEEN +,- 18 MILS & +,- 12 MILS 80 %
C  BETWEEN +,- 12 MILS & +,- 6 MILS 20 %
C  BETWEEN +6 AND -6 MILS 70 % OF TIME
      IF(IOS-7) 71,72,73
   71 WF=.1000/(2.*3.)
      GO TO 74
   72 WF=.2000/(2.*3.)
      GO TO 74
   73 WF=.7000/(3.*3.)
C  AVE WEIGHTED PROB KILL FOR DRAWS AND FIRE TIMING
   74 AWPKOT=WF*APKOT
C  AVE WEIGHTED PROB KILL FOR DRAWS, FIRE TIMING, AND OFFSETS
      AWPKOTO=AWPKOTO+AWPKOT
      PRINT 76,AWPKOT
   76 FORMAT(//,31X,33HAVE PROB KILL FOR DRAWS+TIMING  =,F6.3,///,)
  300 CONTINUE
      PRINT 77,AWPKOTO
   77 FORMAT(//,25X,39HAVE PROB KILL FOR DRAWS+TIMING+OFFSET =,F6.3,//,)
  200 CONTINUE
  100 CONTINUE
   20 CONTINUE
   10 CONTINUE
   99 STOP
      END
```

```
      SUBROUTINE BTRI(R,AC,VI,VT,RB,DELTA,LAM,TF,ALPHA,UO,UBAR,UP,USK,
     1GLFI,TLC,IPALT)
      REAL LAM
C  BALLISTIC RANGE ITERATION
      EKI = 2. * VT/(UC*(1.+ EXP(-ALPHA * R)))
      FK = 1.0 + EKI
      RB = FK * R
  150 FRAC = ALPHA * VT * RB * RB/(UO * (1.-EXP(-ALPHA*RB)))
      ERRR =(RB*RB-R*R-2.*R*COS(AO)*FRAC-FRAC**2)/(R*R)
      DERR = FK - SQRT(FK**2-ERRR)
      FK = FK-DERR
      RB = FK*R
      IF(ABS(DERR).LE..001) GO TO 160
      GO TO 150
C  AVERAGE PROJECTILE VELOCITY
  160 UBAR = UO * (1.-EXP(-ALPHA*RB))/(RB*ALPHA)
C  TIME OF FLIGHT
      TF = RB/UBAR
C  PROJECTILE VELOCITY AT IMPACT
      UF = UO * EXP(-ALPHA*RB)
C  PREDICTED LEAD ANGLE
      DELTA=ASIN(VT*SIN(AC)/UBAR)
C  PREDICTED COLLISION ANGLE (FRL VS PROJ VEL VECTOR)
      LAM = AC-DELTA
C  PROJECTILE IMPACT VELOCITY
      USK = UP - VT*COS(LAM)
C  ATTACKER ACCELERATIONS IN G,S SQUARED
      AISQ=(VI*VT*SIN(LAM)/(RB*32.2))**2
C  ATTACKER LOAD FACTOR
      GLFI=SQRT(AISQ+1.)
C  PITCH RATE OF ATTACKER AT 5.6 G,S (6.0 G,S - .4 G,S)
      AMLC=193.2/VI-.020
      IF(IPALT.EQ.5) GO TO 165
      AMLC=144.9/VI-.02
C  TARGET CROSSING RATE
  165 TCR = VT*SIN(LAM)/RB
C  TRACKING LEAD CAPABILITY (TF=1 SEC)
      TLC=AMLC-TCR
      RETURN
      END
```

```
      SUBROUTINE TGTPTS (LAM,HWT,LT,COT,COY)
      DIMENSION HWT(8,4),COT(8,4),COY(8,4)
      REAL LAM,LT(8,4),LFT
C     1ST ARGUMENT IS TARGET PART (1 THRU 8)
C     2ND ARGUMENT IS DRAW OF FIRE PATTERN (1 THRU 4)
C         DRAW 1 IS TAIL VIEW WITH DRAW PARALLEL TO FRL
C         DRAW 2 IS TAIL VIEW WITH DRAW PERPENDICULAR TO FRL.
C         DRAW 3 IS SIDE VIEW WITH DRAW PERPENDICULAR TO FRL
C         DRAW 4 IS SIDE VIEW WITH DRAW PARALLEL TO FRL
C           THEREFORE HWT (HALF WIDTH TARGET) AND LT (LENGTH TARGET) DEPEND ON
C           THE PARTICULAR DRAW
      HWT(1,1) = 2.0
      LT(1,1) = 4.*COS(LAM) + 40.*SIN(LAM)
      COT(1,1) = 0.
      HWT(2,1) = 2.5
      LT(2,1) = 0.5*COS(LAM) + 15.*SIN(LAM)
      COT(2,1) = 4.5
      HWT(3,1) = HWT(2,1)
      LT(3,1) = 0.5*COS(LAM) + 5.*SIN(LAM)
      COT(3,1)=9.5
      HWT(4,1) = HWT(1,1)
      LT(4,1) = LT(3,1)
      COT(4,1) = 4.0
      HWT(5,1) = 0.25
      LFT=6.0-40.*SIN(LAM)
      LT(5,1)=AMAX1(LFT,0.)
      COT(5,1) = COT(1,1)
      HWT(6,1) = HWT(2,1)
      LT(6,1) = LT(2,1)
      COT(6,1) = -COT(2,1)
      HWT(7,1) = HWT(2,1)
      LT(7,1) = LT(3,1)
      COT(7,1) = -COT(3,1)
      HWT(8,1) = HWT(1,1)
      LT(8,1) = LT(3,1)
      COT(8,1) = -COT(4,1)
```

```
      HWT(1,2) = 0.5*LT(1,1)
      LT(1,2) = 2.0*HWT(1,1)
      COT(1,2) = COT(1,1)
      HWT(2,2) = 0.5*LT(2,1)
      LT(2,2) = 5.0
      COT(2,2) = -2.5*SIN(LAM)
      HWT(3,2) = 0.5*LT(3,1)
      LT(3,2) = LT(2,2)
      COT(3,2) = -7.5*SIN(LAM)
      HWT(4,2) = 0.5*LT(4,1)
      LT(4,2) = LT(2,2)
      COT(4,2) = -20.*SIN(LAM)
      HWT(5,2) = 0.5*LT(5,1)
      LT(5,2) = 2.0*HWT(5,1)
      COT(5,2) = 5.*COS(LAM) - 20.*SIN(LAM)
      HWT(6,2) = HWT(2,2)
      LT(6,2) = LT(2,2)
      COT(6,2) = COT(2,2)
      HWT(7,2) = HWT(3,2)
      LT(7,2) = LT(3,2)
      COT(7,2) = COT(3,2)
      HWT(8,2) = HWT(4,2)
      LT(8,2) = LT(2,2)
      COT(8,2) = COT(4,2)
      HWT(1,3) = HWT(1,2)
      LT(1,3) = LT(1,2)
      COT(1,3) = COT(1,1)
      LT(2,3) = LT(5,2)
      Q1 = 2.5*COS(LAM)-11.25*SIN(LAM)
      HWT(2,3) = AMAX1(Q1,0.)
      COT(2,3) = 7.0*COS(LAM)-HWT(2,3)
      LT(3,3) = LT(5,2)
      Q2 = 5.*COS(LAM)-13.75*SIN(LAM)
      Q3 = AMAX1(Q2,0.)
      A1 = 2.5*COS(LAM)
      HWT(3,3) = AMIN1(Q3,A1)
```

```
      CCT(3,3) = 12.*COS(LAM)-HWT(3,3)
      LT(4,3) = LT(5,2)
      Q4 = 2.*COS(LAM)-20.*SIN(LAM)
      HWT(4,3) = AMAX1(Q4,0.)
      CCT(4,3) = 6.*COS(LAM)-HWT(4,3)
      HWT(5,3) = 0.5*(0.5*COS(LAM)+8.*SIN(LAM))
      LT(5,3)=6.0
      CCT(5,3) = CCT(4,2)
      Q5 = 2.5*COS(LAM)-8.75*SIN(LAM)
      HWT(6,3) = AMAX1(Q5,0.)
      LT(6,3) = LT(5,2)
      CCT(6,3) = -7.*COS(LAM)+HWT(6,3)
      Q6 = 5.*COS(LAM)-6.25*SIN(LAM)
      Q7 = AMAX1(Q6,0.)
      HWT(7,3) = AMIN1(Q7,A1)
      CCT(7,3) = -12.*COS(LAM)+HWT(7,3)
      LT(7,3) = LT(5,2)
      HWT(8,3) = HWT(1,1)
      CCT(8,3) = -4.*COS(LAM)-20.*SIN(LAM)
      LT(8,3) = LT(5,2)
      HWT(1,4) = HWT(1,1)
      LT(1,4) = LT(1,1)
      CCT(1,4) = CCT(1,1)
      HWT(2,4) = HWT(5,1)
      LT(2,4) = 2.0*HWT(2,3)
      CCT(2,4) = CCT(1,1)
      HWT(3,4) = HWT(5,1)
      LT(3,4) = 2.0*HWT(3,3)
      CCT(3,4) = CCT(1,1)
      HWT(4,4) = HWT(5,1)
      LT(4,4) = 2.0*HWT(4,3)
      CCT(4,4) = CCT(1,1)
      HWT(5,4)=0.5*LT(5,3)
      LT(5,4) = 2.0* HWT(5,3)
      CCT(5,4) = 3.0
      HWT(6,4) = HWT(5,1)
      LT(6,4) = 2.0*HWT(6,3)
      CCT(6,4) = CCT(1,1)
      HWT(7,4) = HWT(5,1)
```

```
      LT(7,4) = 2.0*HWT(7,3)
      COT(7,4) = COT(1,1)
      HWT(8,4) = HWT(5,1)
      LT(8,4) = 2.0*HWT(8,3)
      COT(8,4) = COT(1,1)
      COY(1,1) = COT(1,2)
      COY(2,1) = COT(2,2)
      COY(3,1) = COT(3,2)
      COY(4,1) = COT(4,2)
      COY(5,1) = COT(5,2)
      COY(6,1) = COT(6,2)
      COY(7,1) = COT(7,2)
      COY(8,1) = COT(8,2)
      CCY(1,2) = CCT(1,1)
      COY(2,2) = COT(2,1)
      CCY(3,2) = CCT(3,1)
      COY(4,2) = COT(4,1)
      CCY(5,2) = CCT(5,1)
      CCY(6,2) = CCT(6,1)
      CCY(7,2) = COT(7,1)
      COY(8,2) = COT(8,1)
      COY(1,3) = COT(1,1)
      CCY(2,3) = CCT(2,4)
      CCY(3,3) = COT(3,4)
      COY(4,3) = COT(4,4)
      CCY(5,3) = CCT(5,4)
      COY(6,3) = COT(6,4)
      CCY(7,3) = CCT(7,4)
      COY(8,3) = CCT(8,4)
      COY(1,4) = CCT(1,3)
      COY(2,4) = CCT(2,3)
      CCY(3,4) = COT(3,3)
      COY(4,4) = COT(4,3)
      CCY(5,4) = COT(5,3)
      COY(6,4) = COT(6,3)
      COY(7,4) = COT(7,3)
      CCY(8,4) = CCT(8,3)
      RETURN
      END
```

```
      SUBROUTINE COVER(SIGB,RB,OS,OSL,PHW,PHL,PNR,DFD,CUHIT,I)
      DIMENSION DPD(2),CUHIT(8)
C  FIRE PATTERN DENSITY
C     IDP=1 REPRESENTS 68% OF PROJECTILES AND IDP=2 REPRESENTS 32%,
C     12% OF WHICH ARE COMBINED WITH IDP=1 TO GENERATE 80% DISPERSION
      DO 700 IPD = 1,2
C  HALF WIDTH OF SQUARE APPROXIMATION TO CIRCULAR UNIFORM DISTRIBUTION
C     80% OF PROJECTILES WITHIN ONE STND DEV, REMAINING WITHIN THREE STND DEV
      HWP=1.6*SIGB*RB/1000.
      IF(IPD.EQ.2) HWP=1.66*HWP
C  NO COVERAGE, MISS IN BOTH WIDTH AND LENGTH DIRECTIONS
      IF(OS.GE.PHW+HWP.OR.OSL.GE.PHL+HWP) GO TO 700
C  COMPLETE OR PARTIAL COVERAGE IN WIDTH AND/OR LENGTH DIRECTIONS
      ROL = PHL/HWP
      POL = AMIN1(ROL,1.0)
      ROW = PHW/HWP
      POW = AMIN1(ROW,1.0)
      SAR=POW*POL
C  COMPLETE COVERAGE IN WIDTH DIRECTION
      IF(HWP.GE.PHW+OS) GO TO 435
C  PARTIAL COVERAGE IN WIDTH DIRECTION
      IF(OS.GE.PHW) GO TO 430
      FP = HWP
      HMO = PHW-OS
      SP = AMIN1(HMO,HWP)
      OSC=0.5*(FP+SP)/PHW
      GO TO 450
  430 OSC=0.5*(PHW+HWP-OS)/PHW
      GO TO 450
  435 OSC = 1.0
  450 CONTINUE
C  COMPLETE COVERAGE IN LENGTH DIRECTION
      IF(HWP.GE.PHL+OSL) GO TO 465
```

```
C  PARTIAL COVERAGE IN LENGTH DIRECTION
      IF(CSL.GE.PHL) GO TO 460
      FPL=HWP
      HMP=PHL-OSL
      SPL=AMIN1(HMP,HWP)
      OSLC=0.5*(FPL+SPL)/PHL
      GO TO 470
  460 OSLC=0.5*(PHL+HWP-OSL)/PHL
      GO TO 470
  465 CSLC=1.0
C  AREA OF COVERAGE
  470 COV=OSC*OSLC
C  HITS ON PART
      CUHIT(I)=CUHIT(I)+PNR*SAR*COV*DPD(IPD)
  700 CONTINUE
      RETURN
      END
```



```
      SUBROUTINE VAREA(I,L,LAM,TABV,AVP)
C  VULNERABLE AREA TABLE (PART, ANGLE OFF <0,15,30,45 DEG>, ASPECT <REAR,SIDE>)
      DIMENSION TABV(8,4,2)
      REAL LAM
C  TARGET ASPECT
      KK=1
      IF(L.GT.2) KK=2
C  INTERPOLATION FACTORS
      RP1=LAM/.2618+1.
      JJ=INT(RP1)
C  VULNERABLE AREA OF PART
C     INTERPOLATION BETWEEN TWO CLOSEST 15 DEG INCREMENTS OF ANGLE-OFF
      AVP=TABV(I,JJ,KK)+(RP1-JJ)*(TABV(I,JJ+1,KK)-TABV(I,JJ,KK))
      RETURN
      END
```

```
      SUBROUTINE TGUNCTY(VT,TF,YDIS,ZDIS,PRESGAM)
      PRINT 5
    5 FORMAT(/1X,14HTIME OF FLIGHT,3X,10HTARGET VEL,3X,11HLOAD FACTOR,3X
     1,10HBANK ANGLE,3X,17HFLIGHT PATH ANGLE,3X,12HRADIAL ACCEL,3X,6HX-D
     2IST,3X,6HY-DIST,3X,6HZ-DIST,/,5X,5H(SEC),9X,8H(FT/SEC),8X,3H(G),10
     3X,5H(DEG),12X,5H(DEG),9X,11H(FT/SEC**2),4X,4H(FT),4X,4H(FT),4X,4H(
     4FT))
C  INITIAL FLIGHT PATH ANGLE
      DO 25 IGAM=4,4
      GAMMA=0.2618*(IGAM-4.0000)
C  INITIAL LOAD FACTOR
      DO 45 NG=4,4
      GLF=NG-3.00
C  INITIAL BANK ANGLE
      DO 55 IPHI=1,1
      PHI=0.26180*(IPHI-1.00000)
C  INITIAL RADIAL ACCELERATION (FT PER SEC**2)
      RA=32.16*(GLF-COS(PHI)*COS(GAMMA))
C  DISPLACEMENTS FROM INITIAL POSITION AFTER TIME,TF,FOR CONSTANT RA,PHI, GAMMA
      XDIS=VT*TF
      YDIS=RA*SIN(PHI)*TF*TF/2.00
      ZDIS=RA*COS(PHI)*TF*TF/2.00
C  PRINT OUT INITIAL CONDITIONS AND DISPLACEMENTS USING INITIAL RA OVER TF
      PHID=PHI*57.2956
      GAMMAD=GAMMA*57.2956
      PRINT 65,TF,VT,GLF,PHID,GAMMAD,RA,XDIS,YDIS,ZDIS
C  NUMBER OF TIME INCREMENTS
      NDELTAS=100
C  SIZE OF TIME INCREMENTS
      DELT=NDELTAS
      DELTF=TF/DELT
C  ROLL RATE CAUSING CHANGE IN BANK ANGLE DURING TF
      DO 56 IPHIDOT=1,1
C  INCREASED G LOADING DUE TO G-RATE DURING TF
      DO 56 IGLFDOT=3,3
      PHIDOT=0.78540*(IPHIDOT-1.00000)
```

```
      GLFDOT=IGLFDOT-3.00
      PHI=0.52360*(IPHI-1.00000)
      GLF=NG-3.00
C  ITERATION COUNTER
      K=0
C  INITIAL DISPLACMENTS
      XDIS=0.0
      YDIS=0.0
      ZDIS=0.0
C  INITIAL VELOCITY COMPONENTS
      SUMU=0.0
      SUMV=0.0
      SUMW=0.0
C  INITIAL VELOCITY INCREMENTS
      DELU=0.0
      DELV=0.0
      DELW=0.0
C  KINEMATIC (EFFECTIVE) RADIAL ACCEL (FT PER SEC**2)
   10 RA=32.16*(GLF-COS(PHI)*COS(GAMMA))
C  INCREMENTAL DISTANCES DURING DELTF (ACCEL FOR NEW DELTF, VEL FOR END OF OLD )
      DELXDIS=VT*DELTF+SUMU*DELTF
      DELYDIS=RA*SIN(PHI)*DELTF*DELTF/2.000+SUMV*DELTF
      DELZDIS=RA*COS(PHI)*DELTF*DELTF/2.000+SUMW*DELTF
C  DISPLACEMENTS FROM INITIAL POSITION
      XDIS=XDIS+DELXDIS
      YDIS=YDIS+DELYDIS
      ZDIS=ZDIS+DELZDIS
C  VELOCITY COMPONENTS AFTER TIME INCREMENT DELTF
      DELU=0.0
      DELV=RA*SIN(PHI)*DELTF
      DELW=RA*COS(PHI)*DELTF
C  VELOCITY COMPONENTS AFTER KTH INCREMENT
      SUMU=SUMU+DELU
      SUMV=SUMV+DELV
      SUMW=SUMW+DELW
      K=K+1
      IF(NDELTAS-K) 200,64,62
```

```
C  CHANGE IN FLIGHT PATH ANGLE DUE TO PITCH RATE DURING INCREMENTAL FLIGHT TIME
   62 GAMDOT=RA/VT
      DELGAM=GAMDOT*DELTF
      GAMMA=GAMMA+DELGAM
C  CHANGE IN BANK ANGLE DUE TO ROLL RATE DURING INCREMENTAL FLIGHT TIME
      DELPHI=PHIDOT*DELTF
      PHI=PHI+DELPHI
C  CHANGE IN G LOADING DUE TO CHANGING LOAD FACTOR DURING INCREMENTAL FLIGHT TIM
      DELGLF=GLFDOT*DELTF
      GLF=GLF+DELGLF
C  MAX ALLOWABLE TARGET G-LOADING IS 7 G,S
      IF(GLF.LT.7.) GO TO 32
      GLF=7.00
   32 GO TO 10
C  BANK ANGLE AND FLIGHT PATH ANGLE IN DEGREES
   64 PHIT=PHI*57.2956
      GAMMAT=GAMMA*57.2956
      PRINT 65,TF,VT,GLF,PHIT,GAMMAT,RA,XDIS,YDIS,ZDIS
   65 FORMAT(4X,F6.4,11X,F5.0,9X,F5.2,8X,F5.1,12X,F5.1,12X,F6.2,6X,F5.0,
     13X,F5.0,3X,F5.0)
      PRESGAM=GAMMA
      GAMDOD=GAMDOT*57.2956
      PHIDOD=PHIDOT*57.2956
      PRINT 104
  104 FORMAT(/,12X,51HNUMBER OF ITERATIONS, SIZE OF INCREMENTS, AND RATE
     1S)
      PRINT 105,K,DELTF,GAMDOD,PHIDOD,GLFDOT
  105 FORMAT(12X,10HITERATIONS,4X,5HDELTF,4X,6HGAMDOT,4X,6HPHIDOT,4X,6HG
     1LFDOT,/,27X,5H(SEC),3X,9H(DEG/SEC),1X,9H(DEG/SEC),2X,7H(G/SEC),/,1
     24X,I4,6X,F6.4,4X,F4.0,7X,F4.0,5X,F5.2,/)
      GAMMA=0.2618*(IGAM-4.0000)
   56 CONTINUE
   55 CONTINUE
   45 CONTINUE
   25 CONTINUE
  200 RETURN
      END
```

Unclassified
Security Classification

**DOCUMENT CONTROL DATA - R & D**

*(Security classification of title, body of abstract and indexing annotation must be entered when the overall report is classified)*

1. ORIGINATING ACTIVITY (Corporate author)
Air Force Institute of Technology (AFIT-EN)
Wright-Patterson AFB, Ohio 45433

2a. REPORT SECURITY CLASSIFICATION
Unclassified

2b. GROUP

3. REPORT TITLE
(6) The Effect of Target Maneuvering on Kill Probability in Air-to-Air Gunnery.

4. DESCRIPTIVE NOTES (Type of report and inclusive dates)
AFIT Thesis (9) Master's thesis,

5. AUTHOR(S) (First name, middle initial, last name)
(10) Richard E. Guild
Major USAF

(12) 143p.

6. REPORT DATE
(11) June 1972

7a. TOTAL NO. OF PAGES

7b. NO. OF REFS
9

8a. CONTRACT OR GRANT NO.

b. PROJECT NO. N/A

c.

d.

9a. ORIGINATOR'S REPORT NUMBER(S)
(14) GAW/MC/72-9

9b. OTHER REPORT NO(S) (Any other numbers that may be assigned this report)
TEST

10. DISTRIBUTION STATEMENT
Distribution limited to U.S. Gov't agencies only; covers the evaluation of [redacted] 2 June 1972. Other requests for this document must be referred to Dean of Engineering, Air Force Institute of Technology, (AFIT-EN), Wright-Patterson AFB, Ohio 45433.

11. SUPPLEMENTARY NOTES

12. SPONSORING MILITARY ACTIVITY
Air Force Armament Laboratory (AFATL-DLYD) Eglin Air Force Base, Florida 32542

13. ABSTRACT

A study was made to determine the effect of target maneuvering during projectile flight time on kill probability in air-to-air gunnery. The effect of target uncertainty was analyzed by comparing kill probabilities for a specified non-maneuvering target with kill probabilities for an average defensively maneuvering target. The kill probability of the average maneuvering target was defined as the average kill probability for the specified target when performing a negative-g jink, hard turn, and break. The kill probabilities were calculated using a mathematical model to approximate the gunnery attack. Firing condition were parametrically varied from 500 feet to 3000 feet line of sight range and zero to 45 degrees angle-off. Two dissimilar rapid firing cannons are compared in the analysis. Kill probability was based on trackshoot aiming when the attacker's g-loading to establish lead for target motion was 5.6 g's or less, and snapshoot aiming when greater. It was concluded that target uncertainty has no effect on kill probability when the time of flight is less than .5 seconds, but that it significantly affects kill probability when the time of flight is greater than .8 seconds. It was also concluded, that for air-to-air gunnery, the ballistic dispersion of rapid firing cannons should be such that 80 percent of the rounds are within a circle of nine to ten mils diameter.

DD FORM 1 NOV 65 1473

01225

Unclassified
Security Classification

| KEY WORDS | LINK A | | LINK B | | LINK C | |
|---|---|---|---|---|---|---|
| | ROLE | WT | ROLE | WT | ROLE | WT |
| Air-to-Air Gunnery<br>Ballistic Dispersion<br>Kill Probability | | | | | | |